Segmental dynamics of polymer glasses undergoing deformation: effect of temperature and reversing deformation protocols

By

Kelly Hebert

A dissertation submitted in partial fulfillment of

the requirements for the degree of

Doctor of Philosophy

(Chemistry)

at the

UNIVERSITY OF WISCONSIN-MADISON

2016

Date of final oral examination: 05/11/2016

The dissertation is approved by the following members of the Final Oral Committee:
Mark D. Ediger, Professor, Chemistry
Randall Goldsmith, Assistant Professor, Chemistry
John Wright, Professor, Chemistry
Arun Yethiraj, Professor, Chemistry
John Perepezko, Professor, Materials Science and Engineering

Acknowledgements

This thesis is not only the culmination of my graduate work, but also the culmination of a dream that I've had since I was 11 years old. I'd like to thank the people who were there at the beginning of my journey – my parents, Greg and Lisa Christison – who encouraged me to take ownership of my education and career plans, let me set my own goals and standards of excellence from a young age, and gave me the perfect balance of support and freedom to do so. I would also like to thank my entire family, including my siblings Andrew and Amy, my in-laws, my grandparents, and the rest of my extended family, for encouragement during difficult times.

My experience at the University of Washington strongly influenced my decision to continue my education in graduate school, and I would like to thank the many people who helped me during my undergraduate years. To Larry Dalton – thank you for taking a chance on an enthusiastic college student and for all of your assistance when I was applying to graduate programs! I'd also like to thank the rest of the Dalton and Robinson research groups for creating a supportive atmosphere and treating me like a full colleague from day one. Particularly, I would like to thank Lewis Johnson, whose friendship, encouragement and support continued during my time at UW-Madison. More than anyone else at UW (Seattle), I would like to thank my mentor in the Dalton group, Stephanie Benight. Now that I am completing my own graduate work, I can fully appreciate what a patient mentor she was (and can identify a few occasions where I almost certainly strained the boundaries of that patience – but she was too wonderful to let me know at the time)! I wouldn't have applied for graduate school right away without her encouragement, and I am incredibly lucky to have started my research career with such a talented and supportive mentor.

There are several people in the chemistry department at UW-Madison who helped me so much during my time here; this is a wonderful place to do science! I'd like to thank all of the staff, including everyone in the business office, machine and electronics shops, and all of the divisional coordinators. These people averted mini-crises too many times to count! Arrietta Clauss deserves special mention for invaluable advice and encouragement during my job search. I would also like to thank Mahesh Mahanthappa and John Wright for encouragement and assistance during my 2nd year and 3rd year exams, as well as my job search.

Friendship and support from several people in Madison and Seattle – chemists and non-chemists alike – were integral during the completion of this Ph.D. Of the chemists, there are too many to name individually, although Kate Skog, Jennifer Faust, Shy Bhattacharya, Elvin Morales, Stephen Block, and Leith Samad all deserve special mention and thanks. I would also like to thank all of my friends in Madison Toastmasters Club No. 1, and Margaret Budde in particular, for helping me find my voice and build confidence during my time in Wisconsin.

I'd like to thank everyone I overlapped with in the Ediger group during my time here – it was a privilege to work with each one of you. Jaritza Gomez, in particular, deserves a great deal of thanks for her unwavering friendship – we have gone through so much together, and I've lost track of the number of times she has helped me see clearly when times have been tough! I would like to thank Ben Bending, who first got me interested in polymer glasses, showed me the ropes, and was my mentor during my early years as a graduate student. I'd also like to thank the rest of Team Deformation: Josh Ricci, Kelly Suralik, and Trevor Bennin. It was humbling to work with such a creative and talented team. I am truly impressed by and proud to have worked with each one of you and I am excited to see what the future holds for all of you.

To Mark – no words could be enough to express my gratitude to you, nor could they adequately describe what a wonderful and *patient* mentor you have been over the past several years. It is quite apparent that you put a tremendous amount of thought and energy into being the best advisor possible to all of your students, no matter the circumstance; that effort and consideration have come through during every single interaction I have had with you. Your ability to remain calm, professional, and fair in clearly difficult situations is nothing short of inspirational and kept me going through my worst times in graduate school. Every day of working with you has motivated me to keep improving myself as a scientist, colleague, and person; I know I'll still be asking myself, "What would Mark do?" forty years from now, and perhaps even fifty or sixty if I am lucky enough! I couldn't have made a better choice of advisor, whether at UW-Madison or at any other university in the world, and I think you will find that sentiment to be uncommonly common among those who have worked with you.

More than any other person, I would like to thank my husband, Paul, who is (by a large margin) the most brilliant, humble, and caring person I have met. Paul – your endless support, patience, and impeccable (uncanny, perhaps?) ability to articulate exactly what I need to hear at any given moment has dually allowed me to grow by leaps and bounds as a person and also helped me through the most difficult situations I've ever faced. I could not have possibly made it through graduate school without your support, and of all of the people I've met during my time in Madison, I am the most thankful to have met you. I'm all the more thankful that we got married, because there's no way I would be able to leave Madison without you! I'm happy that in the next phase of our life together, we'll be able to share everything good in store for us, and I certainly couldn't imagine going through the bad times with anyone else.

Finally, to Erwin and Hauska – I couldn't have imagined how much of a difference two small felines could make in the well-being of a graduate student. Thank you for the past five years we've spent together!

Table of Contents

Segmental dynamics of polymer glasses undergoing deformation: effect of temperature and reversing deformation protocols

Kelly Hebert

Under the supervision of Prof. Mark D. Ediger

Department of Chemistry, University of Wisconsin-Madison

Abstract

A probe reorientation technique is used to monitor changes in the segmental dynamics of polymer glasses as they undergo physical aging and deformation. This thesis focuses on lightly cross-linked poly(methyl methacrylate) (PMMA) glasses in which the optical probe N,N'-Dipentyl-3,4,9,10-perylenedicarboximide (DPPC) is dilutely dispersed. Deformations are performed within a home-built deformation apparatus which allows optical access to the samples. The work of this thesis provides a test of existing models and theories in the literature which describe polymer glass deformation. A full understanding of the deformation behavior of polymer glasses may allow these versatile materials to be used in a wider variety of applications.

The effect of temperature on segmental dynamics during flow-state deformation is studied using PMMA glasses between T_g-11 K and T_g-27 K deformed in tension at a series of constant engineering strain rates. These studies demonstrate that thermally-activated transitions are significant during flow, with calculated free energy barriers of ~39 kT_g. Furthermore, these free energy barriers during flow are reduced by only ~10-15% as compared to the pre-deformation values, indicating that although deformation reduces thermal effects on dynamics, thermally-activated transitions remain a significant feature of flow-state dynamics. The reported

effect of temperature is significantly larger than anticipated in the literature; a comparison of the results to existing models and simulations is discussed.

A series of reversing constant strain rate deformations is performed on a PMMA glass at T_g-7 K to separate contributions of proposed mechanisms which enhance segmental dynamics during deformation. We quantify the activity of the proposed rejuvenation mechanism using both probe reorientation and a mechanical experiment and find that for both techniques, rejuvenation gradually increases with strain, saturating at strains several times the yield strain. Our results describing the rejuvenation mechanism broadly agree with a theory of Chen and Schweizer. However, at low strains, the probe reorientation results show higher activity of the rejuvenation mechanism; these optical results agree with a recent simulation study. The difference between the optical and mechanical measurements, as well as a comparison to theoretical work in the literature is discussed.

Chapter 1

Introduction

Kelly Hebert

Overview

Polymer glasses are easily-processed, lightweight, yet mechanically tough materials which are finding increasing use in applications previously reserved for inorganic glasses or metals. Polycarbonate, for example, is prized for its ductility and durability; it is often used in eyeglass lenses and is a major component of bulletproof glass. The glossy luster of poly(methyl methacrylate) has made it an attractive material for display windows. Biodegradable poly(lactic acid) has been an increasingly popular material for disposable drinkware. In many of the applications of polymer glasses, a structural or load-bearing capacity is valued; however, a full understanding of the mechanical properties of these versatile materials is far from being attained.

The nonequilibrium nature of polymer glasses adds a layer of complexity to attaining a full understanding of their mechanical properties. The properties of a glass can strongly depend on their thermal history; two glasses at a constant temperature may show varying degrees of brittleness purely because their thermal history is different. Because polymer glasses are out of equilibrium, their properties, including volume, relaxation times, and enthalpy do not stay constant, but evolve over time. However, there are other factors which complicate an understanding of the mechanical behavior of polymer glasses. Unlike their rubbery counterparts, many deformation protocols do not show a simple linear relationship between mechanical variables; the purely elastic regime of many polymer glasses is encompassed at strains far less than 1%.[1, 2] Additionally, relaxation times within glasses and supercooled liquids (including polymer glasses and melts) can span several orders of magnitude in what has been termed dynamic heterogeneity.[3-6]

Attempts to model the deformation of polymer glasses spans several decades, and several conflicting theories currently exist in the literature. In spite of a disagreement in the exact form,

several researchers have postulated that a control parameter associated with deformation allows segmental dynamics to speed up, allowing these glassy materials to flow. By understanding how segmental dynamics change during deformation, we may be able to determine which mechanisms associated with deformation allow flow to occur. This understanding may in turn lead to better predictions of the mechanical properties of these materials, facilitating their use in more applications. A probe reorientation method developed by Lee et al.[7] allowed for the first direct measurements of changes in segmental dynamics during deformation. The experiments of Lee et al. focused on single[7-12] and multi-step[13] constant stress (creep) deformation and recovery; a flexible deformation apparatus developed by Bending et al.[14] allowed for additional deformation protocols to be investigated, including constant strain rate deformation.[14, 15] The work described in this thesis builds upon prior work using this flexible deformation apparatus to provide critical testing of prominent theories of polymer glass deformation that exist in the literature.

This introductory chapter provides a discussion of background related to the work in this thesis. Section I describes features of glassy materials relevant to the deformation of polymer glasses. Section II discusses mechanical features of polymer glasses, as well as the concept of mechanical rejuvenation. Section III introduces modeling, simulation, and experimental work which aims to understand facets of glassy deformation from a molecular perspective and also introduces the probe reorientation technique featured in this thesis. Section IV discusses general findings from probe reorientation experiments which are consistent with other experimental, simulation, and theory studies. Section V outlines the contributions and scope of this thesis.

Section I. : What are glasses, and how are they formed?

Glasses are materials which are frequently formed by cooling from the equilibrium liquid, as shown in Figure 1. If a liquid is cooled at a fast enough rate to avoid the first-order phase transition into the crystal, the system follows the trajectory of the equilibrium liquid and below the melting temperature, becomes a metastable supercooled liquid. As the supercooled liquid continues to be cooled, the system must continue to densify at rate dictated by the imposed cooling rate in order to remain in equilibrium. Eventually, the slowed dynamics of the system prevent further densification on a time scale consistent with the cooling rate. It is at this point the system falls out of equilibrium and a glass is formed with a glass transition temperature T_g. The value of T_g is dependent on the cooling rate. For example, by using a slower cooling rate, the system is better-able to keep up the required rate of densification to remain in equilibrium; in Figure 1, this is demonstrated by the difference between glass #1, and a glass of slower cooling rate glass #2. It is important to note that Figure 1 is represented as a plot of volume as a function of temperature; however, a similar plot could be made by using entropy or enthalpy as the dependent variable.

As glasses are not equilibrium materials, their properties evolve with time toward the equilibrium supercooled liquid (referred to as aging or physical aging in this thesis) and are dependent on their thermal history. This is in contrast to an equilibrium solid or liquid, whose properties may be defined by their temperature and pressure. In Figure 1, aging is indicated by

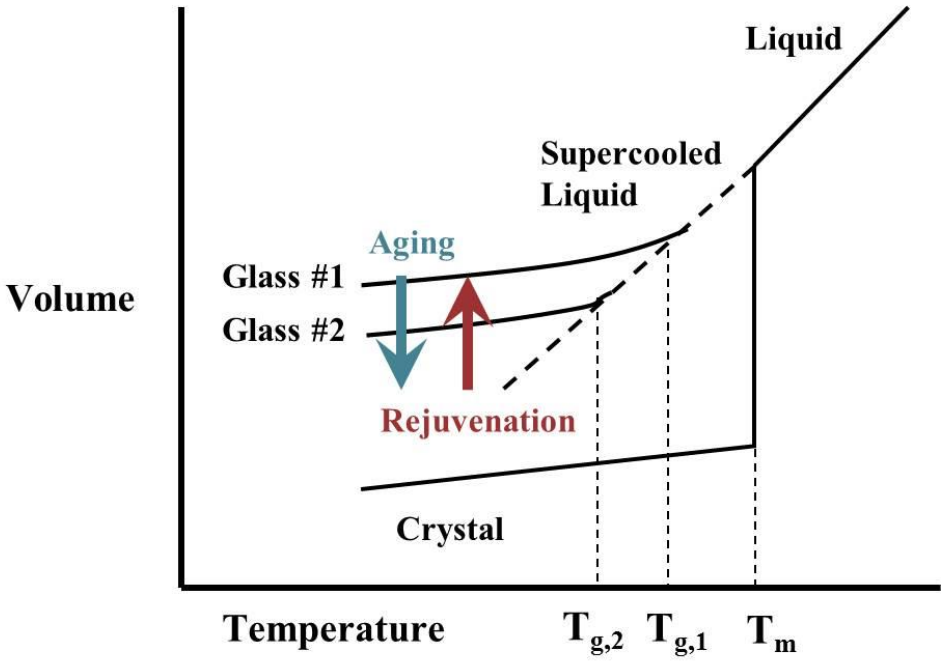

Figure 1. Volume vs. Temperature diagram illustrating the relationships between the equilibrium liquid, supercooled liquid and crystal states and glassy materials. Glasses 1 and 2 are formed at $T_{g,1}$ and $T_{g,2}$, respectively, by cooling at different rates. The effect of physical aging and mechanical rejuvenation are illustrated by colored arrows. Figure adapted from reference 6.

the downward arrow toward the equilibrium supercooled line. It should be noted that volume changes toward equilibrium are not required to show densification; in some instances, a fast increase in temperature of an equilibrium or near-equilibrium state may result in a glass which is more dense than the equilibrium supercooled liquid. This would then result in a volume expansion in order to reach equilibrium.[16]

The potential energy landscape (PEL) is a frequently-invoked framework to describe the glass transition and changes in glassy dynamics due to physical aging or deformation.[17, 18] A schematic of the PEL is shown in Figure 2. The glassy system rests in a metabasin, or local energy minimum, with a characteristic barrier size associated with α-relaxation (segmental relaxation, for a polymer glass). Metabasins may contain a collection of much smaller basins associated with β relaxation (for example, side-chain relaxations for a polymer glass such as poly(methyl methacrylate)). Changes to the glassy system as a result of aging can be described by movement further down the PEL stepwise down the jagged landscape toward a lower-energy state; movements between basins are achieved by the glass crossing the barriers of its resident basin. A glassy system's initial position on the PEL is defined by the protocol of glass formation. For example, glasses formed by a very fast cooling rate start out trapped much higher on the PEL than those formed by slow cooling, consistent with the idea that fast-cooled glasses are initially further from equilibrium than their slow-cooled counterparts. However, basins are also typically shallower at these higher positions on the PEL, translating to faster initial aging.

In addition to changes due to physical aging, the properties of glasses (and by extension their position on the PEL) may also be modified by mechanical deformation. This interplay of deformation and aging has thus far been most extensively studied in polymer glasses,[10, 11, 19-21] but colloidal glasses[22-24] and metallic glasses[25, 26] have also been investigated. In order for a

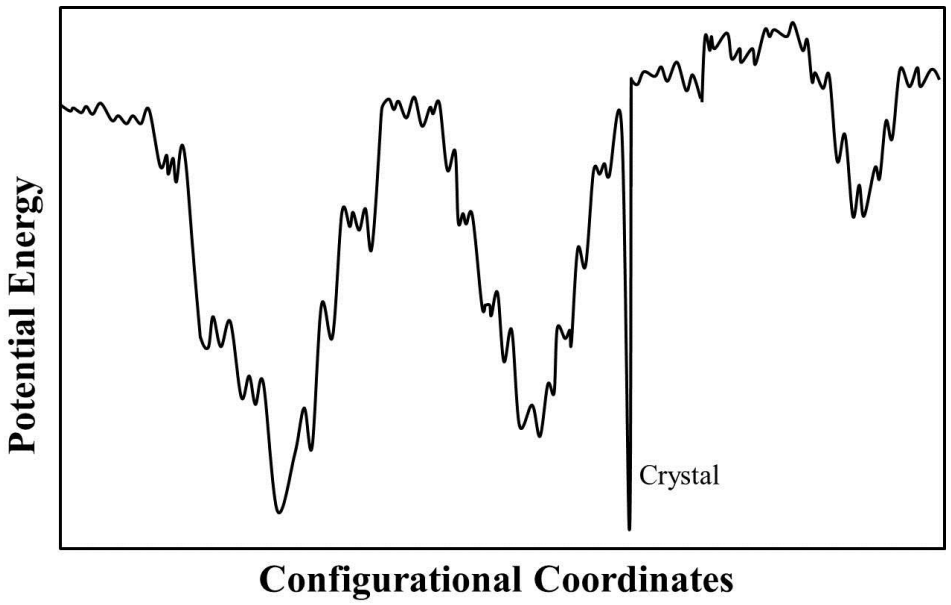

Figure 2. Schematic representation of the potential energy landscape. Adapted from reference 18.

glass to change its position on the PEL, it must overcome barriers associated with its resident metabasin. The question of how deformation alters the barriers associated with these metabasins is explored in Chapter 2 and briefly introduced in Section II of this chapter. After mechanical deformation of large magnitude, some properties of polymer glasses have been shown to be closer to those of a less-aged glass; this process has interpreted to 'erase' prior deformation of a glass and is referred to as "mechanical rejuvenation". This process is shown as an upward arrow on Figure 1. There are, however, several indications in the literature that mechanical rejuvenation does not result in exact erasure of aging.[27-29] The concept of mechanical rejuvenation is integral to the work detailed in this thesis and will be detailed in Section II of this introductory chapter.

Section II: Deformation of Polymer Glasses, Mechanical Rejuvenation, and Thermally-Activated Transitions

When a polymer glass is pulled (tensile deformation) or pushed (compressive deformation) with sufficient force and does not exhibit brittle failure, the glass may flow much like a viscous liquid. The evolution of stress with increasing strain for a poly(methyl methacrylate) glass deformed close to T_g in tension at a constant strain rate is shown in Figure 3. The variables reported in Figure 3 are engineering stress σ and engineering strain ε, which are defined in the following manner:

$$\sigma = F/A_0$$

$$\varepsilon = (L - L_0)/L_0$$

Here, F is the force, A_0 is the initial cross-sectional area of the sample, L is the instantaneous length of the sample along the axis of deformation, and L_0 is the initial sample length. At very

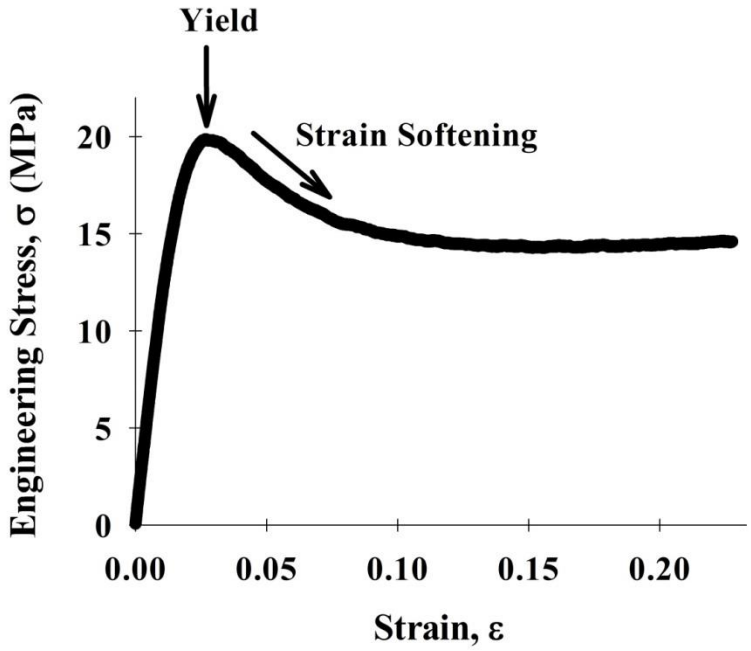

Figure 3. Engineering stress vs. strain mechanical response for a lightly cross-linked poly(methyl methacrylate) glass deformed at a constant engineering strain rate of 3.1×10^{-5} s^{-1} at T_g-22 K. Data illustrates the stress overshoot associated with yield as well as the strain softening regime. The range of strain shown in Figure 3 is representative of the strains sampled for the work presented in this thesis; the strain hardening regime is not extensively explored.

low strains (typically less than 1%), [1, 2] the relationship between stress and strain is linear and the glass behaves like an elastic solid such that the imposed strain is reversible. Outside of this small strain window, if the deformation is reversed to zero stress, a non-zero strain will remain in the glass. As strain continues to increase, stress increases nearly in a linear fashion until peaking at the yield stress σ_y. The strain at the yield stress is termed the yield strain ε_y. As strain continues to increase after yield, stress decreases in what is termed the strain softening regime. The mechanical data shown in Figure 3 represents a typical strain range explored for the experiments reported this thesis. At larger strains than shown in Figure 3, stress again continues to increase in what is termed strain hardening; this increase in stress continues until the polymer glass experiences failure, or breaks. It should be emphasized that the engineering stress and engineering strain reported in Figure 3 are calculated using the initial dimensions of the specimen to be deformed; however, the dimensions of a sample (necessarily!) change during deformation. To report a more instantaneous measure of stress and strain during deformation, true stress σ_T and true strain ε_T are frequently reported in the literature. For a specimen deforming homogeneously at constant volume, true stress and true strain may be related to engineering stress and engineering strain in the following manner:

$$\sigma_T = \sigma(1 + \varepsilon)$$

$$\varepsilon_T = \ln(1 + \varepsilon)$$

However, when some polymer glasses are deformed, they do not deform homogeneously upon yield. In this case, the increase of strain after yield is preferentially focused in (typically) one area of the deforming sample; this phenomenon is known as necking, and the area of inhomogeneous deformation is known as a neck. The samples studied in this thesis are not uniform in thickness and display necking-like behavior after yield because stress is highest at the

thinnest area of the sample. As a result, if one were to calculate the strain within the necking-like region of the sample, this *local strain* would be higher than the engineering strain calculated from the dimensions of the entire sample (*global strain*). In the experiments of this thesis, the strain in the local measurement area of the sample is monitored by taking images of lines photobleached into the measurement area; this procedure is described in detail elsewhere.[7, 14]

The mechanical properties of polymer glasses are influenced by the mechanical protocol employed as well as the thermal history of the glass. As strain rate used for the deformation increases or temperature of the deformation decreases, the yield stress increases. Additionally, as a glass is held isothermally at a temperature below T_g, its yield stress will increase with time. Because of this observation, the magnitude of the overshoot peak associated with yield is often used as a macroscopic indicator of physical aging.[30]

Prior mechanical deformation of a polymer glass may also strongly influence mechanical properties during subsequent deformations. In the context of a constant strain rate deformation, this is most clearly manifested in a decrease of the yield stress in a subsequent deformation. Figure 4 shows a poly(methyl methacrylate) glass deformed at a constant strain rate; the strain is then reversed at a constant rate to zero stress. Immediately after the stress reaches zero, a second constant strain rate deformation is performed. As can be seen in the second tensile deformation, the yield stress is greatly decreased as compared to the first constant strain rate deformation. However, if the first deformation does not reach yield before reversing the stress, a negligible decrease in the yield stress is observed, as will be illustrated further in Chapter III of this thesis. Because the magnitude of the yield peak overshoot has been traditionally associated with physical aging, this decrease in the yield peak due to prior deformation has been interpreted to reverse physical aging in the glass in what has been termed "mechanical rejuvenation".[27, 31, 32]

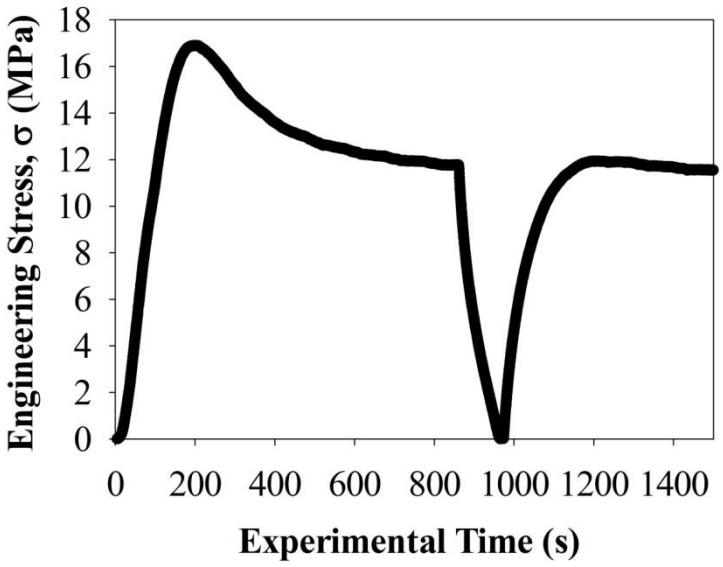

Figure 4. Engineering stress as a function of time during a reversing constant strain rate deformation, followed by a second constant strain rate deformation. In this experiment, poly(methyl methacrylate) was held at T_g- 7 K for ~4500 seconds; a constant engineering strain rate of 1.6×10^{-4} s^{-1} was employed for both tensile and retractile phases of the deformation.

An erasure of physical aging due to deformation of a polymer glass is an idea that dates back to the 1970's from the work of Struik.[19] In this pioneering work, Struik applied stress to a polymer glass at varying intervals during physical aging. After removing the stress, the creep compliance was measured; it was found that the creep compliance of a glass which had undergone prior deformation was similar to a younger glass. This observation led to the interpretation that deformation directly erased the effects of physical aging. Although the concept of mechanical rejuvenation is not new, it remains to be fully understood and is still a controversial topic in the glassy deformation community.

Since the work of Struik, several researchers have investigated the mechanical rejuvenation phenomenon to determine whether physical aging is exactly erased by deformation. McKenna and coworkers have found that for pre-yield deformations, the underlying volume recovery behavior of the glass is not permanently changed by the deformation, suggesting that rejuvenation is not active in this regime.[27, 33] Post-yield deformation was found to change the equilibrium yield stress as compared to the undeformed material; McKenna and coworkers consequently interpreted post-yield deformation to induce a polyamorphic phase transition.[27] Probe reorientation experiments of Lee and Ediger are consistent with the idea that flow-state deformation causes an apparent erasure of aging; pre-flow deformation transiently enhanced dynamics, but the underlying aging behavior was recovered at short times.[10] The question of mechanical rejuvenation has also been extensively studied by the simulation and modeling community;[21, 28, 34-38] several studies have found that deformation brings glasses to distinct states on the PEL rather than causing a literal erasure of aging. For example, molecular dynamics simulations of polystyrene glasses by Chung and Lacks found differing populations of torsional states after shear deformation as compared to those populated a temperature increase.[28]

Although many authors agree that significant deformation is associated with changes to a system on the PEL, the manner in which the glassy system can transition out of its resident metabasin during deformation is unclear. For example, Chung and Lacks[29, 39] have proposed that deformation (at least nearly) eliminates barriers between neighboring metabasins via a "fold catastrophe" mechanism; the elimination of the barrier then allows the system to roll into a neighboring metabasin. In this view, the deformation and segmental relaxation rates are strongly correlated to the extent that effects on temperature on dynamics are mostly eliminated. This is in contrast to a view where thermally-activated transitions are prominent during deformation. Chapter 2 of this thesis provides a more thorough discussion of this topic.

Section III: Attempts to understand segmental dynamics during deformation

The idea that segmental dynamics become significantly accelerated during deformation and allow polymer glasses to flow is a common theme in many theories which aim to predict deformation behavior from a fundamental physics perspective. Many models use the idea that a mechanical or physical property associated with the deformation acts as a control parameter for enhanced segmental dynamics. Modeling efforts date back to Eyring,[40] who in 1936 postulated that stress acts to lower barriers for rearrangements in a solid, allowing flow to occur; since Eyring,[40] other models[30, 41] have been developed which also feature stress as a link to enhanced dynamics during deformation. However, several models associating other parameters with enhanced dynamics have been developed, with control parameters such as the strain, [42] strain rate, [43] free volume, [44] or configurational internal energy. [45] Although these models do not agree on what aspect of deformation is associated with flow, enhanced dynamics are seen as a key feature of deformation. As a result, it may not be surprising that there have been several efforts

to monitor the degree to which segmental dynamics are accelerated during deformation, which is also called molecular mobility.

Simulation work which explores glassy deformation has provided valuable gains to an understanding of the fundamental behavior of how segmental dynamics are enhanced during deformation. Several systems have been explored, including both atomistic[46, 47] and coarse-grained models.[12, 13, 21, 28, 29, 35, 39, 48, 49] Protocols surveyed include constant stress,[12, 13, 48, 49] constant strain rate,[35, 46-48] step strain,[48] shear,[28, 29, 39] and monitoring of recovery behavior after deformation.[12, 13, 21] These simulations show significant enhancements of mobility during deformation, with results consistent to those found using the probe reorientation technique which will be featured later in this chapter and throughout this thesis.

Historically, mechanical measurements have been a common, but indirect experimental method in order to infer molecular mobility of a polymer glass undergoing deformation. Many of these methods involve investigating the stress relaxation behavior immediately after a mechanical perturbation. When a viscoelastic material such as a polymer glass is significantly deformed and then held at a fixed strain, stress begins to decrease upon halting the deformation; this feature is known as stress relaxation. Several relaxation processes in glassy materials can be described by a Kohlrausch-Williams-Watts (KWW) stretched exponential function:

$$\varphi(t) = \varphi_0 e^{(t/\tau)^{\beta}}$$

Where φ is the time-dependent measured property associated with relaxation with initial value φ_0, τ is a characteristic relaxation time, and β is the stretching exponent with value $0 \leq \beta \leq 1$. Physically, β can be related to the degree of dynamic heterogeneity in the glass. Some authors have directly fitted the stress relaxation response of a nonlinear deformation to a stretched exponential function and find enhanced dynamics during deformation,[50] although it is argued by

others that the nonlinear deformation makes this approach invalid.[51, 52] Other workers monitor stress relaxation after a nonlinear deformation but do not use the KWW form to extract τ. For example, Caruthers,[51, 53, 54] Wang,[55] and their coworkers have investigated the initial rate of stress relaxation or use of a time shift factor to infer molecular mobility during a prior constant strain rate deformation. Both sets of authors find that in the post-yield regime, the mechanically-derived mobility is correlated with strain rate.

Other authors have also fitted stress relaxation behavior to a KWW form to infer segmental relaxation, but instead look at relaxation associated with a smaller deformation (~0.1-0.2% strain) superimposed onto a much larger deformation, also called a "tickle" experiment.[52, 56] The key assumption in these experiments is that the magnitude of the smaller deformation is within the linear response regime of the polymer and should be an accurate reporter for the underlying dynamics without affecting the larger deformation. Yee et al.[52] investigated molecular mobility in this manner by imposing "tickle" step strains at varying temperatures and also during much larger step strains on polycarbonate at T_g-115 K. During the larger step strain experiments, mobility increased by more than 10 orders of magnitude before yield; the post-yield regime was not investigated. The results of Yee et al.[52] were also consistent with segmental dynamics becoming more homogeneous with increasing strain, with stretching parameters increasing as a function of strain and approaching those observed in the absence of nonlinear deformation at T_g. This is in contrast to results which fit a nonlinear relaxation response to a KWW form, where the stretching parameter does not change during deformation.[50, 51] Martinez-Vega et al.[56] used torsional "microcreep" tickle experiments to investigate physical aging, creep, and post-deformation recovery of PMMA. These microcreep experiments found results consistent with enhanced dynamics when the larger stress was imposed on the polymer glass

sample; during recovery, dynamics recovered the generic aging behavior after a transient period of enhanced dynamics. Unlike the experiments of Yee et al.,[52] the experiments of Martinez-Vega et al.[56] displayed only slight effects in the stretching exponent, indicating that the spectral width of relaxation times did not significantly change during deformation.

Although mobilities extracted from mechanical techniques demonstrate results consistent with enhanced segmental dynamics during deformation, these techniques are indirect. They rely on a macroscopic mechanical measurement to be an accurate reporter for molecular-level rearrangement, which may involve incorrect assumptions.[57] Other researchers have instead aimed to look at other techniques to get closer to a molecular-level description of glassy deformation dynamics. Other indirect measurements of enhanced dynamics include experiments of Zhou et al.,[58] which found that during deformation, diffusion of a plasticizer in a poly(ether imide) glass was consistent with diffusion at T_g. Additionally, Loo et al.[59] used NMR to investigate molecular mobility of the amorphous regions within nylon 6 and found results consistent with enhanced segmental dynamics during deformation. The first direct measurements of molecular mobility during deformation were from a probe reorientation technique,[7] which will be described shortly. Since the development of the probe reorientation technique, dielectric spectroscopy[60] has been used to directly monitor segmental dynamics during deformation; however, this technique has not yet been able to quantify the factor by which segmental dynamics are enhanced during deformation.

A method developed by Lee et al.[7, 8] allowed, for the first time, direct measurements of molecular mobility of a polymer glass undergoing active deformation. This method involves monitoring the reorientation of an ensemble of fluorescent reporter probes which are dispersed at a concentration of ~10^{-6} M in the polymer matrix. During a single measurement, anisotropy

within the fluorescing probes is created by photobleaching with a linearly-polarized laser beam; molecules whose transition dipoles are aligned with the polarization of the light are preferentially photobleached. After this photobleaching step, fluorescence of the unbleached probes is induced by irradiating with weak, circularly-polarized light; fluorescence intensities perpendicular and parallel to the original photobleaching polarization are monitored, from which anisotropy can be calculated:

$$r(t) = \frac{\Delta I_{II}(t) - \Delta I_{\perp}(t)}{\Delta I_{II}(t) + 2\Delta I_{\perp}(t)}$$

Here, $\Delta I_{II}(t)$ and $\Delta I_{\perp}(t)$ are the time-dependent relative intensities parallel and perpendicular to the photobleaching polarization; a nearby unbleached area is also monitored to correct for any dye alignment effects or minor differences between the orthogonal intensities in the absence of photobleaching or deformation.[7] The decay of the induced anisotropy can be described by the KWW function:

$$r(t) = r(0) \cdot e^{-(t/\tau)^{\beta}}$$

Here, r(t) and r(0) are the time-dependent and initial anisotropy values, respectively. As discussed earlier, the stretching exponent β indicates the nonexponentiality of the decay and can be physically related to how heterogeneous dynamics are during deformation. The time τ is the time for anisotropy to decay by a factor of e and will be the dynamical reporter for much of the work described in this thesis. In addition to the time reporter τ, τ_c has also been used as a time reporter in probe reorientation studies; τ_c is obtained by integrating the correlation function $C_f = r(t)/r(0)$.[7-11, 13]

It is important to note that although τ is not equivalent to the segmental relaxation time τ_α, there is strong evidence that τ is an accurate reporter for changes in segmental dynamics (also termed molecular mobility) during deformation. The reorientation of several probe molecules in

poly(methyl methacrylate) and other polymer systems demonstrates that above the glass transition temperature and in the absence of deformation, probe reorientation displays the same temperature dependence as τ_α, as determined via dielectric spectroscopy.[7, 61] Additionally, changes in segmental dynamics during deformation as determined by probe reorientation are consistent with simulation[12, 13, 35] and theoretical work,[38] which does not employ probes. Section IV includes a more thorough comparison between the results of the probe reorientation technique and other work.

For much of the work of Lee et al.[8-11, 13] and for all of the work detailed in this thesis, the polymeric system of choice is PMMA cross-linked at 1.5 weight percent with EGDMA (ethylene glycol dimethacrylate), and the reporting probe is DPPC (N,N'-Dipentyl-3,4,9,10-perylenedicarboximide). The chemical structures of these three molecules are provided in Figure 5. As compared to the segmental relaxation time τ_α, recent experiments by Bending and Ediger suggest that τ obtained by the DPPC probe in PMMA is roughly 2-3 times slower.[62] Results obtained using the probe reorientation method are anticipated to be generic to other polymer glass systems; reorientation of DPPC probes in polystyrene glasses undergoing deformation show quantitatively similar trends in τ as compared to PMMA when data at the same temperature relative to T_g is compared.[62]

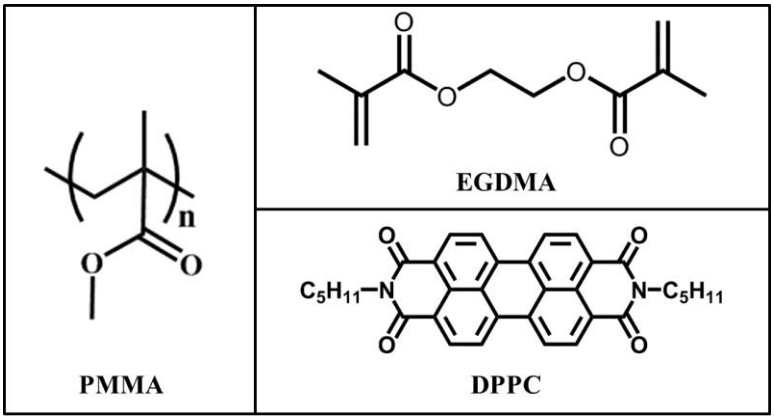

Figure 5. Chemical structures of the polymer, cross-linker, and probe used in this thesis. Full names for each abbreviation are poly(methyl methacrylate) (PMMA), ethylene glycol dimethacrylate (EGDMA), and N,N'-Dipentyl-3,4,9,10-perylenedicarboximide (DPPC).

Section IV: What happens to segmental dynamics during deformation?

Although points of disagreement remain in the literature, several features which have been found in the probe reorientation measurements qualitatively agree with simulation and theory work. These features will be outlined in this section:

During deformation, segmental dynamics can speed up by several orders of magnitude

Probe reorientation experiments have found that during flow, segmental relaxation can be orders of magnitude faster, as compared to a glass which had not undergone deformation. This was first confirmed by Lee et al.,[7-9] who found that segmental dynamics were up to 1000 times faster during the flow portion of constant stress experiments than in the absence of deformation. Probe reorientation experiments which investigated a constant strain rate deformation protocol[14] also found enhancement of segmental dynamics by more than a factor of 100 during the post-yield deformation period as compared to the undeformed glass.

Simulations have also found evidence of segmental dynamics which are greatly enhanced during deformation. Simulation work which mimicked the constant stress deformation protocol work of Lee et al. found qualitatively similar behavior of τ during deformation as was found in the experiments.[12, 13, 49] Constant strain rate simulations of Riggleman et al.[35] found that the segmental relaxation time changes by several orders of magnitude during deformation, similar to what was shown experimentally using probe reorientation.[14] Although a variable equivalent to τ was not calculated, other simulation work[21, 46-48] is consistent with the idea that segmental dynamics are significantly enhanced during deformation.

Theoretical work in the literature also demonstrates strong evidence that segmental dynamics are much faster during deformation. The Nonlinear Langevin Equation theory of Chen

and Schweizer calculates that segmental dynamics during constant stress[20] and constant strain rate[38] deformation can be orders of magnitude faster than in the absence of deformation. A recent model of Medvedev and Caruthers[45] calculates the full distribution of segmental relaxation times during different stages of constant strain rate deformation and also demonstrates that the average segmental relaxation time changes by orders of magnitude during deformation.

During flow, the instantaneous segmental dynamics and strain rate are correlated

During the flow stages of creep, Lee et al. found a linear correlation between log(τ) and log(strain rate) during the deformation of lightly cross-linked PMMA using the probe reorientation technique.[8] Furthermore, this relationship appears to be a general feature of flow-state deformation rather than a feature that is particular to a certain deformation protocol. Bending et al.[14] found that post-yield τ from a constant strain rate experiment and flow-state creep values of τ show a single relationship between strain rate for an identical material and thermal protocol. This relationship is demonstrated in Figure 6, which shows flow-state values of τ during constant stress deformation (black symbols) and average post-yield values of τ during a constant strain rate deformation (colored symbols). An interesting feature of the constant stress deformation is that during creep, the strain rate first undergoes a rapid increase during flow, and then decreases as strain hardening occurs. Figure 6 encompasses data as the strain rate increases to a maximum, and also in the strain hardening regime where strain rate decreases. The relationship between τ and strain rate is identical for both regimes.

The data in Figure 6 is also consistent with the idea that large-magnitude deformation erases prior physical aging in a glass. Figure 6 also includes post-yield data from glasses which had been held below T_g for different periods of time before the deformation was performed. For

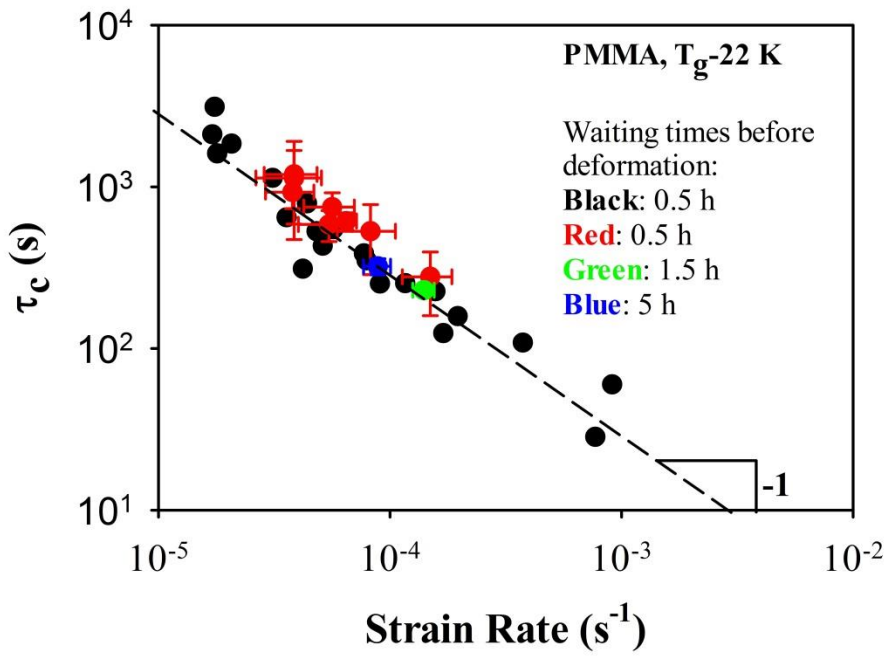

Figure 6. Values of τ_c during the flow phase of constant stress (black data points) or average post-yield values of τ_c for constant strain rate deformation (colored data points) of a lightly cross-linked PMMA glass at T_g-22 K. Glasses are formed by cooling at 1 K/min to the testing temperature and holding isothermally for a set waiting time before deformation. Black and red data points represent a 0.5 h waiting time; green and blue data points represent a 1.5 h and 5 h waiting period before deformation, respectively. Dashed line shows slope of -1 and is a guide to the eye.

these tests with additional waiting time before deformation, τ immediately before deformation is at a higher value because more physical aging occurs before deformation begins; however, the figure demonstrates that during flow τ is independent of this aging time.

This correlation between segmental dynamics and strain rate is consistent with simulation, theoretical, and other experimental studies. Similarly to the probe reorientation studies, Riggleman et al. found a similar relationship between flow-state segmental dynamics and strain rate for both constant stress[13, 49] and constant strain rate[35] deformation. This relationship was also found in the NLE theory of Chen and Schweizer.[38] Dielectric experiments which were performed during deformation of a polymer glass also yielded findings consistent with a correlation between strain rate and segmental dynamics.[60] Additionally, purely mechanical experiments showed correlation between mobility and strain rate during flow.[51, 53-56]

During deformation, dynamics can become more spatially homogeneous

Supercooled liquids and glasses are known to display spatially heterogeneous dynamics;[3-6] within these materials, regions which are spaced nanometers apart may have relaxation rates that are different by several orders of magnitude. Deformation acts to speed up segmental dynamics; however, it is nontrivial whether deformation equally affects segments of all relaxation rates. For example, if one were to monitor the spectrum of relaxation times before and during deformation, would deformation act to shift the spectrum to shorter times without changing its shape, or would the shape of the distribution change as a result of deformation?

In addition to the evolution of segmental relaxation times during deformation, probe reorientation also provides a window into changes in the distribution of relaxation times through the KWW stretching parameter β. In the absence of deformation, the value of β is roughly 0.31

for DPPC probes in a cross-linked PMMA matrix.[14] An increase in β is consistent with a decrease in the spectral width of relaxation times, while a decrease in β is associated with a broadening of the relaxation spectrum.

Probe reorientation experiments have found that the stretching parameter β can increase during deformation, which is consistent with dynamics becoming more spatially homogeneous. This observation was experimentally first reported by the work of Lee et al.[8] Similar to changes in τ during deformation, β was found to have a correlation with the strain rate during deformation, with higher values of β observed with increasing strain rates. Physically, this indicates that during a constant stress deformation, segmental dynamics become more homogeneous during flow, but then during the strain hardening regime this degree of homogeneity decreases.

A model of Medvedev and Caruthers[45] which predicts mechanical properties of polymer glasses incorporates a spectrum of relaxation times and has provided a physical framework for understanding the increase in β observed in probe reorientation experiments. Caruthers and coworkers provide calculations of the spectrum of relaxation times at different points during a constant stress[9] and constant strain rate[45] deformation. These calculations find that the width of this spectrum significantly decreases during deformation, consistent with an increased value of β in the probe reorientation experiment. Furthermore, as the model of Medvedev and Caruthers calculates the shape of the spectrum at different points during deformation, the model can provide more specific information on what population of segments is most affected by deformation. As can be seen in calculations from the model, deformation acts to narrow the distribution of segmental relaxation times by preferentially enhancing dynamics of the slowest-relaxing segments. Dynamics of the fastest-relaxing segments are not typically altered by

deformation, and thus the "slow side" of the distribution is effectively cut off during deformation.

In addition to the probe reorientation experiments, simulations[12, 48, 49] and a dielectric spectroscopy study[60] have also demonstrated that dynamics become more spatially homogeneous during deformation. Additionally, "tickle" experiments of Yee et al.[52] have found evidence of more homogeneous dynamics during deformation.

No one mechanical parameter is correlated to dynamics during all phases of deformation

Although probe reorientation experiments demonstrate strong correlation between log(τ) and log(strain rate) during flow, the same correlation is not observed when comparing data in the pre-flow regime. However, as reported by Lee et al.,[8, 9] pre-flow data is consistent with the Eyring model[40] $\tau \propto \sigma/\sinh\left(\frac{\sigma \cdot V}{2 \cdot k_b T}\right)$, where V is the activation volume and only free fitting parameter; deviations from the fit are clearly observed upon the onset of flow. As a correlation with strain rate, rather than stress, is observed in the flow regime, it is apparent that there is no one mechanical control parameter that acts during all phases of deformation. Simulations,[12, 13, 21, 48, 49] theoretical studies,[20, 38, 53] and mechanical experiments[51, 53, 54] also support the idea that segmental dynamics are not controlled by any one parameter during deformation.

Section V. Contributions of this thesis

At the time I started my Ph.D. work, the Ediger group had developed the probe reorientation technique for use during the deformation of polymer glasses and characterized changes in segmental dynamics of PMMA during constant stress deformation and recovery. However, the mechanism (at the time) to apply stress was to hang weight off of the polymer glass sample using a pulley system; in this respect we were limited in our ability to critically test

models which employ different deformation mechanisms. To broaden the range of experiments available to us, former graduate student Ben Bending designed a programmable deformation instrument which would provide optical access to our samples. I worked closely with Ben to build and optimize this new instrument and additionally performed several checks to ensure that we could reproduce previously-published experiments with this new deformation instrument. For example, some of my early tasks as a graduate student included determining how to best grip samples to minimize compliance and slip, developing or updating LabVIEW programming to allow for constant stress and constant strain rate deformations, and troubleshooting noise observed in our mechanical data. Other projects that Ben and I worked together on during my early years as a graduate student included (unsuccessful) attempts to perform probe reorientation experiments on polycarbonate, as well as preliminary work on poly(lactic acid) with visiting scholar Professor Shogo Nobukawa (Japan Advanced Institute of Science and Technology). This optimization process and other work will not be described in this thesis, but is described in detail elsewhere.[14, 62]

After this new deformation instrument was optimized, I performed work with Ben Bending, Josh Ricci, and M.D. Ediger to characterize the evolution of segmental dynamics in a polymer glass undergoing constant strain rate deformation. This study described the new deformation apparatus and found that during constant strain rate deformation, segmental dynamics speed up until yield, after which dynamics remain relatively constant through the strain softening regime. Additionally, it was found that post-yield τ_c values from constant strain rate experiments and flow-state τ_c from constant stress experiments showed an identical relationship with the instantaneous local strain rate. Samples which were aged for differing periods of time before deformation also showed this identical relationship between post-yield $\log(\tau_c)$ and

log(strain rate), indicating that prior thermal history is erased by aging. This study was published in a paper in *Macromolecules*,[14] on which I am second author.

Chapter 2 of this thesis builds upon the optimization of the deformation instrument and established behavior of segmental mobility during constant strain rate deformation to investigate the effect of temperature on post-yield deformation. In the absence of deformation, probe reorientation experiments indicate that for glasses with an identical cooling rate and isothermal waiting period, the relationship between temperature and segmental dynamics is roughly a 10 K increase per 10-fold enhancement of dynamics (decade).[8] Because deformation can also act to enhance segmental dynamics, there is no reason why this relationship must hold during deformation. Additionally, it was unclear in the literature what role thermally-activated transitions play during deformation. Simulations comparing the athermal quasistatic limit of deformation to finite-temperature molecular dynamics simulations were interpreted to indicate that deformation acts to deplete barriers for rearrangements and that thermally-activated transitions are not significant during flow.[29, 39] However, modeling work indicates that temperature has some impact on flow-state dynamics down to at least T_g-60 K.[38] Probe reorientation experiments were performed during constant strain rate deformation of lightly cross-linked PMMA glasses. It was found that temperature not only has a significant effect on flow-state dynamics, but these effects are several times stronger than predicted by the most directly applicable model in the literature.[38] Additionally, barriers crossed during deformation were estimated at ~39 kTg and were only reduced by 10-15% from the undeformed material. These results are discussed in light of simulation and theoretical work in the literature. Chapter 2 has been previously published in an article in *Macromolecules*,[15] on which I am the first author; the coauthors are Ben Bending, Josh Ricci, and M.D. Ediger.

Chapter 3 of this thesis describes experiments which test mechanisms of a prominent polymer glass deformation theory by monitoring segmental dynamics before and after a reversing constant strain rate deformation, using the probe reorientation technique. The Nonlinear Langevin Equation (NLE) theory of Chen and Schweizer[20, 38] has previously provided strong qualitative agreement with observed changes in segmental dynamics during constant stress and constant strain rate deformation. The theory incorporates two mechanisms which allow segmental dynamics to become enhanced during deformation. In the first mechanism, which we term the landscape tilting mechanism, stress lowers barriers for rearrangements via a molecular-level Eyring mechanism, but this mechanism is reversible with reversing stress. The second mechanism is the rejuvenation mechanism, which is active at sufficiently high strains and acts by pulling the system to a higher place on the PEL where barriers are lower. The rejuvenation mechanism is irreversible, unlike the landscape tilting mechanism. We separate contributions of the two mechanisms by performing a series of constant strain rate deformations to varying strain values, which are then reversed at the same constant rate to zero stress. Changes in segmental dynamics are monitored before and after the reversing deformations via probe reorientation. We interpret that per the NLE theory, any remaining enhancement of dynamics after these reversing deformations are solely due to the rejuvenation mechanism; the protocol we use allows us to remove any effects of landscape tilting as there is no stress on the sample. We quantify the activity of the rejuvenation mechanism as a function of strain by investigating the departure of τ from the quiescent aging trajectory after these reversing deformations. Additionally, we perform a series of purely mechanical experiments and quantify the rejuvenation mechanism by the reduction of the yield stress in a subsequent constant strain rate deformation. We compare quantified rejuvenation vs. strain for the probe reorientation and

mechanical experiments with the amplitude of local density fluctuations in the NLE theory (the marker for rejuvenation) and find broad qualitative agreement. However, for pre-yield strains, probe reorientation demonstrates significantly higher levels of rejuvenation than observed in the mechanical experiment or theory. These results are discussed in the context of the theory and recent molecular dynamics simulations which show similar trends to the probe reorientation results. Chapter 3 will be submitted for publication at a later time.

Chapter 4 describes broad conclusions from the thesis as well as outlines future experiments which may be performed.

References

1. Papakonstantopoulos, G. J.; Riggleman, R. A.; Barrat, J.-L.; de Pablo, J. J. *Physical Review E* **2008,** 77, (4), 041502.
2. Yannas, I. V. *Journal of Polymer Science: Macromolecular Reviews* **1974,** 9, (1), 163-190.
3. Ediger, M. D. *Annual Review of Physical Chemistry* **2000,** 51, 99-128.
4. Thurau, C. T.; Ediger, M. D. *Journal of Polymer Science Part B-Polymer Physics* **2002,** 40, (21), 2463-2472.
5. Richert, R. *Journal of Physics-Condensed Matter* **2002,** 14, (23), R703-R738.
6. Ediger, M. D.; Angell, C. A.; Nagel, S. R. *Journal of Physical Chemistry* **1996,** 100, (31), 13200-13212.
7. Lee, H. N.; Paeng, K.; Swallen, S. F.; Ediger, M. D. *Journal of Chemical Physics* **2008,** 128, (13), 134902.
8. Lee, H. N.; Paeng, K.; Swallen, S. F.; Ediger, M. D. *Science* **2009,** 323, (5911), 231-234.
9. Lee, H. N.; Paeng, K.; Swallen, S. F.; Ediger, M. D.; Stamm, R. A.; Medvedev, G. A.; Caruthers, J. M. *Journal of Polymer Science Part B: Polymer Physics* **2009,** 47, (17), 1713-1727.
10. Lee, H. N.; Ediger, M. D. *Macromolecules* **2010,** 43, (13), 5863-5873.
11. Lee, H. N.; Ediger, M. D. *Journal of Chemical Physics* **2010,** 133, (1), 014901.
12. Riggleman, R. A.; Lee, H. N.; Ediger, M. D.; de Pablo, J. J. *Soft Matter* **2010,** 6, (2), 287-291.
13. Lee, H. N.; Riggleman, R. A.; de Pablo, J. J.; Ediger, M. D. *Macromolecules* **2009,** 42, (12), 4328-4336.

14. Bending, B.; Christison, K.; Ricci, J.; Ediger, M. D. *Macromolecules* **2014,** 47, (2), 800-806.

15. Hebert, K.; Bending, B.; Ricci, J.; Ediger, M. D. *Macromolecules* **2015,** 48, (18), 6736-6744.

16. McKenna, G. B.; Vangel, M. G.; Rukhin, A. L.; Leigh, S. D.; Lotz, B.; Straupe, C. *Polymer* **1999,** 40, (18), 5183-5205.

17. Stillinger, F. H. *Science* **1995,** 267, (5206), 1935.

18. Debenedetti, P. G.; Stillinger, F. H. *Nature* **2001,** 410, 259-267.

19. Struik, L. C. E. *Polymer* **1997,** 38, (16), 4053-4057.

20. Chen, K.; Schweizer, K. S. *Physical Review E* **2010,** 82, (4), 041804.

21. Smessaert, A.; Rottler, J. *Macromolecules* **2012,** 45, (6), 2928-2935.

22. Besseling, R.; Weeks, E.; Schofield, A.; Poon, W. *Physical Review Letters* **2007,** 99, (2).

23. Schall, P.; Weitz, D. A.; Spaepen, F. *Science* **2007,** 318, (5858), 1895-1899.

24. Hunter, G. L.; Weeks, E. R. *Reports on Progress in Physics* **2012,** 75, (6), 066501.

25. Dmowski, W.; Yokoyama, Y.; Chuang, A.; Ren, Y.; Umemoto, M.; Tsuchiya, K.; Inoue, A.; Egami, T. *Acta Materialia* **2010,** 58, (2), 429-438.

26. Cheng, Y. Q.; Ma, E. *Progress in Materials Science* **2011,** 56, (4), 379-473.

27. McKenna, G. B. *Journal of Physics: Condensed Matter* **2003,** 15, (11), S737.

28. Chung, Y. G.; Lacks, D. J. *Journal of Chemical Physics* **2012,** 136, (12), 124907.

29. Chung, Y. G.; Lacks, D. J. *Macromolecules* **2012,** 45, (10), 4416-4421.

30. Klompen, E. T. J.; Engels, T. A. P.; Govaert, L. E.; Meijer, H. E. H. *Macromolecules* **2005,** 38, (16), 6997-7008.

31. Govaert, L. E.; van Melick, H. G. H.; Meijer, H. E. H. *Polymer* **2001,** 42, (3), 1271-1274.

32. Hasan, O. A.; Boyce, M. C.; Li, X. S.; Berko, S. *Journal of Polymer Science Part B: Polymer Physics* **1993,** 31, (2), 185-197.

33. McKenna, G. B.; Santore, M. M.; Lee, A.; Duran, R. S. *Journal of Non-Crystalline Solids* **1991,** 131–133, Part 1, (0), 497-504.

34. Warren, M.; Rottler, J. *Physical Review E* **2008,** 78, (4), 041502.

35. Riggleman, R. A.; Toepperwein, G. N.; Papakonstantopoulos, G. J.; de Pablo, J. J. *Macromolecules* **2009,** 42, (10), 3632-3640.

36. Utz, M.; Debenedetti, P. G.; Stillinger, F. H. *Physical Review Letters* **2000,** 84, (7), 1471-1474.

37. Lacks, D. J.; Osborne, M. J. *Physical Review Letters* **2004,** 93, (25), 255501.

38. Chen, K.; Schweizer, K. S. *Macromolecules* **2011,** 44, (10), 3988-4000.

39. Chung, Y. G.; Lacks, D. J. *Journal of Polymer Science Part B: Polymer Physics* **2012,** 50, (24), 1733-1739.

40. Eyring, H. *Journal of Chemical Physics* **1936,** 4, (4), 283-291.

41. De Focatiis, D. S. A.; Embery, J.; Buckley, C. P. *Journal of Polymer Science Part B: Polymer Physics* **2010,** 48, (13), 1449-1463.

42. Schapery, R. A. *International Journal of Solids and Structures* **1966,** 2, (3), 407-425.

43. Fielding, S. M.; Larson, R. G.; Cates, M. E. *Physical Review Letters* **2012,** 108, (4), 048301.

44. Knauss, W. G.; Emri, I. *Polymer Engineering & Science* **1987,** 27, (1), 86-100.

45. Medvedev, G. A.; Caruthers, J. M. *Journal of Rheology* **2013,** 57, (3), 949-1002.

46. Lyulin, A. V.; Balabaev, N. K.; Mazo, M. A.; Michels, M. A. J. *Macromolecules* **2004,** 37, (23), 8785-8793.

47. Lyulin, A. V.; Michels, M. A. J. *Physical Review Letters* **2007,** 99, (8), 085504.

48. Warren, M.; Rottler, J. *Journal of Chemical Physics* **2010,** 133, (16), 164513.

49. Riggleman, R. A.; Schweizer, K. S.; de Pablo, J. J. *Macromolecules* **2008,** 41, (13), 4969-4977.

50. Legrand, D. G.; Olszewski, W. V.; Bendler, J. T. *Journal of Polymer Science Part B: Polymer Physics* **1987,** 25, (5), 1149-1152.

51. Lee, E. W.; Medvedev, G. A.; Caruthers, J. M. *Journal of Polymer Science Part B: Polymer Physics* **2010,** 48, (22), 2399-2401.

52. Yee, A. F.; Bankert, R. J.; Ngai, K. L.; Rendell, R. W. *Journal of Polymer Science Part B: Polymer Physics* **1988,** 26, (12), 2463-2483.

53. Kim, J. W.; Medvedev, G. A.; Caruthers, J. M. *Polymer* **2013,** 54, (15), 3949-3960.

54. Medvedev, G. A.; Kim, J. W.; Caruthers, J. M. *Polymer* **2013,** 54, (24), 6599-6607.

55. Liu, J.; Lin, P.; Li, X.; Wang, S.-Q. *Polymer* **2015,** 81, 129-139.

56. Martinez-Vega, J. J.; Trumel, H.; Gacougnolle, J. L. *Polymer* **2002,** 43, (18), 4979-4987.

57. McKenna, G. B.; Zapas, L. J. *Polymer Engineering & Science* **1986,** 26, (11), 725-729.

58. Zhou, Q. Y.; Argon, A. S.; Cohen, R. E. *Polymer* **2001,** 42, (2), 613-621.

59. Loo, L. S.; Cohen, R. E.; Gleason, K. K. *Science* **2000,** 288, (5463), 116-119.

60. Kalfus, J.; Detwiler, A.; Lesser, A. J. *Macromolecules* **2012,** 45, (11), 4839-4847.

61. Inoue, T.; Cicerone, M. T.; Ediger, M. D. *Macromolecules* **1995,** 28, (9), 3425-3433.

62. Bending, B. Ph.D. Thesis. University of Wisconsin-Madison, 2014.

Chapter 2

Effect of Temperature on Post-yield Segmental Dynamics of Poly(methyl methacrylate) Glasses: Thermally Activated Transitions are Important

Kelly Hebert, Benjamin Bending, Josh Ricci, and M.D. Ediger

Macromolecules, 2015, Volume 48, 6736-6744. Copyright 2015 American Chemical Society

DOI: 10.1021/acs.macromol.5b01486

http://pubs.acs.org/articlesonrequest/AOR-7rRWHJhqQhAyqaMjE5NQ

Abstract

Optical probe reorientation measurements were utilized to investigate the effect of temperature on the segmental dynamics of a glassy polymer during deformation. Constant strain rate deformations were performed on poly(methyl methacrylate) glasses at temperatures from T_g-27 K to T_g-11 K and engineering strain rates from 3×10^{-6} s^{-1} to 3×10^{-5} s^{-1}. Deformation enhances segmental mobility by up to a factor of 100 in these experiments. In the post-yield flow state at a given strain rate, the effect of temperature on dynamics is reduced, relative to the undeformed polymer glass. However, we still observe a significant effect of temperature on segmental dynamics during flow, with calculated free energy barriers of ~39 kT_g. The Kohlrausch-Williams-Watts parameter β_{KWW}, a measure of spatially heterogeneous dynamics, is observed to increase in the post-yield regime with increasing strain rate and decreasing temperature, indicating more homogenous dynamics. β_{KWW} is correlated with the enhancement of segmental dynamics relative to the undeformed polymer, independent of temperature.

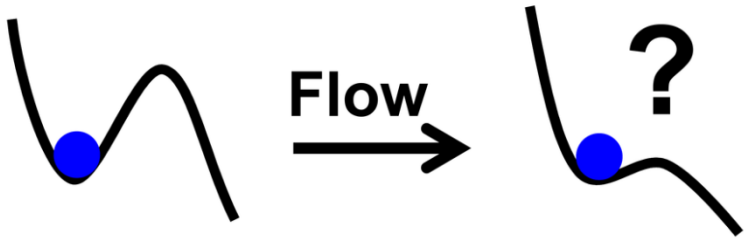

Table of Contents Figure

Introduction

Polymer glasses are crucial to an increasing number of applications because of their processability, low cost, and desirable mechanical properties. However, a fundamental understanding of the deformation behavior of these materials remains elusive. The complex physics of polymer glasses, even in the absence of deformation, makes this a challenging problem. In addition to the presence of spatially heterogeneous dynamics[1-4] and structural relaxation (physical aging),[5-8] polymer glass deformation is generally highly nonlinear.[5, 9-11]

Efforts to understand polymer glass deformation span several decades, and some of the earliest ideas about the plastic deformation of a solid material can be traced back to a 1936 work of Eyring. In this framework, stress acts to lower barriers for molecular rearrangements.[12] Based on Eyring's approach, it has been postulated that during deformation of a polymer glass, molecular rearrangements occur at an enhanced rate, allowing flow to occur. However, it is unclear to what extent the details of the Eyring model are correct. Starting in the 1960s, many models of polymer glass deformation have been developed that incorporate the idea of enhanced dynamics facilitating flow. Some of these models follow Eyring and assume that molecular mobility is directly tied to stress,[13, 14] while others take the control variable to be strain,[15] strain rate,[16] configurational internal energy,[17] or free volume.[18, 19] Several experimental studies and computer simulations have confirmed the presence of enhanced molecular mobility during deformation, deepening what is known about polymer glass deformation and allowing for critical tests of these models. Experimentalists have used mechanical tests,[11, 20-22] NMR,[23] and diffusion[24] to infer segmental mobility during deformation. Direct measurements of enhanced segmental mobility during deformation have been obtained using dielectric spectroscopy[25] and probe reorientation.[26-33] Simulators have found enhanced dynamics during constant strain rate[34-

[37] as well as constant stress[29, 32, 35] mechanical experiments. Although these approaches have advanced our understanding of polymer glass deformation, some critical features remain to be clarified.

One open question is how deformation affects the relationship between temperature and segmental dynamics in a polymer glass. Because both thermal energy and deformation can act to accelerate segmental dynamics, separating the contributions of these two factors is challenging and remains a point of disagreement in the literature. Some researchers have suggested that segmental dynamics can be dictated by the deformation to such an extent that any effect of temperature is largely eliminated.[36, 37] This view, which can be explained through the idea of the potential energy landscape, is consistent with the system being trapped in a particular basin on the landscape as long as a barrier exists between this resident basin and neighboring basins; as deformation proceeds, barriers between neighboring basins evolve in size, and the system escapes the resident basin only when a barrier is completely eliminated by the deformation. An important question is whether this view, which must be correct at sufficiently low temperature, is relevant for polymer glasses under typical laboratory conditions.

An alternate perspective is that temperature has a strong influence on segmental dynamics during deformation and this is often envisioned as thermally-activated transitions between basins on the potential energy landscape. For example, Schall, Weitz, and Spaepen[38] tracked individual particles of a colloidal glass during shear and found particle movement which was consistent with thermally-activated rearrangements during deformation. Furthermore, Schall et al. calculated substantial activation energies (~18 kT) during shear, and that these barriers had only been reduced by ~1 kT during deformation. Chen and Schweizer provide calculations from their theory indicating that for a poly(methyl methacrylate) (PMMA) glass,

thermally-activated transitions are relevant down to at least T_g-60 K during post-yield constant strain rate deformation.[39]

In order to understand the complex dependence of segmental dynamics on temperature and deformation, we have performed tensile constant strain rate deformations on lightly cross-linked PMMA glasses at multiple temperatures near T_g. Engineering strain rates from 3.1×10^{-6} s^{-1} to 3.1×10^{-5} s^{-1} were used and tests were performed at four temperatures ranging from T_g-27 K to T_g-11 K**.** Segmental dynamics were monitored during active deformation using a previously-reported probe reorientation technique.[26] Average segmental relaxation times and the Kohlrausch-Williams-Watts (KWW) β parameter, β_{KWW}, in the post-yield regime were investigated at different strain rates and temperatures to determine how these quantities are influenced by temperature.

We find that, at a fixed strain rate, the temperature dependence of segmental dynamics is significantly reduced during post-yield deformation, relative to the undeformed glass. An analysis of the data indicates that molecular rearrangements during flow take place through thermally-activated transitions involving substantial free energy barriers; we estimate the relevant free energies to be 39 ± 3 kT_g. We also find that at a fixed strain rate, dynamics become more homogeneous during deformation at lower temperatures, as indicated by a larger increase of β_{KWW} during deformation. Independent of temperature, β_{KWW} is found to be correlated to the factor by which dynamics are enhanced in the post-yield regime relative to the undeformed state. Some of these results have been anticipated by modeling and theoretical approaches in the literature, and a detailed comparison will be presented in the Discussion section. The observed dependence of segmental dynamics on temperature is at least three times stronger than predicted for a similar system by the theory of Chen and Schweizer.[39]

Experimental Methods

Sample Preparation

Lightly cross-linked poly(methyl methacrylate) (PMMA) samples were made using the following method.[26, 33] Methyl methacrylate (MMA, Polysciences, Inc.) and ethylene glycol dimethacrylate (EGDMA, Polysciences, Inc.) were passed through separate alumina columns to remove inhibitors. From these, a solution of 1.5 weight percent EGDMA in MMA was prepared. The fluorescent probe N, N'-Dipentyl-3,4,9,10-perylenedicarboximide (DPPC, Aldrich) was added to the mixture of EGDMA and MMA to make a stock solution that was ~10^{-6} M in DPPC. A portion of this stock solution was added to a vial, along with 0.1 weight percent of the free radical initiator benzoyl peroxide (Polysciences, Inc.). The vial was then sealed and placed into a 65 °C bath for 30 minutes to partially polymerize the mixture, and then transferred to a mold which consisted of two 2" × 3" glass slides with aluminum foil spacers held together by binder clips. The sample was further polymerized within the mold under nitrogen in a 90 °C oven for 24 hours, after which the temperature was increased to 140 °C for an additional 24 hours. After removal from the oven, PMMA films were removed from their molds through sonication. PMMA films created through this procedure had a glass transition temperature T_g of 395 ± 1 K, as determined by differential scanning calorimetry using the onset of the second heating scan at 10 K/min.

Samples were cut using a custom-made steel rule die, based upon a miniaturization of the "dog-bone" style shape specified in ASTM method D1708-10.[40] The samples varied in thickness, with dimensions of 35-50 μm near the dogbone ends and 25-30 μm at the thinnest part of the sample, as measured by a micrometer.

Deformation Instrumentation

Samples were deformed using a custom-built apparatus which has been previously described.[33] In this instrument, samples are held by two sandpaper-lined clips inside of a temperature-controlled brass cell. One of these clips is fixed in place inside of the brass cell. The other clip is attached to a polyetherimide rod which extends outside of the cell and attaches to a load cell (Measurement Specialties Inc., Model XFTC300). The load cell and a U-shaped aluminum bar are fixed to a single-axis roller stage. A high-resolution linear actuator (Physik Instrumente Gmbh & Co., model M-227.50) pushes against the opposite end of this U-shaped bar, driving tensile deformation of the sample.

Force is monitored by the load cell for a short period before and during the entirety of deformation. The initial cross-section of the sample used to calculate engineering stress is typically 25-30 μm × 2.0 mm, which are the dimensions of the thinnest area of the sample and the width of the midsection of the dogbone, respectively. Before deformation, the sample is allowed to sag slightly; the onset of deformation is apparent by a clear uptick from the baseline reading of the load cell. Global strain is calculated from the time of the onset of deformation, the speed of the linear actuator, and the initial length of the sample between the clips.

Probe reorientation measurements are performed in a roughly 500 μm × 500 μm area of the sample, and local strain is monitored by capturing images of bleached lines in the local measurement area as described in previous studies. [26-31, 33] In the post-yield regime, these samples deform inhomogeneously at all of the temperatures examined. Typically, the local measurement area is chosen to be near or at the thinnest location in the sample, where strain develops most prominently in the post-yield regime. Instantaneous local strain rates during deformation are determined by taking the derivative of a polynomial fit to the local strain versus

time data as described in a previous publication.[33] Local strain rates match the global strain rates until yield, but after yield are typically three to five times larger than the global strain rate.

Probe reorientation technique

Measurements of segmental dynamics were obtained using a previously-described probe reorientation technique and occurred as the sample was actively deformed.[26-31, 33] A linearly-polarized 532 nm laser preferentially photobleaches an ensemble of DPPC probe molecules whose transition dipoles are aligned with the polarization of the light. After this photobleaching step, a weak, circularly-polarized 532 nm laser induces fluorescence in the unbleached population of probes. The fluorescence intensities with polarizations perpendicular and parallel to the original bleaching polarization are monitored to determine the decay of anisotropy in the ensemble of probe molecules in the bleached area.

The time-dependent anisotropy of the ensemble of unbleached probe molecules, as measured by the fluorescence intensities discussed above, can be described by the Kohlrausch-Williams-Watts (KWW) function:

$$r(t) = r(0) \cdot e^{-(t/\tau_{1/e})^{\beta_{KWW}}}$$

Here $r(t)$ is the anisotropy at time t, $r(0)$ is the anisotropy at time 0, $\tau_{1/e}$ is the time for the function to decay by a factor of e, and β_{KWW} denotes the nonexponentiality of the decay. Anisotropy data from probe reorientation measurements are fit to the KWW function to obtain $\tau_{1/e}$ and β_{KWW}, which are presented in the current work. We also show the probe rotational correlation time, τ_c, which is obtained by integrating the orientational autocorrelation function: $CF = r(t)/r(0)$. Several previous studies[26-31, 33] use τ_c as the main experimental reporter for dynamics. The two dynamical reporters τ_c and $\tau_{1/e}$ emphasize different portions of the segmental

relaxation time distribution, with $\tau_{1/e}$ more strongly weighted by the fastest-relaxing segments as compared to τ_c.[28] It has been previously shown that the DPPC probe is a good reporter for the α (segmental) relaxation of PMMA, with probe reorientation above T_g in the absence of deformation displaying the same temperature dependence as τ_α as determined by dielectric spectroscopy.[28] Recent simulation[34] and theory[39] work, which do not use fluorescent probes, also report similar dynamical trends to what is reported here, further supporting the probe as a good reporter of segmental dynamics during deformation.

In order to obtain multiple measurements of segmental dynamics during a single deformation experiment, we stopped monitoring the anisotropy decay well before $r(t)$ decayed to zero. In several previous publications using the probe reorientation technique, each anisotropy decay was monitored for a fixed period of time.[28-31, 33] We have changed our procedure for the experiments reported here, and instead the time window for data collection is varied during the deformation such that $r(t)/r(0)$ is measured to a value lower than 0.5. For results presented here, at least two-thirds of post-yield decay curves have decayed to a value of $r(t)/r(0) = 0.5$ or lower.

Thermal History

Samples were held in a brass temperature-controlled cell during the entirety of the experiment, including annealing, cooling to the testing temperature, and deformation. Prior to deformation, samples were held at 408 K for at least three hours. Samples were cooled 1 K/min to the testing temperature and then held isothermally for 30 minutes prior to deformation. The temperature remains constant to within 0.2 K during deformation. The reported temperature for

these tests is accurate to ± 1 K, based upon melting point tests performed inside the temperature cell.

Results

In the following section, we present mechanical results and the evolution of segmental dynamics during deformation. In the Discussion section, we will compare our results with existing theoretical approaches in the literature which anticipate some of the qualitative features discussed in the Results section. The Discussion section also provides further quantitative analysis of the effect of thermally-activated transitions.

The results presented in this work focus on how temperature affects the segmental dynamics of a polymer glass during deformation, and we begin by showing the effect of temperature on the mechanical response of the samples. Figure 1 shows the stress-strain response of cross-linked PMMA glasses at four different temperatures deformed in extension at a constant engineering strain rate of 3.1×10^{-5} s^{-1}. For the data displayed in Figure 1, the yield stresses span a factor of 1.8, with the yield stress decreasing as temperature increases. For the present work, tests were conducted to a maximum global strain of 0.38, and thus this work does not extensively explore the strain hardening regime at larger strains. The yield strain and yield stress for the T_g-22 K curve are consistent with previously-reported mechanical tests of this material with the same thermal history.[33]

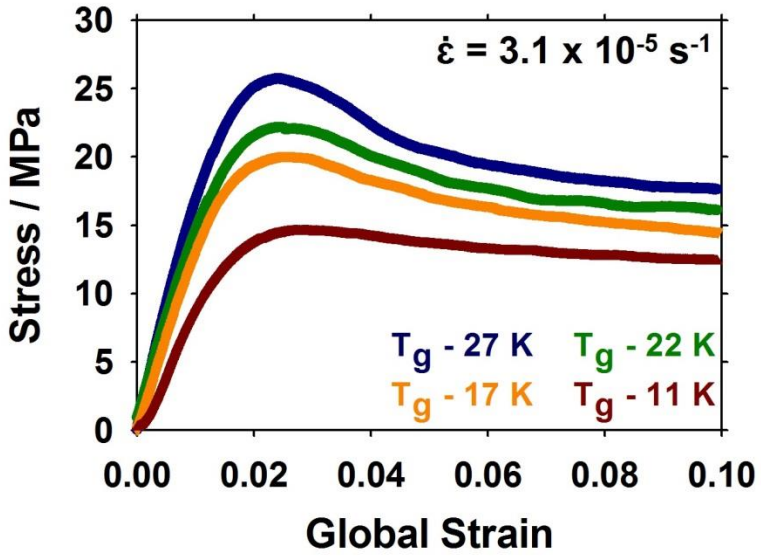

Figure 1. Engineering stress plotted against global strain for cross-linked PMMA glasses deformed at a constant global strain rate of $3.1 \times 10^{-5}\ s^{-1}$. Data are presented for experiments at four temperatures.

The evolution of the segmental dynamics of PMMA during constant strain rate deformation at T_g-17 K is shown in Figure 2a for various strain rates. The y-axis plots $\tau_{1/e}$, a characteristic time for reorientation of the probe DPPC in the PMMA matrix, as described in the Experimental Methods section. It has been previously reported that the reorientation of this probe is a good reporter for segmental dynamics in the polymer melt in the absence of deformation[28] and additional arguments support the connection between probe reorientation and segmental dynamics during deformation.[29, 33] The x-axis shows the local strain in the region of the sample in which the probe reorientation measurement occurs. After the start of deformation, $\tau_{1/e}$ decreases until yielding (at a local strain of ~0.05). After yield, in the strain softening regime, $\tau_{1/e}$ decreases more slowly or remains constant. The value that $\tau_{1/e}$ approaches in the post-yield regime depends upon the average post-yield local strain rate, provided in the legend. After yield, the glass with the highest local strain rate displays dynamics which are 35 times faster than the undeformed glass (indicated by the arrow). It should be noted that local strains attained during the deformation are significantly larger than the global strains experienced by the entirety of the sample. Because of inhomogeneous deformation in these samples upon yield near the measurement location, local strain typically increases 3-5 times faster than the global strain. The general behavior reported in Figure 2a is consistent with the behavior observed for τ_c and in a previous study.[33]

The effect of temperature on the segmental dynamics of PMMA during deformation at a single strain rate is demonstrated by Figure 2b. This panel shows $\tau_{1/e}$ for constant strain rate deformation at four different temperatures; for each experiment, the average post-yield local strain rate was within the range $(1.3 \pm 0.2) \times 10^{-4}$ s^{-1}. For each of the four temperatures, the value of $\tau_{1/e}$ in an undeformed glass with the same thermal history is indicated by an arrow. In all four

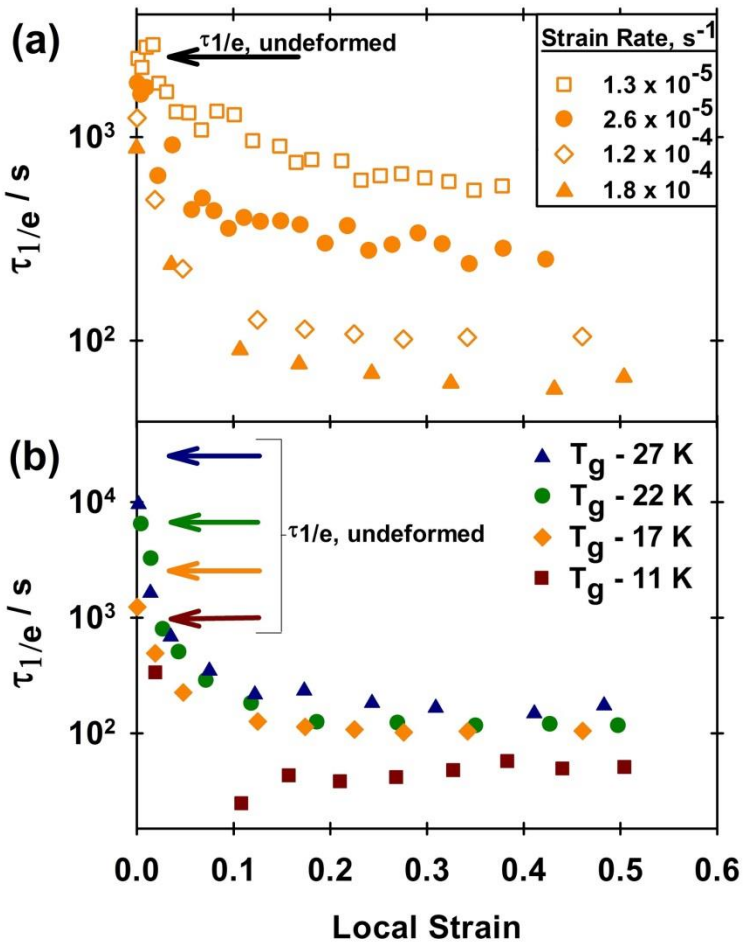

Figure 2. Evolution of segmental dynamics as a function of local strain for a PMMA glass during constant strain rate deformations. The y-axis shows the average segmental relaxation time $\tau_{1/e}$, measured using the probe mobility technique. Panel a shows deformation at T_g - 22 K at four strain rates. The lower panel shows $\tau_{1/e}$ for tests with a local strain rate of $(1.3 \pm 0.2) \times 10^{-4}$ s^{-1} at the four different temperatures investigated. The arrows in both panels indicate the value of $\tau_{1/e}$ in the absence of deformation. As seen in panel b, in the post-yield regime, $\tau_{1/e}$ decreases as temperature increases, indicating faster dynamics at this strain rate.

data sets, $\tau_{1/e}$ decreases from its pre-deformation value until yielding at ~0.05 strain, after which it decreases more slowly or remains constant.

Based upon the data in Figure 2b, there are three observations that should be noted. First, for a particular strain rate, the value of $\tau_{1/e}$ in the post-yield regime depends upon temperature, with faster dynamics observed at higher temperature. Secondly, the effect of temperature on segmental dynamics during deformation at a particular strain rate is significantly smaller than the effect of temperature in the PMMA glass in the absence of deformation. In the absence of deformation, $\tau_{1/e}$ differs between the lowest and highest temperature by a factor of 25; after yield, this decreases to a factor of 4. Lastly, relative to the undeformed state, segmental dynamics in the post-yield regime are enhanced by a greater factor at lower temperatures. By comparing the pre-deformation and average post-yield values of $\tau_{1/e}$ in Figure 2b, it can be observed that for this strain rate, segmental dynamics were enhanced by a factor of 120 at T_g-27 K. In contrast, this enhancement is only a factor of 18 for the deformation at T_g-11 K. These three observations will be further illustrated in Figures 3 and 4 and explored in more detail in the Discussion section.

To illustrate how the combined effect of temperature and strain rate affects the segmental dynamics of a polymer glass in the post-yield regime, $\tau_{1/e}$ values are shown as a function of local strain rate in Figure 3a for experiments at four temperatures. Each constant strain rate deformation is represented by one data point with error bars indicating one standard deviation in the post-yield averages. In Figure 3a, within each temperature series, $\log(\tau_{1/e})$ demonstrates an approximately linear decrease with log(local strain rate), indicating further enhancement of segmental dynamics as strain rate is increased. However, at a given local strain rate, $\tau_{1/e}$ is systematically lower with increasing temperature, indicating faster segmental dynamics at higher temperatures. Figure 3b shows an analogous plot where τ_c is used as the measure of segmental

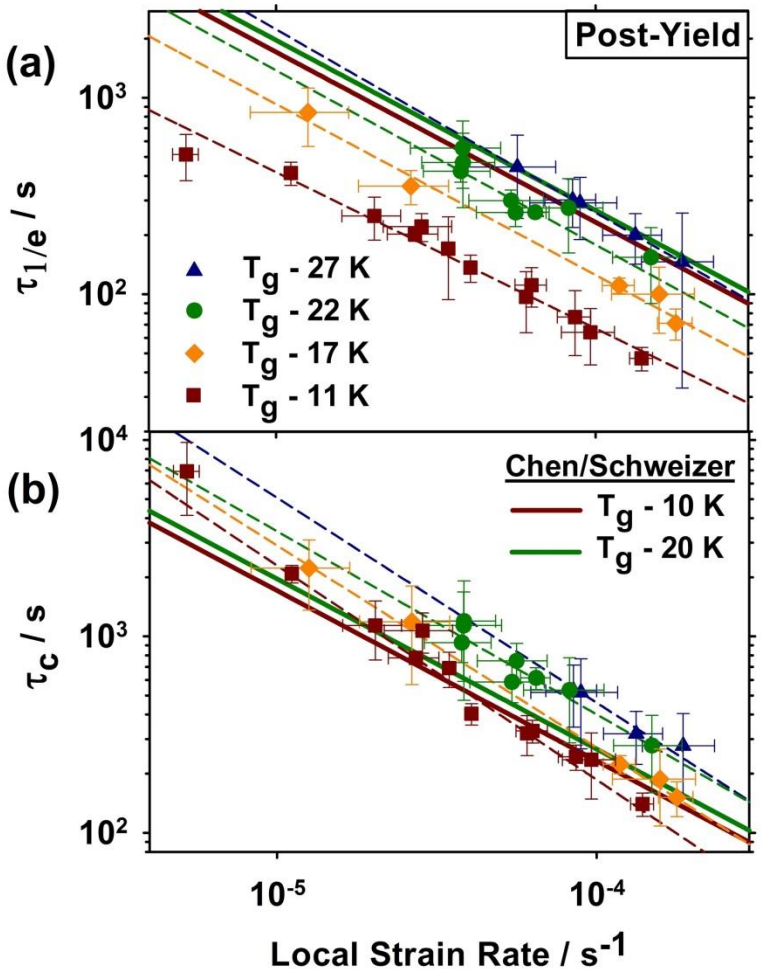

Figure 3. $\tau_{1/e}$ (panel a) or τ_c (panel b) versus local strain rate for constant strain rate experiments in the post-yield regime, at the four temperatures investigated. Individual data points are average values of post-yield data for a single constant strain rate experiment. Error bars represent one standard deviation. Solid lines are extracted from Figure 7 of reference 39. Fit lines to the data are shown as dashed lines and were determined through an orthogonal distance regression; slopes with standard deviations from top to bottom in panel a are: -0.93 ± 0.62, -0.89 ± 0.33, -0.87 ± 0.15, -0.80 ± 0.06. In panel b, slopes with standard deviations from top to bottom are: -0.93 ± 0.75, -0.93 ± 0.37, -1.03 ± 0.19, -1.09 ± 0.07.

dynamics; τ_c is the integral of the orientation correlation function for the probe, as described in the Experimental Methods section, and is expected to be more strongly influenced by slowly-relaxing segments in comparison to $\tau_{1/e}$. Figures 3a and 3b show similar trends, but the difference in log(τ) between temperature series is larger for $\tau_{1/e}$ than τ_c.

The dashed lines in both panels of Figure 3 correspond to best fits of the data using an orthogonal distance regression. Slope values with errors representing one standard deviation are provided in the figure caption. These slopes and the solid lines that are replicated from Figure 7 of reference 39 will be further described in the Discussion section. Particularly at lower temperatures, the size of the standard deviations in individual measurements can be partly attributed to the experimental control of the global, rather than local, strain rate. In the post-yield regime for some tests (such as those shown in Figure 2a), the local strain rate gradually increases while the segmental relaxation time decreases; in the format of Figure 3a, the individual post-yield measurements would lie along a small line segment (parallel to the dashed line) instead of being randomly scattered around the post-yield averages. Because the orthogonal distance regression assumes uncorrelated errors in x and y, the standard deviations provided for the slopes of lines overestimate the error in the slope. One test from the T_g-27 K data was removed from Figure 3b due to a particularly high variance.

Figure 4 demonstrates how the distribution of segmental relaxation times is modified during deformation. Deformation has been previously reported to narrow the distribution of segmental relaxation times within a polymer glass[17, 27-31] and Figure 4 provides an opportunity to investigate this for constant strain rate measurements over a range of temperatures. The two panels of Figure 4 display the average post-yield β_{KWW} values, with error bars representing one standard deviation. A smaller value of β_{KWW} indicates a broader distribution of segmental

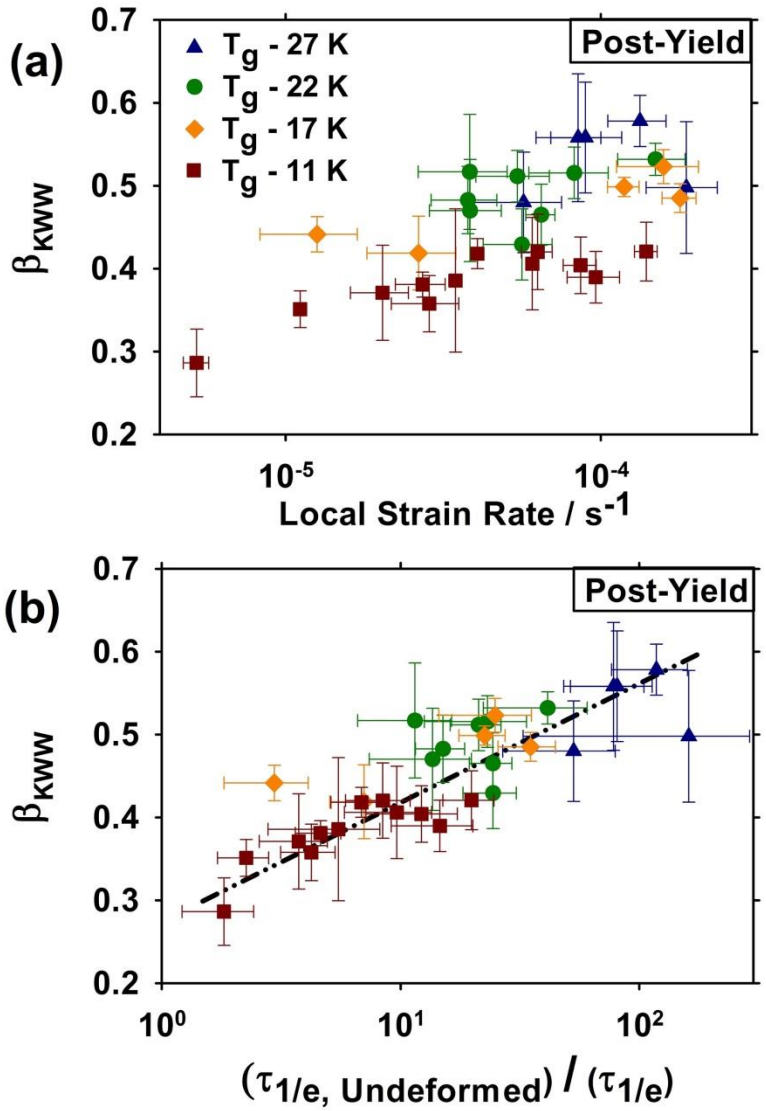

Figure 4. Evolution of the KWW β parameter with local strain rate (panel a) or mobility enhancement (panel b) for constant strain rate experiments. Individual data points represent average values of post-yield data for one constant strain rate experiment. Panel a shows evolution of β_{KWW} with strain rate for all temperatures. In panel b, the x axis is displayed as a mobility axis, which is scaled to show the factor by which $\tau_{1/e}$ is enhanced relative to the absence of deformation; the dashed line is a guide to the eye.

relaxation times, and has been previously interpreted as an indication of spatially heterogeneous dynamics; higher β_{KWW} values correspond to more homogeneous dynamics.[27-31] For PMMA glasses, β_{KWW} in the absence of deformation close to T_g has been found to be 0.31 ± 0.04. During a constant strain rate deformation, β_{KWW} increases as yielding occurs and then becomes nearly constant. Figure 4a displays the average post-yield β_{KWW} as a function of local strain rate for the tests shown in Figure 3. It can be seen in Figure 4a that at a given temperature, the post-yield value of β_{KWW} increases as the local strain rate increases, indicating that segmental dynamics are becoming more homogeneous. Figure 4a also illustrates that at a given strain rate, β_{KWW} in the post-yield regime tends to be lower at higher temperatures. This may be interpreted to mean that the quiescent distribution of relaxation times is perturbed to the smallest extent during deformation at high temperatures.

Figure 4b demonstrates how the distribution of segmental relaxation times correlates with the enhancement of segmental mobility during post-yield flow, relative to the undeformed state. For this panel, the average post-yield $\tau_{1/e}$ value is scaled by its value in the absence of deformation to obtain a factor which describes how much faster segmental dynamics are in the averaged post-yield data than in an undeformed glass. β_{KWW} values from deformations at all temperatures demonstrate a correlation with this scaled mobility value. This indicates that the change in the distribution of relaxation times is related to the extent to which dynamics are perturbed from the undeformed state, apparently independent of temperature.

Discussion

Figures 3 and 4 demonstrate that temperature plays a significant role in determining the post-yield segmental dynamics of a polymer glass, and these results form the basis for our discussion. In this section, we compare our results with recent simulations and theory. In addition, we compare our results with previous creep deformation experiments.

Comparison to Simulations in the Quasistatic Limit

Recently, several simulations[36, 37, 41-43] have investigated the behavior of glasses as they undergo quasistatic deformation in the limit of zero temperature and strain rate (also known as athermal quasistatic deformation). In such simulations, the system undergoes deformation in small strain steps (typically ~ 10^{-6}) and is quenched after each step. The system is always at the minimum of a basin after each step and thus thermally-activated transitions cannot occur.[42] Deformation acts to lower barriers between neighboring basins, and at the point at which a barrier is completely eliminated, the system falls into the neighboring basin in what is termed a "fold catastrophe" or plastic event. In contrast, at finite temperature, the system has enough thermal energy to overcome a barrier at a strain less than that needed to completely eliminate the barrier.[42] Many of these simulations have investigated the deformation of colloidal or atomic systems.[41-45]

Chung and Lacks[36, 37] have recently used the quasistatic approach to investigate the deformation of glassy polystyrene. For comparison, these authors also performed molecular dynamics simulations of the deformation of the polystyrene glass at finite temperature (T_g-70 K), for shear rates in the range of 10^3 to 10^9 s^{-1}.[36, 37] They characterized the mobility in the polymer glass during deformation by examining translational displacements, as characterized by the van Hove function. When the van Hove function was plotted as a function of strain (rather than

time), the mobility during the finite temperature deformations (except for the two highest strain rates) was found to be nearly quantitatively consistent with mobility in the quasistatic limit. Because the conditions of the molecular dynamics simulations are far from the limit of zero temperature and deformation rate, it is surprising that most of this mobility data agrees with the quasistatic limit. Chung and Lacks interpreted their results to mean that thermally-activated transitions are not a significant contributor to mobility during deformation under the conditions of these simulations.

In contrast, the results presented here indicate a significant influence of thermally-activated transitions, based upon three observations. First, the dependence of $\tau_{1/e}$ or τ_c upon temperature for a given strain rate in Figure 3 indicates that the segmental dynamics are being influenced by thermal energy. Second, in the quasistatic limit, the segmental relaxation time must be proportional to the inverse of the strain rate. In this limit, the system experiences precisely the same rearrangements and motions, regardless of the rate of deformation. Therefore, a doubling of the strain rate would precisely double the rate of these rearrangements. In the format of Figure 3, the quasistatic limit predicts a slope of -1. Our best estimates of the values of the slopes in Figure 3a are greater than -1, and in particular the highest temperature data in Figure 3a has a slope of -0.80 ± 0.06 that is inconsistent with -1. A similar observation has been made by Besseling et al. in a colloidal glass system undergoing shear deformation. Besseling et al. noted that the local shear rate $\dot{\gamma}$ and the α relaxation time τ_α demonstrated a relationship of $\tau_\alpha = \dot{\gamma}^{-0.8}$.[46] As an additional point of comparison, the theory of Chen and Schweizer yields a slope of ~ -0.86 for PMMA glass undergoing constant strain rate deformation, as displayed by the solid lines in Figure 3.[39] Lastly, we note that in the quasistatic limit, the distribution of relaxation times should be independent of the strain rate. Thus, we would expect the post-yield

β_{KWW} values in Figure 4a to be the same at all strain rates and temperatures, in contradiction to the experimental results.

There are several important differences between our experiments and the simulations of Chung and Lacks, and these differences need to be considered in light of the apparently contradictory results. In comparison to the work of references 36 and 37, our experiments are performed closer to T_g and at much lower deformation rates. At the higher temperatures and slower deformation protocol used in our work, the system is much more likely able to thermally escape a basin on the potential energy landscape, in comparison to the conditions simulated by Chung and Lacks. Therefore, the deformation conditions simulated by Chung and Lacks may act to suppress thermally-activated transitions, relative to the conditions of the present work. Another major difference between the work of Chung and Lacks and the present work is the strain attained during each deformation. The mobility data in the simulation work is calculated for a number of different shear strains. Chung and Lacks observed strong agreement with the quasistatic limit for shear deformation to a strain of 1.09, as indicated by the observed mobility (as a function of strain) being nearly identical for shear rates spanning four orders of magnitude. However, when the shear was performed to 11% strain, the observed mobility over this same shear rate range spanned more than a decade. For the data presented in this work, the deformation is typically ended at or before a local strain of 0.5. In a few experiments, the dependence of mobility on strain has been measured to a local strain of 1. In that case, it was found that τ_c changed less than 0.3 decades after yield and much of this change was accounted for when normalized to the local strain rate.[33] Thus, the experimental data currently available does not indicate the transition towards the quasistatic limit with increasing strain that was observed in the simulations.

A more direct comparison to the work of Chung and Lacks[36, 37] could be made if the simulation conditions could be matched by experiments. Unfortunately, the lowest shear rate used in their simulations, 10^3 s^{-1}, is about six orders of magnitude faster than the strain rates available with our experimental apparatus. However, deformations at lower temperatures may be possible to attain.

Thermally-activated transitions with and without deformation

We now explore several methods to quantify the influence of temperature on the segmental dynamics during deformation. Just above T_g, the reorientation of probe molecules in cross-linked PMMA shows the same temperature dependence as τ_α measured by dielectric spectroscopy; an increase of 3 K in the melt corresponds to roughly a one decade decrease in τ_c.[27, 28] For cross-linked PMMA glasses with the same pre-deformation thermal history as glasses presented here, it has been shown that a 10 K increase in temperature corresponds to roughly a decade decrease in τ_c.[27, 28] Figures 2b and 3 demonstrate a weakening in the relationship of temperature increase and enhancement of segmental dynamics during post-yield flow. Based on the spacing between the dashed lines in Figure 3b, the relationship between τ_c and temperature during post-yield flow is roughly 45 K/decade, at a fixed strain rate. For $\tau_{1/e}$, this number is 28 K/decade, as shown in Figure 3a. By either of these measures, our data displays a significant effect of temperature on segmental dynamics, although it is clear that this effect is suppressed relative to the undeformed state. We emphasize that these post-yield relationships are expected to be independent of thermal history.

Our results indicate a significant influence of thermally-activated transitions during flow, and we will now estimate the height of the corresponding barriers. One could calculate an

apparent barrier height $E_{apparent}$ during flow by investigating the evolution of τ in the post-yield regime across tests at a fixed local strain rate, or in essence by looking at how τ changes across a vertical line through Figure 3. A calculation of $E_{apparent}$ for the data in Figure 3a using an Arrhenius form $\tau = Ae^{E_{apparent}/kT}$ provides an estimate of $E_{apparent}$= 100 ± 30 kJ/mol, or ~ 30 kT_g. We note that a similar activation energy of ~109 kJ/mol for PMMA has been obtained by fitting values of the compressive yield stress to an Eyring-based model.[47] However, the approach used in our calculation of $E_{apparent}$ assumes that the structure of the polymer glass system during flow is identical at each of the four temperatures. With differing flow stresses for the deformations at each temperature, there is no reason for this to be the case.

We expect that a more reliable estimate of a typical free energy barrier E_A can be obtained from the post-yield average value of $\tau_{1/e}$ or τ_c by assuming the Arrhenius form $\tau = \tau_0 e^{E_A/kT}$, with τ_0 as the relaxation time in the limit of high temperature, which can be approximated as 10^{-14} s^{-1}.[48] For each constant strain rate experiment, this equation is used to calculate E_A from the assumed value of τ_0 and the observed value of $\tau_{1/e}$ and τ_c in the post-yield regime. Based upon this approach, E_A during flow at all strain rates shown in Figure 3a ranges from 41 ± 3 kT_g at T_g-27 K to 38 ± 3 kT_g at T_g-11 K. In the absence of deformation (using the values of $\tau_{1/e}$ indicated by the arrows in Figure 2b), the same calculation yields E_A values of 45 kT_g and 40 kT_g at the lowest and highest temperatures, respectively. Using the data for τ_c in Figure 3b, barrier heights during flow at all temperatures are 40 ± 3 kT_g, with values in the absence of deformation ranging from 48 ± 3 kT_g at T_g-27 K to 42 ± 3 kT_g at T_g-11 K. Although there are certainly assumptions built into this calculation of E_A, we cannot escape the conclusion that thermally-activated transitions are very significant during deformation (and only slightly reduced relative to the quiescent state). While several arguments indicate that the reorientation

time of the DPPC probe is proportional to the average segmental relaxation time during deformation, the numerical values of τ_c or $\tau_{1/e}$ are not equal to the segmental relaxation time; one may ask how this difference affects the calculations above. Our best indications show τ_c to be a factor of 2-10 larger than τ_α. This difference corresponds to a maximum decrease in E_A by 3 kT_g.

The approach used above to calculate E_A was previously utilized by Schall, Weitz, and Spaepen[38] to investigate how deformation changes the activation energy for shear transformation zone formation in a colloidal glass, basing their calculation on the rate at which shear transformation zones are induced. Through this method, they found that the activation energy was ~19 kT in the absence of deformation and only reduced by a few kT during deformation. Because they also observed the microscopic rearrangements of the particles during deformation, they were able to validate their estimate of E_A by estimating the energy required for the observed particle rearrangements. This strengthens our confidence in the estimates of E_A provided in the paragraph above. In addition, the results of reference 38 suggest that simulations of polymer glasses should be able to estimate energy barriers during deformation by these same two routes.

Some simulations have explored the effect of temperature on the yielding behavior or dynamics of a glassy material.[49, 50] For example, Lyulin et al.[50] simulated an atomistic model of polystyrene and tracked the total translational displacement of segments during constant strain rate deformation at several different temperatures. However, we are unaware of simulations which calculate the evolution of an observable comparable to τ_c or $\tau_{1/e}$ at multiple finite temperatures. Based upon the results presented here, such studies may provide insight about the role of thermally-activated transitions during polymer glass deformation.

The above calculations indicate the significance of thermally-activated transitions during the post-yield flow of a polymer glass and yet we observe a nearly inverse relationship between

τ_c or $\tau_{1/e}$ and strain rate, as can be seen in Figure 3. The latter is often considered a signature of "zero temperature" processes and one may ask how these two seemingly contradictory features can coexist in the same experiments. Below we discuss the theory of Chen and Schweizer[39] which provides an example of how these features can be reconciled.

Theory and Modeling Considerations

Some of the trends seen in the results presented in this work have been anticipated by modeling and theoretical approaches in the literature, and we will focus this section on a comparison of our results with two of these recent approaches. The results seen in both panels of Figure 3, which show higher segmental mobility at higher temperatures for a fixed strain rate, are qualitatively consistent with the non-linear Langevin equation (NLE) theory of Chen and Schweizer;[39] this approach incorporates a molecular-level Eyring mechanism to reduce barriers during deformation, and accounts for aging before and during deformation, and post-yield rejuvenation. The theory describes the pre-yield, yield, and strain softening regimes of constant strain rate deformation. In their work, calculations are presented for PMMA deformed in tension at constant strain rates ranging from 10^{-1} s^{-1} to 10^{-5} s^{-1} and temperatures from T_g-10 K to T_g-60 K.

The theory of Chen and Schweizer predicts several of the features seen in Figure 3 and is reasonably consistent with the experimentally-observed relationship between dynamics and strain rate. Figure 7 of reference 39 shows calculations[39] which are analogous to Figure 3a in the present work, and the solid lines in the two panels of Figure 3 are based on these results. The theory and experimental data of Figure 3a have several features in common. First, both theory and experiment show a linear relationship between strain rate and segmental dynamics on a log-log plot with a slope slightly shallower than -1 (~ -0.86 in the theory). Additionally, each

displays a noticeable enhancement of the post-yield segmental dynamics at higher temperature for deformation at a fixed strain rate. The calculations of Chen and Schweizer show near-quantitative agreement in both the slope and absolute value of the data for the lower of the two temperatures shown. In reference 39, a change in temperature corresponds to a smaller change in log τ than seen in the present work. Based upon the spacing between temperature series in Figure 7 of their work, one decade of dynamical enhancement for PMMA in the theory of Chen and Schweizer can be extrapolated to a temperature change of close to 170 K, which may be compared to 28 K/decade for $\tau_{1/e}$ in the present work.

It is important to note that several factors may account for the difference seen between the theory and experimental work. One major difference is that the theory calculates a mean barrier hopping time and does not provide information about the distribution of relaxation times. Thus, the difference in behavior of τ_c and $\tau_{1/e}$, as well as the behavior of β_{KWW} seen in the present work, cannot be compared to the work of Chen and Schweizer. We note that the theory utilizes a truly constant strain rate deformation, while our experiment controls the global, rather than local strain rate. However, we find that variations in the post-yield local strain rate within individual experiments occur with corresponding changes in τ_c or $\tau_{1/e}$, and thus, it is reasonable to expect that slow variations in the local strain rate do not significantly affect the comparison with the theory. Although the theoretical calculations assume a different thermal history prior to deformation than used in our experiments, the theory demonstrates an erasure of thermal history in the post-yield regime and predicts that post-yield segmental dynamics are only a function of temperature and strain rate.

The relationship between β_{KWW} and local strain rate shown in Figure 4 (and also results previously reported for deformations at constant stress)[28] are qualitatively consistent with the

model of Medvedev and Caruthers.[17] These authors use a stochastic model of polymer glass deformation which predicts a spectrum of domain relaxation times. Some of the main features of this approach include the ability to model strain softening, as well as a description of how the relaxation spectrum evolves during deformation. In reference 17, these authors present calculations for a lightly cross-linked PMMA glass during tensile and compressive constant strain rate deformation within the temperature range surveyed in the present work. During constant strain rate deformation, this model predicts that the domain relaxation time distribution narrows as yielding occurs, after which there is little change in the width of the spectrum. This behavior is consistent with a pre-yield increase and post-yield leveling-off of β_{KWW} observed in constant strain rate deformations of the present work. In the model detailed in reference 17, this narrowing of the relaxation spectrum is primarily due to the preferential enhancement in dynamics of the slowest-moving domains, while the fastest-moving domains are less impacted by deformation. Based on this model, it is reasonable to anticipate that for higher strain rates, a greater portion the relaxation spectrum should be affected during deformation. Conversely, for slow strain rates, only a very small portion of the relaxation spectrum will be perturbed during deformation. Thus, the general trends seen in Figure 4a, where an increase in strain rate at a single temperature yields a higher value of β_{KWW}, is consistent with the model of Medvedev and Caruthers. As temperature increases and domain relaxation becomes faster on average, a smaller portion of the relaxation spectrum should be impacted by deformation at a given strain rate, in agreement with the experimental results.

Influence of temperature upon segmental dynamics for different deformation protocols

The data shown in Figures 3a and 3b indicate a systematic decrease of the average segmental relaxation time with increasing temperature at a given strain rate, and here we compare these results to previously-reported creep experiments. Lee et al.[27] used the probe orientation technique to monitor changes in segmental dynamics during creep for a lightly cross-linked PMMA glass. Figure S3 in the supplemental material of reference 27 is similar in format to Figure 3b and indicates that, within experimental error, log τ_c is independent of temperature over a similar temperature range as that employed here. In this section, we briefly discuss this apparent discrepancy.

In the present work, the effect of temperature on log τ_c is much more subtle than for log $\tau_{1/e}$, as shown by the comparison between Figure 3a and Figure 3b. While an analogous plot of log $\tau_{1/e}$ is not presented in reference 27, such a plot would show an obvious and significant variation with temperature, given the systematic changes in the β_{KWW} values reported there. Thus, in terms of log $\tau_{1/e}$ values, both creep and constant strain rate experiments indicate a significant influence of temperature on segmental dynamics in the flow state.

Smaller quantitative differences between the results of reference 27 and those presented here might be related to two features of the deformation protocols. In the creep experiments of Lee et al., over two orders of magnitude in local strain rate were typically sampled during one experiment.[27] Although global, rather than local strain rate is controlled in the present study, the local strain rate is typically changing less than 0.3 decades in the post-yield regime of one deformation. Thus the present experiments are much closer to a steady flow state and this may have an influence on the results. In addition, different strain levels were investigated in the two experiments. In the present study, local strains achieved are typically less than 0.5. For many of

the experiments of Lee et al.[27-31], local strains achieved were more than 1. Experiments which utilize constant strain rate deformation across different temperatures and achieve local strains similar to those of Lee et al. may elucidate whether strain affects the temperature dependence of post-yield dynamics at high strains. This may be important for understanding the role of segmental dynamics in the strain hardening regime.

Conclusion

We find that temperature has a significant influence on the segmental dynamics of a polymer glass during post-yield flow, indicating that sizeable thermal barriers are being crossed during deformation. These results were obtained using a probe reorientation technique during constant strain rate deformation of lightly cross-linked PMMA samples. Although the effect of temperature on dynamics during deformation is reduced relative to the quiescent state, it is significantly larger than anticipated for the deformation protocol and material used, based upon the theory of Chen and Schweizer.[39] We anticipate that these experiments may assist in a deeper understanding of polymer glass deformation and the testing of models and simulations, ultimately leading to improved predictions of the deformation properties of polymer glasses.

The results presented in this paper span a 16 K temperature range just below T_g, and it would be interesting to determine how segmental dynamics during post-yield flow depends on temperature far below T_g. Such experiments would be expected to come closer to the quasistatic limit that can be accessed in simulations.[36, 37] For the strain rates that we utilized in this work, we anticipate that thermally-activated transitions will remain the dominant contribution to segmental dynamics at any accessible temperature. Experiments far below T_g would clearly

separate the deformation and aging time scales, and this would aid in understanding the fundamental mechanisms by which deformation influences segmental dynamics.

Acknowledgements

We thank the National Science Foundation (DMR-1104770 and DMR-1404614) for support for this research. We thank Ken Schweizer, Dan Lacks, and Kelly Suralik for helpful discussions. We thank Lian Yu and Travis Powell for assistance with DSC measurements.

References

1. Ediger, M. D.; Harrowell, P. *Journal of Chemical Physics* **2012,** 137, (8), 080901.
2. Richert, R. *Journal of Physics-Condensed Matter* **2002,** 14, (23), R703-R738.
3. Ediger, M. D. *Annual Review of Physical Chemistry* **2000,** 51, 99-128.
4. Smessaert, A.; Rottler, J. *Soft Matter* **2014,** 10, (42), 8533-8541.
5. Struik, L. C. E. *Polymer Engineering & Science* **1977,** 17, (3), 165-173.
6. Angell, C. A.; Ngai, K. L.; McKenna, G. B.; McMillan, P. F.; Martin, S. W. *Journal of Applied Physics* **2000,** 88, (6), 3113-3157.
7. McKenna, G. B. *Journal of Physics: Condensed Matter* **2003,** 15, (11), S737.
8. Thurau, C. T.; Ediger, M. D. *Journal of Chemical Physics* **2002,** 116, (20), 9089-9099.
9. McKenna, G. B.; Zapas, L. J. *Polymer Engineering & Science* **1986,** 26, (11), 725-729.
10. Meijer, H. E. H.; Govaert, L. E. *Progress in Polymer Science* **2005,** 30, (8-9), 915-938.
11. Kim, J. W.; Medvedev, G. A.; Caruthers, J. M. *Polymer* **2013,** 54, (15), 3949-3960.
12. Eyring, H. *Journal of Chemical Physics* **1936,** 4, (4), 283-291.
13. Klompen, E. T. J.; Engels, T. A. P.; Govaert, L. E.; Meijer, H. E. H. *Macromolecules* **2005,** 38, (16), 6997-7008.
14. De Focatiis, D. S. A.; Embery, J.; Buckley, C. P. *Journal of Polymer Science Part B: Polymer Physics* **2010,** 48, (13), 1449-1463.
15. Schapery, R. A. *International Journal of Solids and Structures* **1966,** 2, (3), 407-425.
16. Fielding, S. M.; Larson, R. G.; Cates, M. E. *Physical Review Letters* **2012,** 108, (4), 048301.
17. Medvedev, G. A.; Caruthers, J. M. *Journal of Rheology* **2013,** 57, (3), 949-1002.
18. Knauss, W. G.; Emri, I. J. *Computers & Structures* **1981,** 13, (1–3), 123-128.

19. Knauss, W. G.; Emri, I. *Polymer Engineering & Science* **1987,** 27, (1), 86-100.

20. Lee, E. W.; Medvedev, G. A.; Caruthers, J. M. *Journal of Polymer Science Part B: Polymer Physics* **2010,** 48, (22), 2399-2401.

21. Martinez-Vega, J. J.; Trumel, H.; Gacougnolle, J. L. *Polymer* **2002,** 43, (18), 4979-4987.

22. Yee, A. F.; Bankert, R. J.; Ngai, K. L.; Rendell, R. W. *Journal of Polymer Science Part B: Polymer Physics* **1988,** 26, (12), 2463-2483.

23. Loo, L. S.; Cohen, R. E.; Gleason, K. K. *Science* **2000,** 288, (5463), 116-119.

24. Zhou, Q. Y.; Argon, A. S.; Cohen, R. E. *Polymer* **2001,** 42, (2), 613-621.

25. Kalfus, J.; Detwiler, A.; Lesser, A. J. *Macromolecules* **2012,** 45, (11), 4839-4847.

26. Lee, H. N.; Paeng, K.; Swallen, S. F.; Ediger, M. D. *Journal of Chemical Physics* **2008,** 128, (13), 134902.

27. Lee, H. N.; Paeng, K.; Swallen, S. F.; Ediger, M. D. *Science* **2009,** 323, (5911), 231-234.

28. Lee, H. N.; Paeng, K.; Swallen, S. F.; Ediger, M. D.; Stamm, R. A.; Medvedev, G. A.; Caruthers, J. M. *Journal of Polymer Science Part B: Polymer Physics* **2009,** 47, (17), 1713-1727.

29. Lee, H. N.; Riggleman, R. A.; de Pablo, J. J.; Ediger, M. D. *Macromolecules* **2009,** 42, (12), 4328-4336.

30. Lee, H. N.; Ediger, M. D. *Journal of Chemical Physics* **2010,** 133, (1), 014901.

31. Lee, H. N.; Ediger, M. D. *Macromolecules* **2010,** 43, (13), 5863-5873.

32. Riggleman, R. A.; Lee, H. N.; Ediger, M. D.; de Pablo, J. J. *Soft Matter* **2010,** 6, (2), 287-291.

33. Bending, B.; Christison, K.; Ricci, J.; Ediger, M. D. *Macromolecules* **2014,** 47, (2), 800-806.

34. Riggleman, R. A.; Toepperwein, G. N.; Papakonstantopoulos, G. J.; de Pablo, J. J. *Macromolecules* **2009,** 42, (10), 3632-3640.

35. Warren, M.; Rottler, J. *Journal of Chemical Physics* **2010,** 133, (16), 164513.

36. Chung, Y. G.; Lacks, D. J. *Macromolecules* **2012,** 45, (10), 4416-4421.

37. Chung, Y. G.; Lacks, D. J. *Journal of Polymer Science Part B: Polymer Physics* **2012,** 50, (24), 1733-1739.

38. Schall, P.; Weitz, D. A.; Spaepen, F. *Science* **2007,** 318, (5858), 1895-1899.

39. Chen, K.; Schweizer, K. S. *Macromolecules* **2011,** 44, (10), 3988-4000.

40. D1708-10, Standard Test Method for Tensile Properties of Plastics by Use of Microtensile Specimens. ASTM International: West Conshohocken, PA, 2011; pp 1-5.

41. Karmakar, S.; Lemaître, A.; Lerner, E.; Procaccia, I. *Physical Review Letters* **2010,** 104, (21).

42. Karmakar, S.; Lerner, E.; Procaccia, I.; Zylberg, J. *Physical Review E* **2010,** 82, (3), 031301.

43. Maloney, C.; Lemaître, A. *Physical Review E* **2006,** 74, (1).

44. Utz, M.; Debenedetti, P. G.; Stillinger, F. H. *Physical Review Letters* **2000,** 84, (7), 1471-1474.

45. Tanguy, A.; Wittmer, J. P.; Leonforte, F.; Barrat, J. L. *Physical Review B* **2002,** 66, (17), 174205.

46. Besseling, R.; Weeks, E.; Schofield, A.; Poon, W. *Physical Review Letters* **2007,** 99, (2).

47. Ames, N. M.; Srivastava, V.; Chester, S. A.; Anand, L. *International Journal of Plasticity* **2009,** 25, (8), 1495-1539.

48. Angell, C. A. *Polymer* **1997,** 38, (26), 6261-6266.

49. Rottler, J.; Robbins, M. O. *Physical Review E* **2003,** 68, (1), 011507.

50. Lyulin, A. V.; Balabaev, N. K.; Mazo, M. A.; Michels, M. A. J. *Macromolecules* **2004,** 37, (23), 8785-8793.

Chapter 3

Evolution of mechanical rejuvenation in a polymer glass by monitoring segmental dynamics before and after a reversing constant strain rate deformation

Kelly Hebert and M.D. Ediger

To be submitted

Abstract

Optical probe reorientation measurements were performed to monitor changes in segmental dynamics resulting from the deformation of a polymer glass. Segmental dynamics were monitored in a poly(methyl methacrylate) glass near T_g at stress ~ 0 before and after a series of reversing constant strain rate deformations. Evidence of a rejuvenation mechanism, as quantified by a departure from the quiescent aging dynamics after the reversing deformation, is observed for deformations which reach 60% of the yield strain or greater. By this measure, a saturation of the rejuvenation mechanism is not observed until at least five times the yield strain. Purely mechanical measurements of rejuvenation, which measure the reduction of the yield stress in a subsequent deformation were also performed. These purely mechanical experiments show broad qualitative agreement with the probe reorientation experiments in the post-yield regime, with the rejuvenation mechanism saturating at strains significantly past yield. However, unlike the optical measure of rejuvenation, the mechanical experiment does not demonstrate significant rejuvenation in the pre-yield regime. The results are discussed in the context of recent theoretical approaches and simulations which provide a molecular-level description of polymer glass deformation.

Introduction

Polymer glasses are finding increasing use due to their low cost, manufacturing ease, and mechanical strength. However, in spite of decades of modeling, simulation, and experimental effort, a fundamental understanding of the deformation behavior of these materials has not been attained. Work aiming to elucidate the mechanical behavior of polymer glasses spans several decades, and the earliest efforts in this area date to Eyring,[1] who posited that during the deformation of a solid, stress acts to lower barriers for rearrangements, allowing flow to occur. Since the work of Eyring,[1] several additional models have been formed to attempt to understand the deformation behavior of polymer glasses from a molecular perspective. Integral to the work of Eyring[1] and these additional models is the idea that during deformation, segmental dynamics become significantly faster, which then allows flow to occur; one or more physical or mechanical properties acts as a control parameter for enhanced dynamics. To date, models which control enhanced segmental dynamics via stress,[2, 3] strain,[4] strain rate,[5] configurational internal energy,[6] and free volume[7] have been proposed. However, it is unclear which of these proposed mechanisms, if any, contribute to the enhancement of segmental dynamics during deformation of real materials.

One approach which has been used to model dynamics during polymer glass deformation[2, 8-12] involves the incorporation of two mechanisms to allow for segmental dynamics to become enhanced during deformation. In the first of these mechanisms, which we term the landscape tilting mechanism, stress acts to lower barriers for deformation in an Eyring-like manner. Using the framework of the potential energy landscape (PEL),[13] the landscape tilting mechanism lowers barriers for rearrangements, but does not act to change the system's position on the PEL. The second mechanism in this class of models which allows for changes in

segmental dynamics is the rejuvenation mechanism, which acts to drive the system higher on the PEL. The rejuvenation mechanism is associated with a physical parameter of the system, with different models tying the rejuvenation mechanism to differing parameters.

One such theory incorporating a landscape tilting and rejuvenation mechanism, the Nonlinear Langevin Equation (NLE) theory of Chen and Schweizer[8, 9] has demonstrated changes in segmental dynamics during constant stress and constant strain rate deformation consistent with simulations[14, 15] and probe reorientation experiments.[16-18] Calculations using the theory to investigate constant strain rate deformation of poly(methyl methacrylate) glass undergoing constant strain rate deformation indicate that up until ~60% of the yield strain, the landscape tilting mechanism is the sole mechanism allowing for the enhancement of segmental dynamics.[9] At higher strains, the rejuvenation mechanism also becomes active. In the theory, the rejuvenation mechanism is physically tied to an increase in S_0, the amplitude of local density fluctuations in the glass. As strain increases, S_0 slowly increases and saturates at strains significantly past yield.

Simulations and experimental studies have been paramount to testing ideas proposed to explain the fundamental physics of polymer glass deformation. Over the past two decades, the activity of simulation work in this field has grown tremendously, allowing molecular-level insight into the fundamental physics of glassy deformation. Within this community, several approaches have been used to study deformation of glassy polymeric systems, and enhanced segmental dynamics have been observed during constant strain rate[15, 19-21] and constant stress[19, 22, 23] deformation. Several purely mechanical experimental studies have been used to provide a critical test of deformation models of polymer glasses, including the work of McKenna,[24, 25] Rendell,[26] Govaert,[2, 27] Caruthers,[28, 29] Wang,[30] and their coworkers. Experimentally, changes in

segmental dynamics during deformation have been measured indirectly by NMR[31] and diffusion[32] and directly by dielectric spectroscopy[33] and probe reorientation.[16-18, 22, 23, 34-37]

Here we perform a series of constant strain rate deformations at a rate of 1.55×10^{-4} s^{-1} on a poly(methyl methacrylate) glass at $T_g - 7$ K to varying strains which are then immediately reversed at the same rate to a near-zero stress. Changes in segmental dynamics are tracked before and after the reversing deformations to test the activity of the rejuvenation mechanism. In addition to our probe reorientation measurements, we have performed purely mechanical experiments in which a second constant strain rate deformation is performed after the reversing deformation; the decrease in the yield stress observed in the second deformation is used to provide a second perspective of rejuvenation. We directly compare our rejuvenation results to those calculated based upon the increase of S_0, the amplitude of local density fluctuations, in the NLE theory.[9] Although the theory does not calculate a reversing deformation protocol, we interpret the theory to indicate that after stress is removed, the landscape tilting mechanism of the theory is no longer active, allowing enhancements in dynamics due to this mechanism to be removed. Based upon remaining enhancements in dynamics after the reversing deformation, we are able to quantify the activity of the rejuvenation mechanism. Although calculations from the NLE theory[8, 9] are used for comparison in this study, the findings of the present work may more broadly provide a characterization of the nature of rejuvenation mechanisms as incorporated in other theoretical and modeling work.

We find that for deformations which remain in the pre-yield regime, levels of rejuvenation up to 40% are observed via optical measurements. These pre-yield rejuvenation effects within the optical data are consistent with simulations of Smessaert and Rottler.[38] In contrast, calculations based on an increase of S_0 in the NLE theory[9] and the mechanical

experiments of this work demonstrate little rejuvenation activity in the pre-yield regime. However, all three measures of rejuvenation demonstrate that the rejuvenation develops gradually with strain and does not saturate until at least five times the yield strain. We outline the broad agreement between the theory and experimental results, agreement between the optical results of the present work and simulations of Smessaert and Rottler,[38] and pre-yield differences in levels of rejuvenation observed between the two experimental methods in the Discussion section.

Experimental Methods

Sample Preparation

Lightly cross-linked poly(methyl methacrylate) (PMMA) samples were synthesized following a previously-reported procedure. [17, 34] A solution containing 1.5 weight percent ethylene glycol dimethacrylate (EGDMA, Polysciences, Inc.) in methyl methacrylate (MMA, Polysciences, Inc.) was used to create the cross-linked films. The fluorescent probe N, N'-Dipentyl-3,4,9,10-perylenedicarboximide (DPPC, Aldrich) was also dissolved in this stock solution at a concentration of ~10^{-6} M . The initiator benzoyl peroxide (Polysciences, Inc.) was added to this stock solution at a concentration of 0.1 weight percent, and the resulting mixture was heated at 343 K for approximately 30 minutes, after which the thickened mixture was loaded into molds consisting of two microscope slides lined with aluminum foil spacers, which were then clamped together. The stock solution was then allowed to polymerize in the molds in a 363 K oven for 24 hours under a positive pressure of nitrogen gas. The oven temperature was then increased to 413 K for an additional 24 hours. Films were removed from their molds through ultrasonication in a water bath. Individual samples were cut from the resulting films by a die

cutter. The shape of the die cutter is a 50% miniaturization of the dimensions prescribed by ASTM method D1708-10.[39] The polymerization procedure results in films that typically range from ~35-50 μm at the edges and ~25-30 μm in the middle of the sample. Samples made in this fashion had a glass transition temperature T_g of 395 ± 1 K, determined using differential scanning calorimetry (DSC) from the onset during the second heating scan at a rate of 10 K/min.

For the reported results in this manuscript, one sample was used for the optical measures of rejuvenation and two were used for the mechanical measures of rejuvenation; however, additional tests performed on other samples yielded results consistent with the reported results. Between subsequent optical and mechanical experiments, the sample was allowed to anneal at a temperature of 408 K for at least three hours. This annealing step resulted in the full erasure of imposed strain from prior tests. As a further check, we ran the tests out of order with respect to the maximum strain achieved during deformation and found good overlap in both the mechanical and pre-deformation optical data, as shown in Figures 2 and 3.

Deformation Instrumentation

Samples were held in a previously-described deformation apparatus[17] for the entirety of each experiment, including annealing above the glass transition temperature. A programmable linear actuator is attached to a u-shaped bar which is then coupled to a load cell and the sample. Increasing the position of the actuator drives tensile deformation, while decreasing the position of the linear actuator allows previously-imposed strain to accordingly decrease when the sample is under tension.

Stress was calculated based on the initial cross-section of the thinnest portion of the sample, which was 2.0 mm × 25 - 30 μm, and force reported by the load cell; global strain was

calculated based on movement of the linear actuator. We perform probe reorientation measurements in a ~500 μm × ~500 μm measurement area at the thinnest region of the sample. In addition to monitoring the global strain, we monitor strain in this local measurement area by photobleaching lines into the glass before deformation is applied. We can then calculate local strain by imaging these lines. Our samples are not uniform in thickness, and thus do not deform homogeneously after yielding occurs. Below the yield strain of 0.030, the global and local strains are approximately equal. In the post-yield regime, strain builds up fastest in the thinnest area of the sample where we perform our experiments; the local strain rate is approximately 2-3 times the global strain rate after yielding occurs. We ensured that we were performing the optical measurements in the thinnest portion of the sample by pre-deforming a sample and photobleaching a mark at the location where a neck-like region first formed after yield, which could be easily identified through a wide-field view under our microscope. The sample was then annealed above the glass transition temperature for at least three hours, resulting in the full erasure of strain in the sample, and the bleached location could be visually identified for subsequent experiments. We found that the relationship between the local strain and global strain during deformation was reproducible for experiments within one sample. This was confirmed by capturing several images of the measurement area during the tensile deformation phase of multiple experiments. The local strain vs. global strain data for multiple tests collapsed onto a single curve, which was then fitted to a 7^{th} order polynomial to determine the maximum local strains attained during each experiment.

Thermal Protocol

Samples were loaded into and held within a temperature-controlled cell while annealing above the glass transition temperature, cooling to the testing temperature, and during all phases of the experiment. To erase thermomechanical history, samples were annealed at 408 K for at least three hours and then cooled at 1 K/min to the testing temperature of 388 K. After cooling, the temperature remains constant to 0.2 K. Reported temperatures are accurate to ± 1 K as determined by melting point tests performed within the brass cell. Times reported in this study reflect time spent below the glass transition temperature as determined by DSC (395 ± 1 K). A heating rate of 10 K/min rather than 1 K/min was used for T_g determination; the glass transition temperature of our samples at the imposed cooling rate is likely ~3 K lower, resulting in a slight overestimation (~180 s) in the reported aging times in this study. However, this should not have a significant quantitative effect on the reported results.

Mechanical Protocol

A schematic of the mechanical protocol performed during the probe reorientation experiment is shown in Figure 1a. Prior to deformation, the sample was held without imposed stress while it aged at 388 K. After a predetermined aging time (9300 s), a global engineering strain rate of 1.55×10^{-4} s^{-1} was imposed on the sample up to a pre-determined strain, after which strain was immediately reversed at the same strain rate. This unloading continued until a stress of 0.2 MPa was reached, at which time the linear actuator was programmed to retract in order to maintain ≤ 0.2 MPa stress for the remainder of the experiment. This small imposed stress of 0.2 MPa after the reversing deformation was used to stabilize the sample for further optical experiments; we do not expect this stress to have a measurable impact on measured dynamics.

To test this, we have repeated this procedure while instead imposing a 1 MPa stress after the deformation and found no measurable effect of this stress on the optical data.

Changes in the post-deformation mechanical behavior of a polymer glass have been previously used to investigate the effect of mechanical rejuvenation in a glass; for example, Govaert and coworkers have investigated the reduction and subsequent regrowth of the yield stress after large mechanical deformations.[27, 40] In addition to the optical measurements described below, we employ a purely mechanical protocol to quantify rejuvenation as shown in Figure 1b. The protocol that we employ is identical to that shown in Figure 1a, except that after a waiting period of 1200 seconds after the reversing deformation, a second deformation at a constant global strain rate of 1.55×10^{-4} s^{-1} is performed. We acknowledge that the mechanical procedure and calculation we use to quantify rejuvenation (described in the Results section) is not guided by a theory or model, and is rather an arbitrary choice based on observations of reduced yield stress after large deformations as reported by, for example, Govaert,[27, 40] McKenna,[25] Bauwens,[41] and their coworkers.

Although large deformations are typically associated with full erasure of the overshoot peak in a constant strain rate deformation, we observe a small overshoot in the mechanical data after the largest reversing deformation as can be seen below in Figure 4a. We attribute this remaining overshoot to the imposed 1200 second waiting time between the end of the reversing deformation and second constant strain rate deformation. Measurable regrowth of the overshoot peak was observed almost immediately after a large deformation in the work of Govaert and coworkers,[40] which investigated polystyrene glass held at room temperature. We have performed additional mechanical testing in which no waiting time was imposed between the reversing deformation and subsequent constant strain rate deformation and found near-erasure of

the overshoot peak. The waiting time in our protocol is imposed to provide a fair comparison to probe reorientation data such that both methods reflect the same waiting period after the reversing deformation; further discussion of this point will be provided below.

A temperature increase has been previously reported to accompany the yielding of polymer glasses,[42] such as the glassy PMMA studied in the present work; for the deformations studied in the present work, any such temperature increase should be negligible. Assuming that no heat is dissipated during deformation and all mechanical work directly acts to heat the sample, calculating work based on the maximum force and maximum strain attained during deformation translates to a maximum increase in temperature of 1.2 K. However, a study of Haward and coworkers[42] found that temperature changes during the deformation of a glassy polymer are strongly dependent on the drawing rate, with smaller increases in temperature experienced for slower drawing rates. For drawing rates of 0.016 mm/s (~3 times faster than the draw rates used in the present study), Haward and coworkers found that less than 20% of the applied mechanical work converted to measurable heating of their samples. Additionally, the samples used in the present study are more than 35 times thinner than the thinnest samples used in the study of Haward and coworkers; any heat dissipation during deformation should be accordingly faster.

Probe Reorientation Protocol

Segmental dynamics before and after the reversing deformation were monitored through a previously-described probe reorientation technique.[16-18, 22, 34-37] Reorientation of an anisotropic ensemble of fluorescent DPPC probes tracks segmental dynamics in the PMMA matrix during aging and deformation; this ensemble is induced by photobleaching with a linearly-polarized 532 nm laser beam. Probe reorientation is tracked by inducing fluorescence in the remaining

unbleached population of probe molecules via a weak, circularly-polarized 532 nm laser beam. Fluorescence intensities in the polarizations parallel and perpendicular to the original photobleaching polarization are monitored. Anisotropy of the fluorescing probes can then be calculated from these intensities as described previously.[34] The time-dependent anisotropy decay in the fluorescence can be described by the Kohlrausch-Williams-Watts (KWW) function:

$$r(t) = r(0) \cdot e^{-(t/\tau_{1/e})^{\beta KWW}}$$

Where r(t) and r(0) are the time-dependent and initial anisotropies, respectively. Fitting the time-dependent anisotropy to the KWW function yields the time for the anisotropy to decay by a factor of e, $\tau_{1/e}$, and the stretching exponent β_{KWW}. The reorientation of the DPPC probes has been previously reported to be a good reporter for the α (segmental) relaxation of PMMA above T_g in the absence of deformation as evidenced by probe reorientation and τ_α from dielectric spectroscopy displaying the same temperature dependence under these conditions.[35] Changes in segmental dynamics as reported by probes during constant stress[16, 22, 23, 34-37] and constant strain rate deformation[17, 18] are qualitatively consistent with those observed in simulation work[14, 15, 22, 23] and predicted by theory.[8, 9] As these simulation and theoretical studies do not incorporate fluorescent probes, this agreement yields further support for the probes as a good reporter for segmental dynamics.

For the experiments reported here, β_{KWW} does not significantly change during the course of the experiment, including immediately after the reversing deformation, and is fixed to a value of 0.31 during the r(t) fitting. During both constant strain rate[18] and constant stress[16, 23, 35] deformation, β_{KWW} can increase; this increase is associated with the enhancement of segmental dynamics during deformation.[18, 35] Based on a previously-reported relationship between β_{KWW} and enhancement of dynamics during constant strain rate deformation,[18] we anticipate β_{KWW} to

reach a maximum value of 0.4 during the reversing deformations employed in this study and immediately decrease upon unloading. Prior probe reorientation studies which investigated the recovery period after a constant stress deformation show a rapid decrease of β_{KWW} to its value in the absence of deformation at a temperature close to the one employed in the present study.[37] Data was also analyzed without fixing β_{KWW}; although the data showed more noise, the general trends in the data did not change.

Results

In this section, we present results which outline how reversing constant strain rate deformations of varying magnitude change segmental dynamics and subsequent mechanical properties of a polymer glass. Implications of the data in light of existing theories and simulations in the literature will be outlined in the Discussion section.

Figure 1 shows a schematic of the protocol used in both the probe reorientation and purely mechanical experiments to evaluate rejuvenation. Figure 1a shows the probe reorientation measurement protocol; Figure 1b shows the purely mechanical protocol. In each case, the lightly cross-linked samples were held below T_g in the absence of stress or strain for 9300 seconds, at which time a reversing constant strain rate deformation was applied. For each deformation, a rate of 1.55×10^{-4} s^{-1} was applied to a set strain and then the strain was reversed at the same rate until a stress of 0.2 MPa was reached. The total time elapsed during the reversing deformation ranged from 110 to 1020 seconds for these experiments. Further retraction of the sample was then programmed to maintain a stress of 0.2 MPa or less. The protocol for the mechanical experiment shown in Figure 1b is identical to Figure 1a with the exception of an additional constant strain rate deformation performed 1200 seconds after the reversing

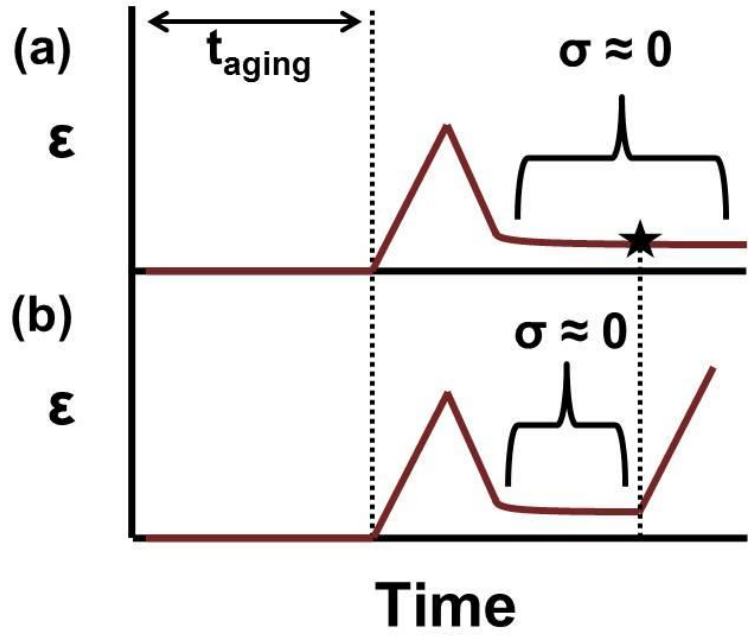

Figure 1. Schematic diagram illustrating the mechanical protocol utilized during probe reorientation experiments (a) and purely mechanical experiments (b). In panel (a), $\tau_{1/e}$ for the purposes of determining rejuvenation was reported for a fixed time after the end of the deformation, as shown by the star. This same fixed time was imposed as a waiting time between the reversing deformation and second constant strain rate deformation in panel (b).

deformation. The time at which rejuvenation is evaluated in the probe reorientation measurement is represented by the star in Figure 1a, which also corresponds to the beginning of the second constant strain rate deformation in Figure 1b. Further discussion of the post-deformation stress and imposed waiting time may be found in the Experimental Methods section. The schematic in Figure 1 is not shown to scale in order to more clearly highlight the deformation protocol.

Figure 2 shows mechanical data collected during the deformation phase of Figure 1a. As can be seen in the data, reversing deformations spanning the pre-yield, yield, and strain softening regimes are represented. Probe reorientation measurements were monitored in a local region of the sample and strains reported in the legend represent the maximum attained strain in the local measurement region. The samples employed in this study are not uniform in thickness and deform inhomogeneously after yield; strain builds up 2-3 times faster in the local measurement region after yield (see Experimental Methods section). The time axis in Figure 2 represents the total elapsed time since the sample reached the DSC T_g of 395 K; deformation commences at a time of 9300 seconds after T_g is reached.

Figure 3 shows the evolution of $\tau_{1/e}$ before and after the reversing deformations shown in Figure 2. In the absence of deformation, $\tau_{1/e}$ evolves toward equilibrium as shown by the solid line, which represents a linear fit to the aging data set on a log-log plot of $\tau_{1/e}$ vs. aging time. After small pre-yield reversing deformations, very little change is seen from this base aging trajectory; however, significant departure from the aging trajectory is seen in the case of large pre-yield deformation. As can be seen in Figure 3, the decrease of $\tau_{1/e}$ from the aging trajectory appears to saturate after deformations which reach several times the yield strain. It should be

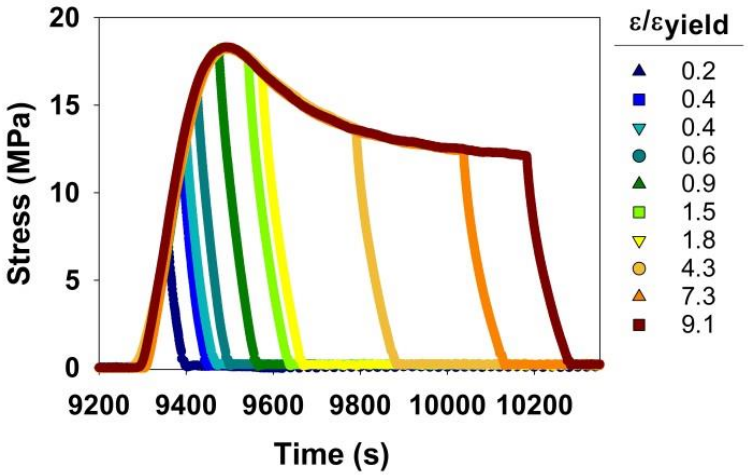

Figure 2. Evolution of stress during the reversing deformation for the protocol outlined in Figure 1a. All deformations were started at a fixed waiting time of 9300 seconds and reversed at different strains. Strains reported in the legend reflect the maximum strain attained in the local measurement area during the deformation, relative to the yield strain. At the conclusion of the deformation, a stress of 0.2 MPa or less was maintained for the remainder of the experiment.

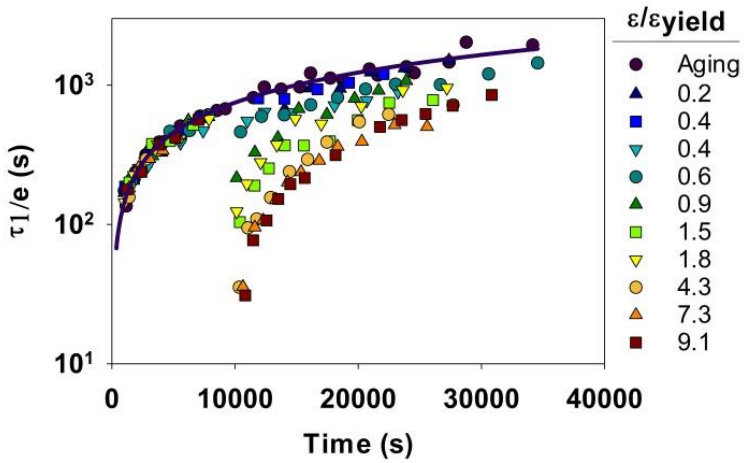

Figure 3. Evolution of $\tau_{1/e}$ before and after the reversing deformation. Deformation was started at a fixed waiting time of 9300 seconds and reversed at different strains. Strains reported in the legend reflect the maximum strain attained in the local measurement area during the deformation, relative to the yield strain. The solid line is a fit to physical aging data obtained in the absence of deformation and represents $\tau_{1/e} \propto t^{+0.72}$.

noted that all data points in Figure 3 were collected at a stress of 0.2 MPa or less; this small stress is not expected to impact $\tau_{1/e}$ as discussed in the Experimental Methods section.

Using the probe reorientation technique, the level of rejuvenation at a fixed time after a reversing constant strain rate deformation was determined by the decrease in $\tau_{1/e}$ relative to the aging curve. Because all of the reversing deformations began at the same aging time and were of varying magnitudes, the end time of each reversing deformation increased with increasing strain; to limit systematic bias due to the end time of each deformation, for each deformation $\tau_{1/e}$ was reported at constant time of 1200 seconds after the end of deformation by interpolation of the data. Rejuvenation was then determined by setting a linear scale from 0% - 100% based on the decrease in $\log(\tau_{1/e})$ from the aging trajectory, where 0% represents no change from the generic aging curve and 100% rejuvenation represents the ~1.3 decade decrease in $\tau_{1/e}$ found after the deformation of the largest strain. Typically, the first optical measurements after the reversing deformation were collected ~1000 seconds after the end of the deformation; this waiting period was chosen to allow for interpolation in the vicinity of collected data. The interpolation was not performed for the deformation which reached lowest strain due to the lack of data at short times after the deformation.

Figure 4 displays two examples of the mechanical data used to evaluate rejuvenation from a purely mechanical experiment. After each reversing constant strain rate deformation, the glass is held for 1200 seconds at ~0.2 MPa before a second constant strain rate deformation is applied as outlined in Figure 1b. The decrease of the yield stress as compared to the yield stress in the absence of prior deformation (difference between the black and green dashed lines) is used to assess rejuvenation. Similar to the probe reorientation measurement, rejuvenation was evaluated on a linear scale of 0% to 100% based on the reduction of the yield stress, where 0%

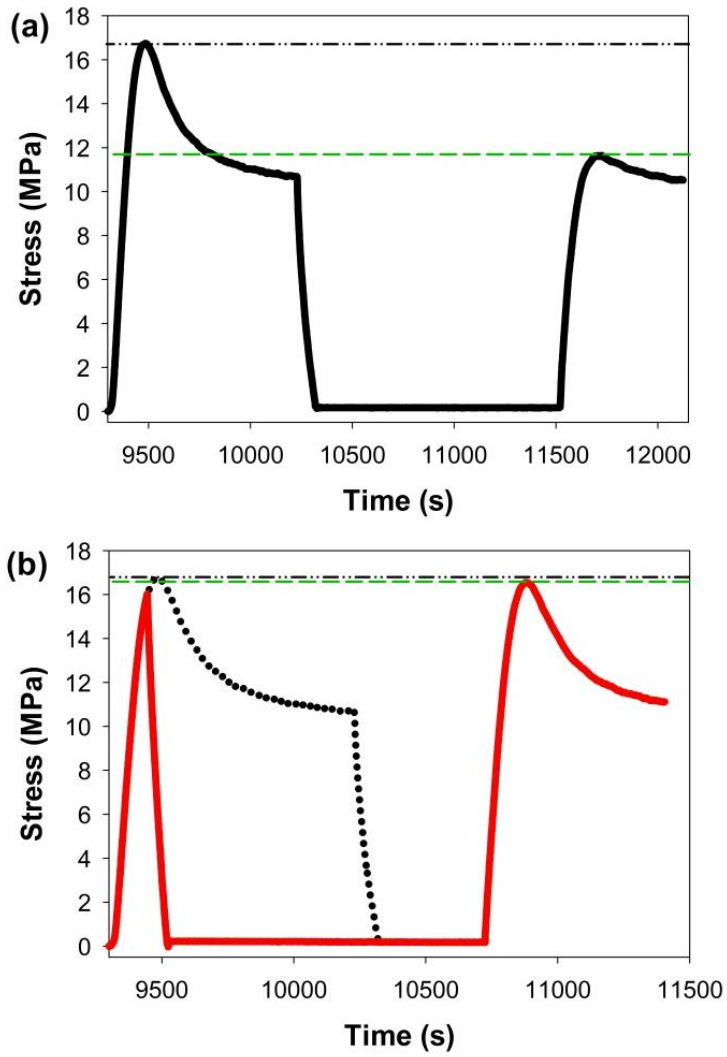

Figure 4. Two representative sets of mechanical data obtained by the protocol described in Figure 1b. Panel (a) shows the largest post-yield deformation (5.6 ε_{yield}), resulting in a significant reduction in the yield stress upon a second constant strain rate deformation. Panel (b) demonstrates that a 0.8 ε_{yield} reversing deformation (red) does not significantly alter the subsequent mechanical properties of the glass. The black and green dashed lines mark the original and post-deformation yield stresses, respectively. The reversing portion of the mechanical data in Figure 4a is overlaid in Figure 4b (black) as a reference of the unaltered mechanical properties of the glass.

rejuvenation corresponded to a yield stress in the absence of prior deformation (16.9 MPa) and 100% rejuvenation corresponded to the maximum reduction seen in the yield stress for a reversing deformation to a maximum of 5.6 ε_{yield} (11.7 MPa). Panel a shows the largest post-yield deformation surveyed which attained a strain of 5.6 ε_{yield}, demonstrating a near-erasure of the large overshoot peak in the second deformation. However, even for large pre-yield deformations, the yield stress is not significantly reduced. This is demonstrated in Panel b, where a reversing deformation that reached a maximum strain of 0.8 ε_{yield} reduced the yield stress during the second constant strain rate deformation from 16.9 MPa to 16.6 MPa. Large post-yield deformation is associated with the reduction or loss of the overshoot peak in a subsequent constant strain rate deformation;[27, 40] we attribute the small overshoot peak we observe at the largest strain surveyed to partial recovery of the overshoot during our imposed 1200 second waiting time (see Experimental Methods section).

Figure 5 shows the calculated percent rejuvenation after reversing deformations from the probe reorientation experiment and purely mechanical experiment. At strains greater than the yield strain (solid vertical line), the mechanical and optical measures of rejuvenation show strong agreement, with % rejuvenation gradually increasing until at least five times the yield strain. For strains lower than the yield strain, the probe reorientation method displays greater evidence of rejuvenation as compared to the mechanical experiments. The solid line shows percent rejuvenation based on theoretical calculations from reference 9. Comparison between rejuvenation measures from the mechanical experiments, optical experiments and theory will be further explored in the Discussion section.

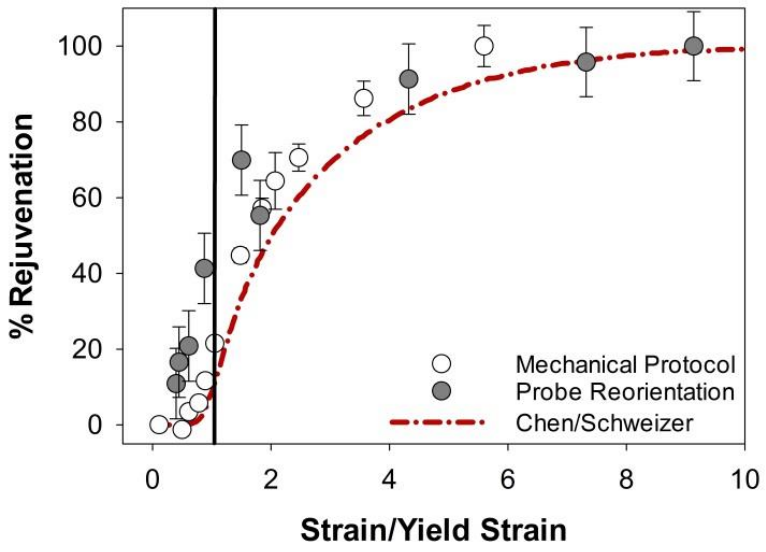

Figure 5. % Rejuvenation vs. normalized strain as analyzed through the purely mechanical protocol (reduction in yield stress), probe reorientation measurement (reduction in $\tau_{1/e}$), and reference 9 (increase in S_0 during constant strain rate deformation). Data points represent measurements conducted 1200 seconds after the conclusion of each deformation. Dashed line represents calculations for PMMA glass deformed in tension at a constant strain rate. Solid line marks strain at yield.

Discussion

Figures 3-5 demonstrate a gradual build-up of rejuvenation signatures with strain and also demonstrate a difference in markers of rejuvenation as measured by probe reorientation and a purely mechanical experiment. These figures will form the basis for this Discussion section. We first use our results to test the mechanisms of the NLE theory.[8, 9] We then explore the apparent difference between markers of the rejuvenation mechanism, as monitored by probe reorientation as compared to other techniques. Finally, we compare the recovery of segmental dynamics after reversing deformations to simulations of Smessaert and Rottler;[38] similar trends are observed in both simulation and experiment.

Comparison to theoretical and modeling work

Several theoretical models exist in the literature which describe the evolution of segmental dynamics during the deformation of polymer glasses; one such theory from Chen and Schweizer[8, 9] has predicted changes in segmental dynamics during constant stress and constant strain rate deformation consistent with reported experimental[16-18] and simulation[14, 15] studies. In their theory, Chen and Schweizer build in two mechanisms to allow for changes in segmental dynamics during deformation. The first of these mechanisms is what we will term the landscape tilting mechanism, in which stress acts to lower free energy barriers for rearrangements, but does not change the position of the system on the potential energy landscape. The second of these mechanisms is the rejuvenation mechanism, which takes effect at sufficiently high strains and can act concurrently with the landscape tilting mechanism. The rejuvenation mechanism accelerates segmental dynamics by driving the system higher on the potential energy landscape where barriers are lower. In the theory, the marker for the rejuvenation mechanism is an increase

in the amplitude of local density fluctuations S_0. During tensile constant strain rate deformation, S_0 remains constant (indicating that the rejuvenation mechanism is not active) up until roughly 60% of the yield strain. As strain continues to increase, the rejuvenation mechanism becomes active and S_0 begins to gradually increase, experiencing the fastest increases early in the strain softening regime. Saturation of S_0 does not occur until strains at least eight times the yield strain, suggesting that saturation of the rejuvenation mechanism does not occur until the system reaches strains far beyond yield.

By monitoring changes in segmental dynamics before and after reversing constant strain rate deformations, we provide a test of the mechanisms employed in the NLE theory.[8, 9] In the framework of this theory, the landscape tilting mechanism is only active when stress is applied to the glass. Thus, when stress is removed after the reversing deformations in the present study, any enhancement of dynamics due to the landscape tilting mechanism should also be removed, and the only remaining active mechanism to enhance dynamics should be the rejuvenation mechanism. By separating out the landscape tilting mechanism contributions from our post-deformation measurements of $\tau_{1/e}$, we determine the level of strain required for the rejuvenation mechanism to become active.

As can be seen in Figure 5, the activity of the rejuvenation mechanism in the NLE theory[8, 9] as characterized by an increase in S_0 as a function of strain shows close agreement with both experimental measurements of rejuvenation in the post-yield regime. In all cases, rejuvenation gradually develops as a function of strain up until at least five times the yield strain. However, investigating the pre-yield regime reveals that the probe reorientation measurements show systematically higher levels of rejuvenation than both the mechanical measurements and the theory. In Figure 5, we have defined rejuvenation for calculations provided by the theory[9]

(PMMA, 10^{-3} s^{-1} constant strain rate, T_g - 10 K, pre-aging time = 10^5 s) by setting a percent rejuvenation scale based on the increase of S_0. A rejuvenation level of 0% corresponds to the value of S_0 at the start of deformation, and 100% rejuvenation corresponds to the value of S_0 at 11 ε_{yield}; minimal increase in S_0 is observed after 7 ε_{yield}. The calculations to which we compare were selected to most closely mimic the conditions we used; however, different temperatures, strain rates, and aging times demonstrate very similar trends in rejuvenation activity.

We emphasize here that although we interpret our protocol to separate out the landscape tilting and rejuvenation mechanisms of the NLE theory, theoretical calculations using exact reversing deformation protocol we employ may allow for a more direct comparison. The calculations used for comparison from reference 9 reflect a PMMA glass undergoing tensile constant strain rate deformation. Such reversing deformation calculations are beyond the scope of the present work. However, particularly in light of the broad qualitative agreement between all measures of rejuvenation of Figure 5, we anticipate that such calculations will support the qualitative conclusions of the present work.

The qualitative differences between the pre-yield probe reorientation and theory calculations of Figure 5 may also be related to the presence of spatially heterogeneous dynamics. The theory provides calculations using a single relaxation time, while it is known that supercooled liquids and glasses display spatially heterogeneous dynamics.[43-46] Using the probe reorientation technique, Lee et al. previously showed that flow-state deformation can narrow the distribution of relaxation times in a polymer glass, as reported by the KWW parameter β.[35] This was also observed in further experimental studies of polymer glasses undergoing constant stress[16, 23, 35] and constant strain rate[17, 18] deformation. In a constant strain rate deformation, β may significantly increase (indicating more homogeneous dynamics) during the pre-yield

regime.[17, 18] Although we do not observe increased values of β for the results reported here, changes after the deformation within the uncertainty of β from these experiments (±0.05) may occur after the reversing deformation, indicating small evolutions in the spectrum of relaxation times. Such small changes in β may be associated with the enhanced values of $\tau_{1/e}$ after pre-yield reversing deformations. We provide further discussion of an alternate explanation for enhanced dynamics after the pre-yield reversing pulses below. Additionally, we discuss of the Stochastic Constitutive Model of Medvedev and Caruthers,[6] which may explain the apparent pre-yield rejuvenation effects we observe in the optical experiment.

Difference between probe reorientation and mechanical measures of rejuvenation

Although differences in the pre-yield regime exist between the probe reorientation and theoretical calculations of rejuvenation, these differences are also present between the mechanical and optical results, as may be observed by investigating the data points of Figure 5. Rejuvenation effects from a mechanical perspective have been well-studied and the absence of significant signs of rejuvenation in the pre-yield regime that we observe in the mechanical data are consistent with previous reports of Struik,[47] Smith,[48] Bauwens,[41] McKenna,[25] and their coworkers. However, it is unclear to what extent these macroscopic mechanical measurements report the molecular-level dynamics within the polymer glass system during all phases of deformation. For example, evidence in the literature exists which may imply that mechanical measurements provide different information in the pre- and post-flow regimes. During a constant strain rate deformation, studies authored by Caruthers,[28, 29, 49] Wang,[30] and their coworkers have found a linear relationship in log-time between the initial rate of stress decrease or a shift factor and applied strain rate during stress relaxation in the post-yield regime. This

relationship is similar to what has been previously reported during flow-state deformation via probe reorientation experiments.[16-18, 22, 35, 36] However, probe reorientation experiments register orders of magnitude increases in segmental mobility between the pre-yield and post-yield regimes; such increases have not yet been qualitatively observed in these nonlinear mechanical measurements.

Our observed rejuvenation after pre-yield reversing deformations demonstrates similarities with recent work of Caruthers and coworkers which investigates the build-up of stress after a reversing mechanical deformation.[50] In their work, the mechanical protocol is similar to that of the present work with the chief difference that the strain is fixed after the deformation (in the present work, strain is allowed to decrease after the deformation to maintain a near-zero stress). The protocol of Caruthers and coworkers results in a subsequent increase of stress, which is termed the stress memory effect. Caruthers and coworkers[50] observe the stress memory effect for deformations of all magnitudes surveyed; the magnitude of the stress overshoot after the reversing deformation increases with strain and appears to reach a maximum at large strains. We note that it is unclear whether the magnitude of the stress memory effect is an indicator of the rejuvenation mechanism, although the qualitative behavior of this stress magnitude is similar to that of the experimental data in the present work.

The Stochastic Constitutive Model (SCM) of Medvedev and Caruthers[6] has been used to investigate multi-step deformations, including those involving the stress memory effect;[50] it may be possible for the SCM to provide insight into the qualitative features of the present results. A major feature of the SCM as compared to other models in the literature is its ability to track how the distribution of relaxation times (also called the relaxation spectrum) changes during aging and deformation. This is in contrast to models which assume only a single relaxation time as

well as those which do not assume that the relaxation spectrum does not change its shape during deformation. The SCM model provides a window into dynamic heterogeneity by calculating changes in dynamics during within a series of domains, which may be characterized as being initially soft (fast-relaxing) or rigid (slow-relaxing). During a constant strain rate deformation, the relaxation spectrum drastically narrows before yield; this narrowing is due to a disproportionate acceleration of dynamics within the slowest-relaxing domains.

The SCM[6] may provide a mechanism through which local rejuvenation effects may be present in the pre-yield regime of deformation, although the glass has not experienced macroscopic yield. Based on the calculated behavior of the relaxation spectrum, it may be qualitatively inferred by the SCM model that in the (macroscopic) pre-yield regime, the slowest-relaxing (rigid) regions become soft and locally yield. In our reversing deformation experiments, enhancements in dynamics associated with these local yielding events would not reverse with stress and may thus remain after the reversing deformation. This explanation from the SCM, however, does not resolve the apparent difference between the mechanical and optical measurements of the present work. However, the difference between the mechanical and optical results of this work may be due to the populations of segments preferentially sampled by the two techniques. For example, work of Kim et al.[49] investigating the initial stress relaxation response following a constant strain rate deformation demonstrated that for deformation conditions closest to the linear viscoelastic response regime, the initial rate of stress relaxation was fastest at low strains. To explain this observation, Kim et al.[49] derived the strain-dependent stress relaxation response for a system with a spectrum of relaxation times in the linear response regime; this derivation is consistent with the idea that at low strains, the mechanical response is more heavily weighted by the fastest-relaxing segments. If this idea can be applied to a nonlinear deformation,

the difference between the optical and mechanical experiments of the present work may be resolved. In this case, the mechanical signatures of rejuvenation may be less influenced by contributions of the slowest-relaxing segments, which are more likely to locally experience yield. Thus, the optical and mechanical measures of rejuvenation may be preferentially sampling differing populations of relaxing segments.

Recovery from mechanical perturbation

Smessaert and Rottler[38] have simulated dynamics of a polymer glass system during the recovery period after reversing constant stress and constant strain rate deformations; our post-deformation optical results are overlaid on select constant strain rate simulations (lines) in Figure 6. Here, the y-axis normalizes τ (simulation) or $\tau_{1/e}$ (experiment) to its value in the absence of deformation at an aging time of t_a (the total elapsed time immediately after the deformation). The x-axis normalizes t_r, the time elapsed in the recovery period after stress is removed, to t_a. For a glass with no imposed deformation, dynamics approximately follow a horizontal line at $\tau_{1/e} / \tau_{1/e,0} = 1$ until a value of $t_r/t_a = 1$ is approached, after which the glass continues to age following a characteristic slope μ associated with the aging dynamics. For highly deformed glasses, dynamics in the simulation follow this characteristic line associated with aging dynamics at times of $t_r/t_a < 1$. Strains reflected in the legend reflect the remaining strain in the glass (simulation) or local measurement area (experiment) at the point where stress reaches ~0 after the reversing deformation. These strains are then normalized to the appropriate yield stress (3.0% in the experiment, 6.0% in the simulation). For the experiment, this local strain was estimated by subtracting the engineering strain decrease during unloading from the maximum strain in the local area attained during the reversing deformation. The lines representing the

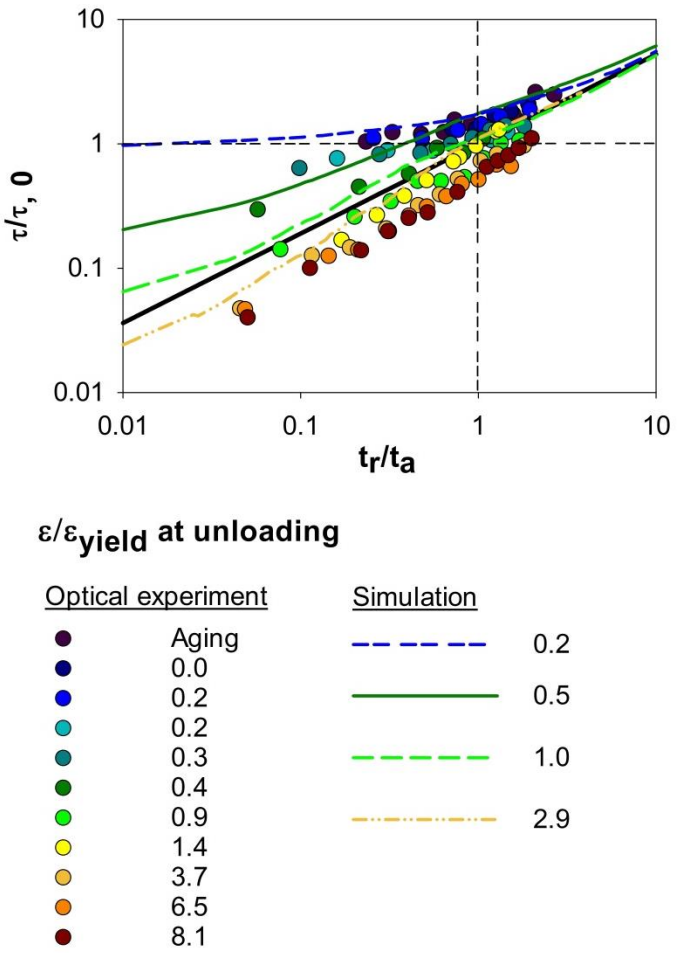

Figure 6. Post-deformation normalized τ vs. normalized time for both the present work (data points) and simulations of reference 38 (lines). The y-axis represents τ (simulation) or $\tau_{1/e}$ (present work) normalized to its quiescent value at the end of deformation; the x-axis normalizes the elapsed time in the recovery regime to the total aging time of the sample at the end of the deformation. Solid black line indicates slope μ associated with the generic aging behavior in the experiment μ = 0.72. Simulation results smoothed and adjusted for differing μ as described in-text. Here, values in the legend represent the remaining strain immediately after the reversing deformation, rather than the maximum strain attained during deformation. In reference 38, the yield strain of the glass is roughly 6.0%, while the yield strain in the present work is 3.0%.

simulation data were obtained by smoothing the raw simulation results; the values of τ within these smoothed lines on a log-log scale were then multiplied by a factor of 0.72/0.89 to account for the difference of μ between experiment and simulation (μ=0.72 in the experiment, μ~0.89 in the simulation).[38]

As can be seen in Figure 6, the enhancement in dynamics and recovery behavior is strikingly similar to that of the optical experiments performed in the present work; particularly notable is the observed agreement at low strains. Based on the measure of rejuvenation used for the optical experiments of our study, the simulation work of Smessaert and Rottler supports our findings of molecular-level rejuvenation activity for some large pre-yield reversing deformations. For example, post-deformation strains which are 30-50% of yield show significant departure from the aging trajectory; the optical data sets within this strain range reflect reversing deformations within the pre-yield regime which show 20-40% rejuvenation in Figure 5, and it may be inferred that the same is true for the simulation data. Simulation results at additional strains reported by Smessaert and Rottler[38] (not shown) are also consistent with a gradual increase in enhanced dynamics, even at very low strains. The agreement of the low-strain simulation and optical results of Figure 6 supports the idea that the rejuvenation mechanism demonstrates significant activity in the pre-yield regime.

As strain increases in the simulations of Smessaert and Rottler,[38] the enhancement of dynamics observed at lower strains increases and then saturates at sufficiently high strains; this feature of the simulations is also consistent with the results reported in this work. In Figure 6, it may be observed that within the optical data, the data sets of the three highest strains nearly overlap. This feature of the simulation is also consistent with the general behavior of Figure 5

observed in the mechanical, optical, and theoretical measures of % rejuvenation, with the rejuvenation mechanism saturating at sufficiently high strains.

Although the simulation[38] and optical results broadly agree, at large strains the experimental results do not recover the generic aging behavior of the glass (solid black line) at a recovery period representing $t_r/t_a = 1$ as anticipated by the simulations. Rather, the optical results show that for the largest deformations, dynamics are still significantly enhanced (relative to the non-deformed glass) at a recovery time equal to the original age of the glass at the end of deformation. This enhancement of dynamics may be associated with large structural changes during deformation associated with a polyamorphic phase transition, as described by McKenna.[25] We point out that slight differences exist in mechanical protocol between simulation and experiment; the experiment applies and reverses deformation at the same rate, while in the simulations, stress is unloaded at a near-instantaneous rate. However, because the unloading period in the experiment represents a small fraction of the pre-deformation aging time (1.1% maximum), this difference in protocol is unlikely to affect the qualitative comparison between simulation and experiment.

An enhancement of dynamics in the pre-yield regime was also observed in the work of Lee et al., who investigated aging after constant stress deformations.[37] In the work of Lee et al, both pre-flow and flow-state constant stress deformations were applied; evolution in dynamics was monitored during all stages of deformation and recovery. After pre-flow deformation, segmental dynamics were transiently faster in recovery; however, the original aging behavior was eventually recovered within an additional time period of t_a.[37] However, for deformations which reached flow, the polymer glass displayed behavior akin to a much younger glass. In the work of Lee et al, the aging behavior following a large-magnitude deformation could be partially

superimposed onto the original aging trajectory by shifting by a time slightly larger than the age of the glass at the time of the removal of stress. This additional time shift is consistent with an observed remaining enhancement of dynamics at $t_r/t_a = 1$ in the current work. We believe that the qualitative similarities between the present work and the work of Lee et al. support the ideas from the work of Rottler and Smessaert,[38] who do not observe fundamental differences between the type of deformation imposed on the recovery behavior in their work.

Lyulin and coworkers[51] investigated signatures of mechanical rejuvenation in a united-atom model of atactic polystyrene during and after large shear cyclic deformations. In these simulations the observed storage and loss moduli continued to decrease or increase, respectively, toward a steady state value during several flow-state shear cycles. This evolution of mechanical properties in the simulations is consistent with the gradual development of the rejuvenation mechanism as described in the present work. Additionally, Lyulin and coworkers[51] provided calculations of segmental dynamics by fitting the –CH–C– (side chain) bond vector orientational autocorrelation function to a stretched exponential form. The behavior of their extracted τ values before and after cyclic deformation are qualitatively consistent with the reported results of Figure 3, with decreased τ immediately after deformation , which then continues to grow after the deformation. We note that the work of Lyulin and coworkers[51] was performed on capped, 5 nm films and demonstrates confinement effects; however, the qualitative features associated with rejuvenation reported in their work are not anticipated to be attributed to confinement.

Concluding Remarks

In this work, we have demonstrated that using both mechanical and optical measures, the rejuvenation mechanism during deformation gradually develops and saturates at strains at least

five times the yield strain. The results of this work are broadly qualitatively consistent with the NLE theory of Chen and Schweizer;[8, 9] however, in the pre-yield regime, significantly larger levels of rejuvenation are found via the optical probe reorientation technique employed in the present work. The pre-yield rejuvenation findings of the optical technique are consistent with reversing constant strain rate and constant stress deformation simulations of Smessaert and Rottler.[38] This work provides a valuable experimental benchmark for theories to test a reversing deformation, which is often difficult to accurately model. With an advanced theoretical understanding of the fundamental physics of polymer glass deformation, these versatile materials may be able to be used in a broader range of applications.

In light of the apparent difference between the mechanical and probe reorientation measures of rejuvenation in the pre-yield regime, additional studies are required to understand the observed difference in measurements using these two techniques. However, we note here that due to the difference in the protocol of the calculations of the theory and the experimental protocol used here, these differences may be able to be resolved through calculations of the theory which use a reversing constant strain rate deformation protocol. Additionally, a theory of Medvedev and Caruthers[6] which takes into account a heterogeneous spectrum of segmental relaxation may be able to resolve this difference.

Acknowledgements

We thank the National Science Foundation (DMR – 1404614) for support of this research. We thank Josh Ricci, Kelly Suralik, and Trevor Bennin for assistance with experiments and helpful discussions. We additionally thank Ken Schweizer, Joerg Rottler, Jim

Caruthers, Grigori Medvedev, Anton Smessaert, and Michael Tylinski for helpful discussions.

We thank Lian Yu and Travis Powell for assistance with DSC measurements.

References

1. Eyring, H. *Journal of Chemical Physics* **1936,** 4, (4), 283-291.
2. Klompen, E. T. J.; Engels, T. A. P.; Govaert, L. E.; Meijer, H. E. H. *Macromolecules* **2005,** 38, (16), 6997-7008.
3. De Focatiis, D. S. A.; Embery, J.; Buckley, C. P. *Journal of Polymer Science Part B: Polymer Physics* **2010,** 48, (13), 1449-1463.
4. Schapery, R. A. *International Journal of Solids and Structures* **1966,** 2, (3), 407-425.
5. Fielding, S. M.; Larson, R. G.; Cates, M. E. *Physical Review Letters* **2012,** 108, (4), 048301.
6. Medvedev, G. A.; Caruthers, J. M. *Journal of Rheology* **2013,** 57, (3), 949-1002.
7. Knauss, W. G.; Emri, I. *Polymer Engineering & Science* **1987,** 27, (1), 86-100.
8. Chen, K.; Schweizer, K. S. *Physical Review E* **2010,** 82, (4), 041804.
9. Chen, K.; Schweizer, K. S. *Macromolecules* **2011,** 44, (10), 3988-4000.
10. Chen, K.; Schweizer, K. S. *Macromolecules* **2008,** 41, (15), 5908-5918.
11. Chen, K.; Schweizer, K. S. *Journal of Chemical Physics* **2007,** 126, (1), 014904.
12. Meijer, H. E. H.; Govaert, L. E. *Progress in Polymer Science* **2005,** 30, (8-9), 915-938.
13. Debenedetti, P. G.; Stillinger, F. H. *Nature* **2001,** 410, 259-267.
14. Riggleman, R. A.; Schweizer, K. S.; de Pablo, J. J. *Macromolecules* **2008,** 41, (13), 4969-4977.
15. Riggleman, R. A.; Toepperwein, G. N.; Papakonstantopoulos, G. J.; de Pablo, J. J. *Macromolecules* **2009,** 42, (10), 3632-3640.
16. Lee, H. N.; Paeng, K.; Swallen, S. F.; Ediger, M. D. *Science* **2009,** 323, (5911), 231-234.

17. Bending, B.; Christison, K.; Ricci, J.; Ediger, M. D. *Macromolecules* **2014,** 47, (2), 800-806.

18. Hebert, K.; Bending, B.; Ricci, J.; Ediger, M. D. *Macromolecules* **2015,** 48, (18), 6736-6744.

19. Warren, M.; Rottler, J. *Journal of Chemical Physics* **2010,** 133, (16), 164513.

20. Chung, Y. G.; Lacks, D. J. *Macromolecules* **2012,** 45, (10), 4416-4421.

21. Chung, Y. G.; Lacks, D. J. *Journal of Polymer Science Part B: Polymer Physics* **2012,** 50, (24), 1733-1739.

22. Lee, H. N.; Riggleman, R. A.; de Pablo, J. J.; Ediger, M. D. *Macromolecules* **2009,** 42, (12), 4328-4336.

23. Riggleman, R. A.; Lee, H. N.; Ediger, M. D.; de Pablo, J. J. *Soft Matter* **2010,** 6, (2), 287-291.

24. McKenna, G. B.; Zapas, L. J. *Polymer Engineering & Science* **1986,** 26, (11), 725-729.

25. McKenna, G. B. *Journal of Physics: Condensed Matter* **2003,** 15, (11), S737.

26. Yee, A. F.; Bankert, R. J.; Ngai, K. L.; Rendell, R. W. *Journal of Polymer Science Part B: Polymer Physics* **1988,** 26, (12), 2463-2483.

27. Govaert, L. E.; van Melick, H. G. H.; Meijer, H. E. H. *Polymer* **2001,** 42, (3), 1271-1274.

28. Lee, E. W.; Medvedev, G. A.; Caruthers, J. M. *Journal of Polymer Science Part B: Polymer Physics* **2010,** 48, (22), 2399-2401.

29. Medvedev, G. A.; Kim, J. W.; Caruthers, J. M. *Polymer* **2013,** 54, (24), 6599-6607.

30. Liu, J.; Lin, P.; Li, X.; Wang, S.-Q. *Polymer* **2015,** 81, 129-139.

31. Loo, L. S.; Cohen, R. E.; Gleason, K. K. *Science* **2000,** 288, (5463), 116-119.

32. Zhou, Q. Y.; Argon, A. S.; Cohen, R. E. *Polymer* **2001,** 42, (2), 613-621.

33. Kalfus, J.; Detwiler, A.; Lesser, A. J. *Macromolecules* **2012,** 45, (11), 4839-4847.

34. Lee, H. N.; Paeng, K.; Swallen, S. F.; Ediger, M. D. *Journal of Chemical Physics* **2008,** 128, (13), 134902.

35. Lee, H. N.; Paeng, K.; Swallen, S. F.; Ediger, M. D.; Stamm, R. A.; Medvedev, G. A.; Caruthers, J. M. *Journal of Polymer Science Part B: Polymer Physics* **2009,** 47, (17), 1713-1727.

36. Lee, H. N.; Ediger, M. D. *Journal of Chemical Physics* **2010,** 133, (1), 014901.

37. Lee, H. N.; Ediger, M. D. *Macromolecules* **2010,** 43, (13), 5863-5873.

38. Smessaert, A.; Rottler, J. *Macromolecules* **2012,** 45, (6), 2928-2935.

39. D1708-10, Standard Test Method for Tensile Properties of Plastics by Use of Microtensile Specimens. ASTM International: West Conshohocken, PA, 2011; pp 1-5.

40. van Melick, H. G. H.; Govaert, L. E.; Raas, B.; Nauta, W. J.; Meijer, H. E. H. *Polymer* **2003,** 44, (4), 1171-1179.

41. Bauwens-Crowet, C.; Bauwens, J. C. *Polymer* **1988,** 29, (11), 1985-1989.

42. Maher, J. W.; Haward, R. N.; Hay, J. N. *Journal of Polymer Science: Polymer Physics Edition* **1980,** 18, (11), 2169-2179.

43. Ediger, M. D. *Annual Review of Physical Chemistry* **2000,** 51, 99-128.

44. Richert, R. *Journal of Physics-Condensed Matter* **2002,** 14, (23), R703-R738.

45. Ediger, M. D.; Harrowell, P. *Journal of Chemical Physics* **2012,** 137, (8), 080901.

46. Smessaert, A.; Rottler, J. *Soft Matter* **2014,** 10, (42), 8533-8541.

47. Struik, L. C. E. *Polymer* **1997,** 38, (16), 4053-4057.

48. Ricco, T.; Smith, T. L. *Polymer* **1985,** 26, (13), 1979-1984.

49. Kim, J. W.; Medvedev, G. A.; Caruthers, J. M. *Polymer* **2013,** 54, (15), 3949-3960.

50. Kim, J. W.; Medvedev, G. A.; Caruthers, J. M. *Polymer* **2013,** 54, (21), 5993-6002.

51. Hudzinskyy, D.; Michels, M. A. J.; Lyulin, A. V. *Macromolecular Theory and Simulations* **2013,** 22, (1), 71-84.

Chapter 4

Concluding Remarks and Suggestions for Future Experimental Directions

Kelly Hebert

Concluding Remarks

Thermally-activated transitions are significant during flow-state deformation

For glassy polymers near T_g, temperature has an observable impact on the mechanical properties; for example, the constant strain rate mechanical curves shown in Chapter 2 differ in yield stress by nearly a factor of 2 across a 16 K temperature window. However, as described in Chapter 2, previously-reported simulations have been interpreted to indicate that during flow, thermally-activated transitions do not significantly contribute to flow-state molecular mobility. Using the probe reorientation technique, this minimal effect of temperature on molecular mobility during flow would most clearly manifest in a single, temperature-independent post-yield relationship between τ and local strain rate. However, experiments described in Chapter 2 demonstrate a significant dependence of flow-state segmental dynamics on temperature. We have estimated that barriers crossed during deformation are roughly $40 \pm 3\ kT_g$; these barriers are reduced ~10-15% relative to the undeformed glass immediately prior to deformation. Considering that barriers at T_g in the absence of deformation are 32 kT, the calculated barriers are indeed significant.

To date, no model (to the author's knowledge) would predict the strikingly large temperature effect on flow-state dynamics of polymer glasses for the deformations described in Chapter 2. For example, as monitored through $\tau_{1/e}$, the flow-state temperature dependence on dynamics in PMMA glasses that we observe in Chapter 2 is at least five times larger than predicted by the Nonlinear Langevin Equation (NLE) theory of Chen and Schweizer.[1] The results reported in Chapter 2 will provide a challenge to models; these results stress the importance of incorporating flow-state temperature effects. As a final note, the experiments of Chapter 2 are performed at a temperature range from T_g-11 K to T_g-27 K; within our group,

lower temperature deformations have proven difficult to achieve with cross-linked PMMA due to sample failure. It is unclear whether the relationship between temperature and flow-state molecular mobility would continue to lower temperatures. If ductile, flow-state deformation can be achieved on glassy systems in our experimental apparatus, a future line of inquiry could involve investigating if (and at what temperature) the relationship between flow-state mobility and temperature ceases to become relevant. Such low-temperature studies may be successful on a more ductile polymer glass system (such as polycarbonate) or a polymer glass which has been made temporarily ductile through pre-deformation.

Rejuvenation effects gradually develop to strains well past yield, as measured mechanically and through the probe reorientation technique

Rejuvenation effects have at times been described in black-and-white terms in the literature; a glass has either been deformed past yield and demonstrates rejuvenation, or the glass has not gone through yield and is not rejuvenated. This view of rejuvenation is not consistent with the work described in Chapter 3, which shows a gradual build-up of rejuvenation that onsets before yield and saturates at strains several times ε_{yield}. For example, the probe reorientation results of Chapter 3 indicate that at yield, the glass is only ~50% rejuvenated. The experimental work described in Chapter 3 broadly agrees with the NLE theory of Chen and Schweizer,[1] as well as simulation work of Smessaert and Rottler.[2]

In the pre-yield regime, probe reorientation and mechanical experiments demonstrate different levels of rejuvenation

As shown in Chapter 3, pre-yield effects of rejuvenation are more strongly observed in probe reorientation measurements than those observed by mechanical measurements. Furthermore, these pre-yield rejuvenation effects are consistent with molecular dynamics simulations of Smessaert and Rottler,[2] which do not incorporate probes. Although there are differences in the pre-yield rejuvenation behavior between optical and mechanical measurements, the origin of this difference is unclear. As discussed in Chapter 3, differences between what is predicted by the NLE theory and the pre-yield optical experiments of this thesis may be related to the absence of spatially heterogeneous dynamics in the theory. Further experiments which compare mechanical and optical measures of molecular mobility may be able to explain the difference in observed pre-yield behavior between the two sets of measurements and provide insight into the populations of segments sampled with each technique.

Suggestions for future experimental directions

The following section discusses two classes of future experiments using the probe reorientation technique. The first set of experiments discussed is based upon reported studies of Roth and coworkers,[3-5] who observe faster aging rates for glasses cooled under stress than those cooled in the absence of stress, as measured via ellipsometry. In combination with our improved deformation apparatus, the probe reorientation technique may provide a molecular-level insight to complement the observations of Roth and coworkers. A second line of inquiry is proposed, seeking to develop rate-switching experiments (i.e. switching the strain rate in the middle of a

constant strain rate experiment) as a possible future experimental tool. Based on these rate-switching deformations, two additional lines of inquiry are proposed.

Investigation of the interaction between deformation and aging in glasses formed under stress

Probe reorientation experiments have been used to investigate the interplay between stress and aging for glasses which were formed stress-free. However, the properties of a glass are also dictated by conditions during the cooling protocol, which includes not only the cooling rate, but stress or strain during cooling. Recent experiments by Roth and coworkers[3-5] have investigated how stress imposed during the formation of a glass affect the subsequent aging rate. In a recent study, Gray and Roth[5] perform their experiments on polystyrene glasses to which a constant stress is applied above T_g. This stress remains on their polymer sample as it is quickly quenched to room temperature. The stress is removed upon cooling, and the aging rate of the glass is then characterized by ellipsometry (by monitoring the evolution of sample thickness over time) at an elevated temperature that is still below T_g. The slope of the normalized film thickness vs. log time is used to calculate the aging rate.

Interestingly, Gray and Roth[5] find two distinct aging rates for the glasses they use, depending on the magnitude of stress applied during the quench. For low stresses (less than ~7 MPa), the glass displays an aging rate characteristic of a glass to which no stress had been applied. At stresses of 7-9 MPa, the aging rate rapidly jumps; glasses to which higher stresses were applied during the quench display a plateau in the aging rate which is ~2 times faster than the low-stress aging rate. The nature of this transition is not yet understood, although the authors found that this transition occurred at a lower stress for a polystyrene sample of lower molecular weight. It should be noted that no stress is applied during measurements of the aging rate.

As described in the introductory chapter of this thesis, the initial position of a glassy system on the potential energy landscape is dependent on the conditions imposed during cooling.[6-8] Roth and coworkers[3, 5] propose that large stresses imposed on the polymer during cooling causes the system to start at a higher position on the potential energy landscape, which is then associated with a faster initial aging rate. However, there are several features of the experiments of Gray and Roth[5] which remain unexplained. A few of these questions include:

1. What is the nature of the sharp transition in aging rate? What is the significance of the stress or strain associated with the transition? In a recent study, Gray and Roth[5] note that the magnitude of applied stress in their studies was limited by sample failure, and that they cannot rule out that an additional transition in aging rate would not occur at higher stresses. Gray has suggested (private communication) that the transition stress or strain in the aging behavior may be associated with yielding during cooling. This is consistent with an idea that flow or post-yield deformation is associated with an erasure of thermomechanical history. Further experiments are necessary to relate the observed aging behavior with mechanical properties of the polymer glass.

2. How is a glass cooled under stress different than a glass cooled in the absence of stress to which stress was applied after cooling? For example, do both glasses age into the same equilibrium state? Mechanical experiments of McKenna,[9, 10] for example, have suggested that deformation acts to induce a polyamorphic phase transition, such that a deformed sample approaches a different equilibrium than an undeformed sample. Although probe reorientation experiments on polymer glasses formed in the absence of imposed stress do not necessarily support the polyamorphic phase transition picture,[11, 12] this may not necessarily hold for glasses

formed under stress. The studies of Gray and Roth are performed far below T_g, where the aging rate reaches a maximum, and thus their measurements do not capture an evolution to equilibrium. However, at temperatures closer to T_g, it may be possible to observe an evolution of properties to equilibrium for a glass cooled in the absence of stress vs. a glass cooled under stress.

3. What is the nature of the role of molecular weight in the observed behavior? The molecular weight of the sample appears to affect the level of stress or strain associated with the transition in aging rate. Would this step in aging rate still occur in a heavily cross-linked system, or is this a feature of uncross-linked, entangled networks?

4. How does aging under stress affect a system's subsequent interaction between aging and stress or mechanical deformation? If cooling under stress does indeed trap the system higher up on the energy landscape as proposed by Gray and Roth,[5] it may be possible for further (small) stresses to accelerate aging instead of acting to counteract aging; this phenomenon has been termed stress aging or overaging. For example, simulations of Lacks et al.[13] and Lyulin et al.[14] found that for glasses trapped high on the energy landscape (for example, by fast cooling[8]), small, cyclic deformations may be associated with faster aging. Earlier work of Kramer[15] indicated that upon resuming a prior flow-state deformation of a polymer glass which had in the intervening time been held under a smaller stress, there was a lag in the deformation before the neck continued to propagate in the sample. Because the sample had appeared to age in the intermittent period between the two larger deformations, Kramer termed this phenomenon stress aging. Work of Klompen et al.[16] found that glasses held under stress prior to a subsequent

constant strain rate deformation exhibited higher yield stresses than those not held under stress. Because growth of the yield stress is associated with physical aging, this result has been interpreted to support the idea of stress aging. Post-yield deformation is also associated with an erasure of prior aging. Although there is no precedence in the literature to suggest that stress during cooling fundamentally changes the flow state of deformation, it may be beneficial to explore whether this relationship still holds for glasses cooled under stress.

5. How does stress during cooling change the distribution of relaxation times in the glass? The ellipsometry measurements of Gray and Roth[5] are able to use the rate of thickness reduction to determine an aging rate; however, these measurements have not yet demonstrated a measure which can provide insight into the distribution of relaxation times within the glass. Medvedev and Caruthers[17] have recently proposed the stochastic constitutive model (SCM) which calculates how deformation changes this distribution of relaxation times during cooling and deformation. The SCM calculates that for a constant strain rate deformation, the distribution of relaxation times significantly narrows. It is reasonable to anticipate that depending on the magnitude, stress imparted during cooling may also significantly alter the shape associated with the spectrum of relaxation times.

Probe reorientation experiments which monitor the evolution of τ, in combination with the improved deformation apparatus developed by our group, may be able to provide further insight into the experimental observations of Gray and Roth.[5] Additionally, probe reorientation experiments may be able to distinguish differences that may exist (or not exist) between the mechanical behavior of glasses cooled under stress or cooled in the absence of stress. Because

the probe reorientation experiments monitor the KWW stretching exponent β (as described in Chapter 1), the probe reorientation experiments may uniquely be able to provide insight into how stress during cooling does (or doesn't) change the distribution of relaxation times upon cooling. To date, probe reorientation experiments have only been used to study glasses which were formed in the absence of imposed stress.[11, 12, 18-24] However, the updated deformation apparatus allows for fixed stress, fixed strain, or a programmed deformation protocol to occur before or during glass formation. Information about how stress imparted during the formation of a glass may provide a test for existing models, which may further guide the processing of these versatile materials.

To study how stress during cooling affects the evolution of τ to equilibrium, our deformation apparatus may be used to impose a set deformation protocol to polymer samples in the melt, which could then be maintained during cooling to a temperature very close to T_g. Because we have developed a flexible deformation apparatus, it would be possible to impose a constant stress, constant strain, or a pre-programmed protocol that would allow us to vary stress or strain during the cooling procedure. It should be noted that a great deal of consideration may need to be taken in planning the deformation procedure during to ensure reproducibility. For example, it may be necessary to precisely control the time that stress or strain is imposed on the sample before beginning the cooling. Additionally, if a constant stress (as monitored by our load cell) is held during cooling, it may be necessary to program the set load cell voltage to adjust during cooling to compensate for any baseline drift in the measurement due to temperature changes. In the absence of stress, our load cell experiences small baseline changes with temperature. Such temperature-dependent changes have not yet affected our measurements, as we have thus far performed experiments at a fixed temperature.

Upon cooling, if a temperature close to T_g is used, τ could be measured as a function of time until equilibrium is reached. A glass not cooled under stress could be used as a comparison system to a glass cooled under stress (the stress may be released upon reaching the testing temperature). Observables obtained during experiments utilizing stress-free and stress-cooled glasses to be compared could include the aging rate, time to equilibrium, value of τ at equilibrium, and the evolution of β over time. Aging rate, as defined by Gray and Roth, is the evolution of the normalized thickness with log time; typical aging rates range from 2 - 8 ($\times 10^{-4}$).[5] In the probe reorientation experiment, aging rates would be defined by the slope of the $\log(\tau)$ vs. log(time) data; Figure 1 shows an example of how this aging rate would be evaluated.

The interaction between stress and aging for glasses cooled under stress and glasses not cooled under stress could also be investigated using the probe reorientation technique and our updated deformation apparatus. For example, does a glass cooled under stress fundamentally behave in the same manner as a glass not cooled under stress, but to which stress is applied after cooling? Additionally, the molecular mobility of these stress-cooled glasses during various deformation protocols could be investigated and compared to those not cooled under stress.

Although all of the published work using the probe reorientation technique uses a lightly cross-linked poly(methyl methacrylate) glass, several other polymer systems are possible for these proposed experiments. For example, Ben Bending has performed preliminary constant stress experiments on polystyrene glasses of varying cross-linking density with the DPPC dye and found that the behavior of molecular mobility during deformation is consistent with published work of poly(methyl methacrylate).[25] Preliminary work in our lab using the DPPC dye dissolved in amorphous, uncross-linked poly(lactic acid)[25] and poly(methyl methacrylate) also show deformation behavior consistent with published work on cross-linked poly(methyl

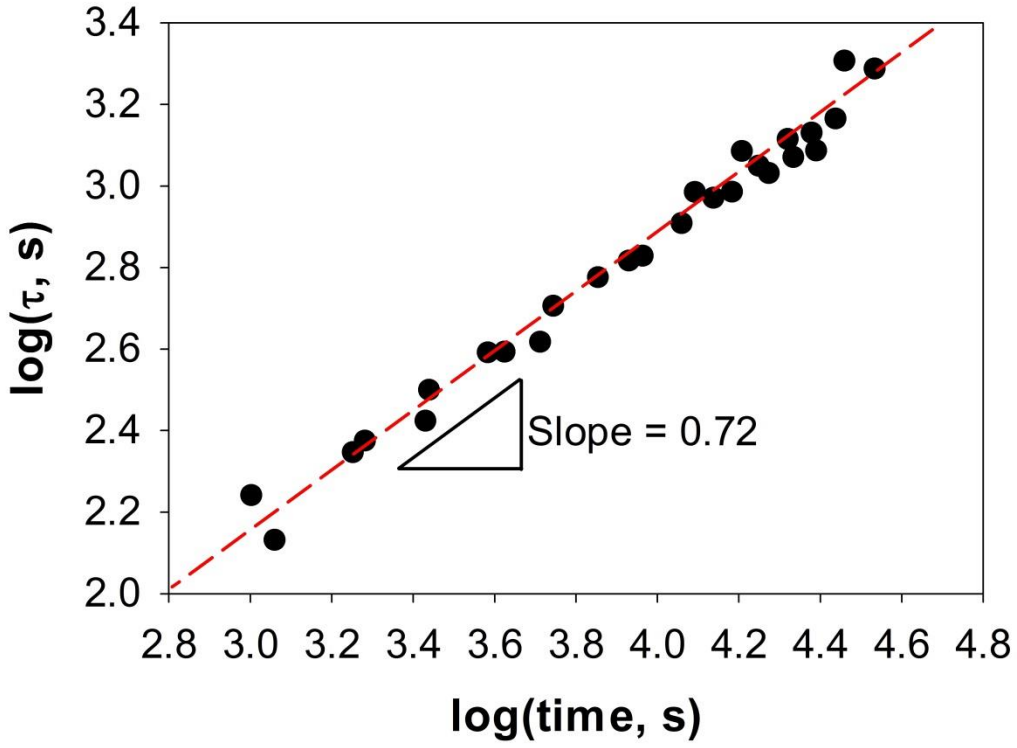

Figure 1. Quiescent log (τ) vs. log(time) behavior for a lightly cross-linked PMMA glass at T_g - 7 K. The slope μ associated with the behavior denotes the aging rate. The y-axis reflects the KWW-derived τ, and the x-axis reflects elapsed aging time, where time = 0 indicates the time at which the sample reached the DSC (10 K/min) T_g of 395 K.

methacrylate).[19] Gray and Roth[5] note that the aging rate effect they observe in their work has a molecular weight dependence. Because of this, it may be necessary to perform experiments using a series of molecular weights.

Under some conditions, glasses have been previously proposed by to experience enhanced aging under stress.[13-16] This concept of overaging (also called stress aging) has been a long-standing interest of our research group; however, overaging has been predicted to most likely occur for low deformation magnitudes and for glasses trapped high on the energy landscape.[13] Unfortunately, below roughly T_g-30 K (in the absence of deformation), relaxation rates in the absence of deformation approaches timescales that are prohibitively slow for our experiments, and many of the polymer glass systems we have previously explored become brittle. If the assertions of Gray and Roth are correct, and stress-cooled glasses do form glasses high on the potential energy landscape, cooling under stress may prove to be a route to study stress aging at temperatures which are more amenable to our experiments. The cooling rate typically used in our experiments (1 K/min) is estimated to be at least three orders of magnitude slower than quenching procedure of Gray and Roth;[5] it may be necessary to cool our samples much more quickly in order to see effects of stress aging at high temperatures. Currently, efforts are underway by Josh Ricci to develop the capability to quickly quench our samples as they are held in the deformation apparatus.

Rate-switching experiments

The experiments described in this thesis impose a constant strain rate deformation, either purely in tension or in a reversing deformation scheme. Experiments performed by former graduate students Ben Bending and Hau-Nan Lee also primarily focus on constant stress or

constant strain rate deformation and recovery. However, work of Lee et al. also has explored multi-step creep experiments,[20] in which a single relationship between τ and strain rate is not found during all phases of the experiment. The experiments that I will be discussing in this section involve running constant strain rate deformations in which the strain rate is switched in the middle of the experiment.

Studies in the literature indicate that it may be possible to reach the same flow state through a rate switching experiment as running an experiment at the final rate. These experiments are interesting from a fundamental perspective of determining how a rate-switching experiment differs from a constant strain rate experiment at the final rate. However, even in the absence of this interest, rate-switching experiments may be used in the future as a tool to more efficiently perform experiments. For example, if an identical flow state at a lower strain rate may be reached by first performing the deformation at a faster strain rate, rate-switching experiments may be used as a more efficient means to explore the strain hardening regime, as will be described below.

This section will also describe experiments which use stress overshoots and undershoots anticipated by rate-switching experiments to explore changes in the stretching exponent β which may be a feature of the stochastic constitutive model of Medvedev and Caruthers.[17] To date, published calculations of their stochastic constitutive model (SCM) have investigated constant strain rate and reversing constant strain rate experiments; however, recently-presented results have indicated that their model may be capable of capturing the behavior of a two-step rate-switching experiment.[26]

Rate-switching experiments - testing the universality of flow

As detailed in the introduction section of this thesis, during a constant strain rate experiment, stress initially increases nearly linearly with strain, followed by an overshoot (yield), the strain softening regime during which stress decreases, and the strain hardening regime during which stress again increases. Instead of imposing a constant rate, some authors[27, 28] have investigated the fundamental behavior of a polymer glass after switching the strain rate in the middle of an experiment.

Some of the earliest strain rate switching work comes from Nanzai,[27] who studies the flow-state behavior of a polymer glass after switching the rate from a high or low strain rate to an intermediate rate. A schematic of the observed behavior of Nanzai[27] is shown in Figure 2. The red curve demonstrates the observed mechanical behavior after switching from a lower strain rate $\dot{\varepsilon}_1$ to a higher strain rate $\dot{\varepsilon}_2$. When switching to a higher strain rate in the middle of an experiment, the stress rapidly increases and experiences a stress overshoot before reaching a steady-state flow. The blue curve shows a schematic of the mechanical behavior after switching from a high strain rate $\dot{\varepsilon}_3$ to a lower strain rate $\dot{\varepsilon}_2$. Upon switching, the stress rapidly decreases and experiences a stress undershoot before displaying steady-state flow. In both curves of Figure 2, which both have the same ending strain rate $\dot{\varepsilon}_2$, the steady-state flow reached is identical, regardless of starting rates $\dot{\varepsilon}_1$ or $\dot{\varepsilon}_3$. This observed mechanical behavior led Nanzai to conclude that the flow state achieved was associated with a particular strain rate and does not depend on how it is reached.[27] Wang and coworkers[28] have also confirmed this mechanical behavior.

Experiments of Hau-Nan Lee et al. have shown that the relationship between log τ and log strain rate during flow can be broken in multi-step experiments.[20] In this set of experiments, Lee et al. performed a four-step constant stress deformation and recovery experiment while

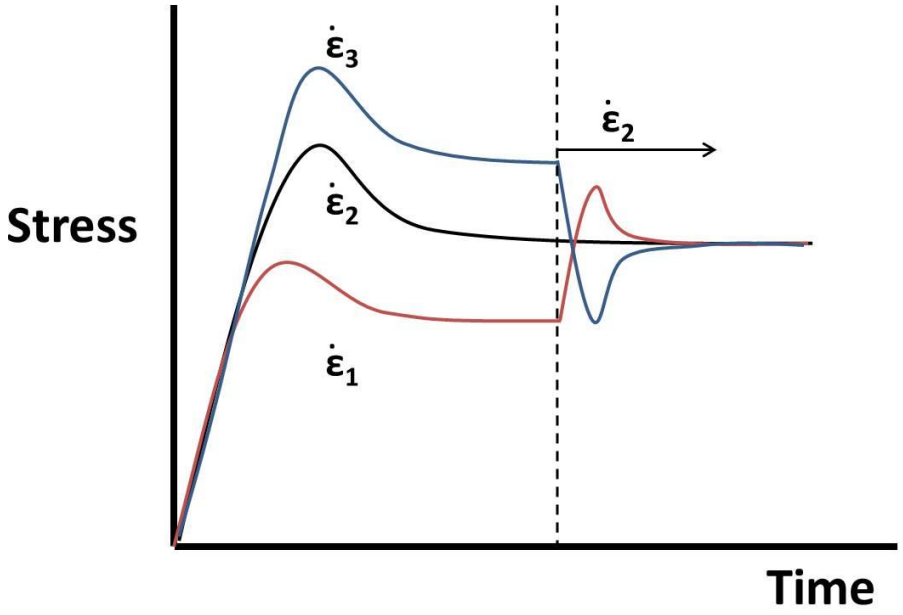

Figure 2. Schematic of a rate-switching experiment. A constant strain rate deformation begins either high rate $\dot{\varepsilon}_3$ (blue) or low rate $\dot{\varepsilon}_1$ (red). At the time indicated by the dashed line, the rate is switched to $\dot{\varepsilon}_2$. If the rate is increased, a stress overshoot is observed. If the rate is decreased, a stress undershoot is observed. Regardless of initial rate, the flow-state mechanical behavior associated with a deformation at a single rate $\dot{\varepsilon}_2$ (black) is recovered after depletion of the overshoot or undershoot. Schematic inspired by results of Nanzai.[27]

monitoring τ_c. In the first phase, a large stress which brought the sample to flow was imposed. In the second phase, stress was greatly decreased and the sample did not flow further. In the third phase, the large stress was again placed on the sample and remained on the sample into the strain hardening regime. In the final phase, all stress was removed from the glass and dynamics were monitored in the recovery regime. When investigating the relationship in flow between $\log(\tau_c)$ and log(strain rate), it was found that the linear relationship typical of a single-step constant stress deformation was only demonstrated for the first step of the multi-step experiment. Simulations which complemented the probe reorientation work also showed similar features to the experiments.

Although the relationship between log(strain rate) and $\log(\tau_c)$ is broken in the multi-step experiments of Lee et al.,[20] it is unclear whether this relationship will be broken during rate-switching constant strain rate experiments. The observed broken relationship may be due to imposing a stress which brought the material outside of the flow regime in the multi-step creep experiments. If performing a rate-switching experiment, it may also be possible that the behavior of τ is transiently different before settling into the flow regime associated with the second strain rate. Such effects will need to be investigated in initial experiments.

To investigate rate-switching experiments, a mechanical protocol similar to that used by Nanzai[27] may be used. Because of our group's extensive experience on cross-linked poly(methyl methacrylate) with DPPC dye (see Chapter 1), this system would be ideal for initial experiments, although uncross-linked poly(methyl methacrylate), cross-linked or uncross-linked polystyrene, or poly(lactic acid) with DPPC are also possible systems of choice which have shown promise in preliminary work. Similar to the protocol described in Figure 2, initial experiments should focus on approaching one strain rate by switching in the post-yield regime from a higher or lower

strain rate as compared to a single constant strain rate experiment performed at the final rate. The behavior of τ and β during the switching experiments and the single constant strain rate experiments could then be compared. If data obtained in the final step of these two-step constant strain rate experiments is consistent with the flow-state single constant strain rate experiment, further experiments which more efficiently investigate the strain hardening regime could be performed, as described in the next section.

Rate-switching as an efficient route to investigate strain hardening

As strain increases past the strain softening regime, stress again begins to increase in what is termed the strain hardening regime. The stress increase in this regime is associated with a resistance to further deformation due to a greater degree of chain orientation.[29-31] Chen and Schweizer have postulated that during strain hardening, molecular mobility decreases,[30] consistent with published work of Lee et al. which investigates the evolution of molecular mobility up to strains of ~1.2.[19, 21] However, much remains unknown about the molecular-level description of strain hardening. Further experiments using the probe reorientation technique which focus systematically on the behavior of strain hardening at a series of temperatures and strain rates may be able to provide further insight into fundamental molecular mechanisms associated with strain hardening. Additionally, because the probe reorientation technique is able to monitor alignment of dye molecules during deformation, these experiments may be able to provide information related to the degree of orientation during strain hardening.

Published results of Lee et al. which investigate constant stress experiments and reach local strains of 1.0 or more (and demonstrate strain hardening behavior) indicate that the relationship between τ and local strain rate which exists in flow does not change during strain

hardening.[19, 21] However, constant stress and constant strain rate deformations investigated through the probe reorientation technique typically do not extensively survey the strain hardening regime. These deformations are often halted well before sample failure due to long experimental times associated with the slow strain rates required to monitor dynamics using the probe reorientation technique. For example, although our current sample cell is able to accommodate a deformation to an engineering strain of 1.4, such an extension at the fastest strain rates currently accessible to us would still take more than 12 hours. Although it is certainly possible to perform these long experiments, they are rather inefficient.

Using the flexible deformation apparatus, it may be possible to efficiently focus measurements in the strain hardening regime by first performing a very fast pre-deformation to a strain which is well past yield. Once the sample is in the strain hardening regime, the velocity of the linear actuator can then be reduced to the desired speed. The validity of these experiments relies on the assumption that, after the observed stress undershoot, the flow state obtained through this rate-switching experiment is indeed identical to the flow state obtained had the rate not been switched. In order to test this assumption, control experiments which measure τ during strain hardening (using a single strain rate) will also need to be performed.

Rate switching - investigating transient period of deformation

During a single-step constant strain rate deformation, we observe that segmental dynamics become faster up until yield, after which dynamics remain comparatively constant in the strain softening regime and are correlated with the local strain rate. During the deformation, we find that β increases from its pre-deformation value up until yield and similarly remains constant in the post-yield regime and is correlated to the enhancement of dynamics from the

undeformed state. In addition to the relationship observed between τ and strain rate in the post-yield regime, one question that may be investigated through rate-switching deformations is how the observed stress overshoot or undershoot is similar to a yield in a single-rate constant strain rate experiment. One route to assess the similarity of these overshoots or undershoots to yield is to observe how β evolves in the post-yield regime in a single-rate vs. a rate-switching experiment.

Although experiments have observed that changes in β are very slight or nonexistent after yield, the SCM predicts that during a constant strain rate deformation, changes to the relaxation spectrum continue during strain softening.[17] These changes are very slight for a polymer which has not been aged for a long period of time before deformation. Because our samples are typically not highly-aged before deformation, such post-yield changes may be within the error associated with our β measurements. However, for a highly-aged sample, such changes become much more dramatic in the SCM. The spectrum of relaxation times is initially slightly narrowed upon cooling in the SCM because the slowest-relaxing segments are unable to shift to slower relaxation times on the timescale of the cooling rate; however, increased aging time causes the relaxation spectrum to widen again. This suggests that the pre-deformation relaxation spectrum will be wider for a highly-aged glass as compared to a glass which is less aged. Interestingly, calculations from the SCM suggest that glasses which are more aged also show greater changes to the spectral width of relaxation times after yield in the strain softening regime as compared to the behavior of a glass which is less aged. We may be able to explore this post-yield narrowing by investigating constant strain rate deformations of PMMA (or other) samples aged to equilibrium, presumably by holding a sample at a temperature just below T_g to make it possible to reach equilibrium in a feasible time window. However, it should be noted that as discussed in

Chapter 2, constant strain rate deformations at these high temperatures may only demonstrate modest increases in β, making slight changes in the strain softening regime difficult to detect.

In a rate-switching experiment, it may be possible to monitor the yielding transition for a system experiencing more dramatic changes in β than we can currently monitor in a single-step constant strain rate experiment. In this way, we may be able to observe in a system anticipated to demonstrate very large changes in the distribution of relaxation times whether measurable changes to β occur during the stress overshoot or undershoot regime. Although calculations of such rate-switching experiments have not been published by Medvedev and Caruthers, recently presented results[26] suggest that the SCM can capture features of a two-step deformation, including a rate-switching experiment. In a single-rate constant strain rate deformation, we are limited to a global strain rate of $\sim 3 \times 10^{-5}$ s^{-1} or less (due to the inability of our instrumentation to adequately track the photobleached area at higher rates). However, large changes in β may be induced during deformation by first deforming at a very high strain rate (during which τ and β would not be monitored) and then rapidly switching the rate to one multiple orders of magnitude slower (after which τ and β could be monitored). As a comparison, post-yield behavior for a single-rate experiment at the lower rate could be used. Such a project would benefit from close collaboration with Medvedev and Caruthers, who may be able to calculate predictions for our experimental data based on the SCM.

References

1. Chen, K.; Schweizer, K. S. *Macromolecules* **2011,** 44, (10), 3988-4000.
2. Smessaert, A.; Rottler, J. *Macromolecules* **2012,** 45, (6), 2928-2935.
3. Gray, L. A. G.; Yoon, S. W.; Pahner, W. A.; Davidheiser, J. E.; Roth, C. B. *Macromolecules* **2012,** 45, (3), 1701-1709.
4. Pye, J. E.; Roth, C. B. *Macromolecules* **2013,** 46, (23), 9455-9463.
5. Gray, L. A. G.; Roth, C. B. *Soft Matter* **2014,** 10, (10), 1572-1578.
6. Debenedetti, P. G.; Stillinger, F. H. *Nature* **2001,** 410, 259-267.
7. Sastry, S.; Debenedetti, P. G.; Stillinger, F. H. *Nature* **1998,** 393, (6685), 554-557.
8. Utz, M.; Debenedetti, P. G.; Stillinger, F. H. *Physical Review Letters* **2000,** 84, (7), 1471-1474.
9. McKenna, G. B.; Santore, M. M.; Lee, A.; Duran, R. S. *Journal of Non-Crystalline Solids* **1991,** 131–133, Part 1, (0), 497-504.
10. McKenna, G. B. *Journal of Physics: Condensed Matter* **2003,** 15, (11), S737.
11. Lee, H. N.; Ediger, M. D. *Macromolecules* **2010,** 43, (13), 5863-5873.
12. Lee, H. N.; Ediger, M. D. *Journal of Chemical Physics* **2010,** 133, (1), 014901.
13. Lacks, D. J.; Osborne, M. J. *Physical Review Letters* **2004,** 93, (25), 255501.
14. Lyulin, A. V.; Michels, M. A. J. *Physical Review Letters* **2007,** 99, (8), 085504.
15. Kramer, E. J. *Journal of Applied Physics* **1970,** 41, (11), 4327-4341.
16. Klompen, E. T. J.; Engels, T. A. P.; Govaert, L. E.; Meijer, H. E. H. *Macromolecules* **2005,** 38, (16), 6997-7008.
17. Medvedev, G. A.; Caruthers, J. M. *Journal of Rheology* **2013,** 57, (3), 949-1002.

18. Lee, H. N.; Paeng, K.; Swallen, S. F.; Ediger, M. D. *Journal of Chemical Physics* **2008,** 128, (13), 134902.

19. Lee, H. N.; Paeng, K.; Swallen, S. F.; Ediger, M. D. *Science* **2009,** 323, (5911), 231-234.

20. Lee, H. N.; Riggleman, R. A.; de Pablo, J. J.; Ediger, M. D. *Macromolecules* **2009,** 42, (12), 4328-4336.

21. Lee, H. N.; Paeng, K.; Swallen, S. F.; Ediger, M. D.; Stamm, R. A.; Medvedev, G. A.; Caruthers, J. M. *Journal of Polymer Science Part B: Polymer Physics* **2009,** 47, (17), 1713-1727.

22. Riggleman, R. A.; Lee, H. N.; Ediger, M. D.; de Pablo, J. J. *Soft Matter* **2010,** 6, (2), 287-291.

23. Bending, B.; Christison, K.; Ricci, J.; Ediger, M. D. *Macromolecules* **2014,** 47, (2), 800-806.

24. Hebert, K.; Bending, B.; Ricci, J.; Ediger, M. D. *Macromolecules* **2015,** 48, (18), 6736-6744.

25. Bending, B. Ph.D. Thesis. University of Wisconsin-Madison, 2014.

26. Medvedev, G. A.; Caruthers, J. M. In *Multi-step deformations -- a stringent test for constitutive models for polymer glasses*, American Physical Society March Meeting, 2016.

27. Nanzai, Y. *Polymer Engineering & Science* **1990,** 30, (2), 96-107.

28. Liu, J.; Lin, P.; Li, X.; Wang, S.-Q. *Polymer* **2015,** 81, 129-139.

29. van Melick, H. G. H.; Govaert, L. E.; Meijer, H. E. H. *Polymer* **2003,** 44, (8), 2493-2502.

30. Chen, K.; Schweizer, K. S. *Physical Review Letters* **2009,** 102, (3), 038301.

31. Hoy, R. S.; Robbins, M. O. *Journal of Polymer Science Part B: Polymer Physics* **2006,** 44, (24), 3487-3500.